1993

Decay Of The Triplet State In A Porphyrin Quinone Molecule

David Donald Fraser

DECAY OF THE TRIPLET STATE IN A PORPHYRIN QUINONE MOLECULE

by

David Donald Fraser

Department of Chemistry

Submitted in partial fulfilment
of the requirements for the degree of
Doctor of Philosophy

Faculty of Graduate Studies
The University of Western Ontario
London, Ontario
October 1992

ISBN 0-315-81281-8

ABSTRACT

Workers in this and many other labs have been studying photoinduced electron transfer seeking to understand the photochemical processes in photosynthesis. Closely related processes also constitute the basis of some photosensitive tissue diseases and of a wide variety of industrial applications. To study the photophysics unhindered by diffusion, a molecule composed of a freebase porphyrin covalently linked to a *p*-benzoquinone by an amide linkage was used.

A nanosecond laser flash photolysis apparatus permitted the observation of the porphyrin triplet state decay, with the quinone fully reduced or with it fully oxidized to allow enhanced quenching of the porphyrin triplet via electron transfer. A difference of rate constants in the two cases yielded the electron transfer rate constant which ranged from $1.0 \times 10^4\ s^{-1}$ in acetonitrile to $2.8 \times 10^5\ s^{-1}$ in methylene chloride. It is shown that the available free energy and the electron transfer rate constants, determined in various solvents over a 40°C temperature range, do not exhibit the relationship put forth by Marcus electron transfer theory.

An alternative hypothesis of a fast equilibrium being established between the triplet porphyrin and a triplet exciplex before the electron reaches a radical-ion-pair state is supported by the observation of negative activation energies in benzonitrile and methylene chloride.

Since neither the radical-ion-pair nor the exciplex were observed as intermediate products, it is not possible to identify conclusively the pathway of deexcitation of the porphyrin triplet state.

ACKNOWLEDGEMENTS

I thank my supervisor, Dr. Jim Bolton for the opportunity to work in this lab and for the continuing encouragement and push he provided.

I thank Drs. Alan Weedon and Bill Ware for the use of their vacuum lines for the freeze-pump-thaw work.

I am grateful to Drs. Aitken Hoy, Te Fu Ho, Alan McIntosh, Lars Forss, and Michael Schindler, Eva Lipczyniska-Kochany, and Jan Kochany for their help with equipment, computers, and synthesis in the course of my work.

It has been wonderful to work with my fellow graduate students Harold Dick, Joyce Stilborn, Liu Jing-yao, Biswajit Choudhury, Georg Riegel, Julio Valladares, and Lizhong Sun.

The technical staff of all facilities helped me with equipment maintenance and occasional new design - John Vanstone, Warren Lindsay, Marty Scheiring, Glen Hall, Laurie Harnick, Bruce Harwood, Leslie Tchorek, Bruce Campbell, Irold Schmidt and Jose Caiero.

Last but not least the secretaries Cheryl O'Meara, Janice Miller, and Susan Bock kept me informed of important things like money and deadlines.

TABLE OF CONTENTS

Page

LIST OF TABLES

LIST OF FIGURES

LIST OF APPENDICES

CHAPTER 1

INTRODUCTION

1.1 Synopsis of thesis

In photosynthetic bacteria the primary reaction is the electron transfer from a bacteriochlorophyll dimer to a bacteriopheophytin, probably via a bacteriochlorophyll monomer, followed by the reduction of a ubiquinone. In green plants and algae (not as well-known) the primary electron transfer is similar, involving chlorins instead of bacteriochlorins and plastoquinone (photosystem II) or an iron-sulfur protein instead of ubiquinone. In both these systems the electron transfer constituents are held in a well-defined orientation by a protein matrix. It is to mimic this electron transfer that the molecule PAQ (5-(4-carboxyphenyl)-10,15,20-tri(*p*-tolyl)porphine linked to methyl-*p*-benzoquinone via an amide group: Fig. 1.1) was synthesized in this lab[1,2] and similar molecules by many others.[3]

The decay of the singlet state of PAQ has been well described by previous studies (using time-correlated single photon counting) and shows excellent agreement with Marcus electron transport theory.[4,5,6] This thesis describes experiments using laser flash photolysis to monitor the decay of the absorbance of the triplet state of PAQ in various solvents and over a 40°C temperature range. Chapter 1 summarizes the overall kinetic scheme of the decay of excited PAQ (based on the above work) and the role of the triplet state within this model, the use of synthetic porphyrins as models of photosynthetic components, Marcus electron transfer theory and the

Figure 1.1. PAQ

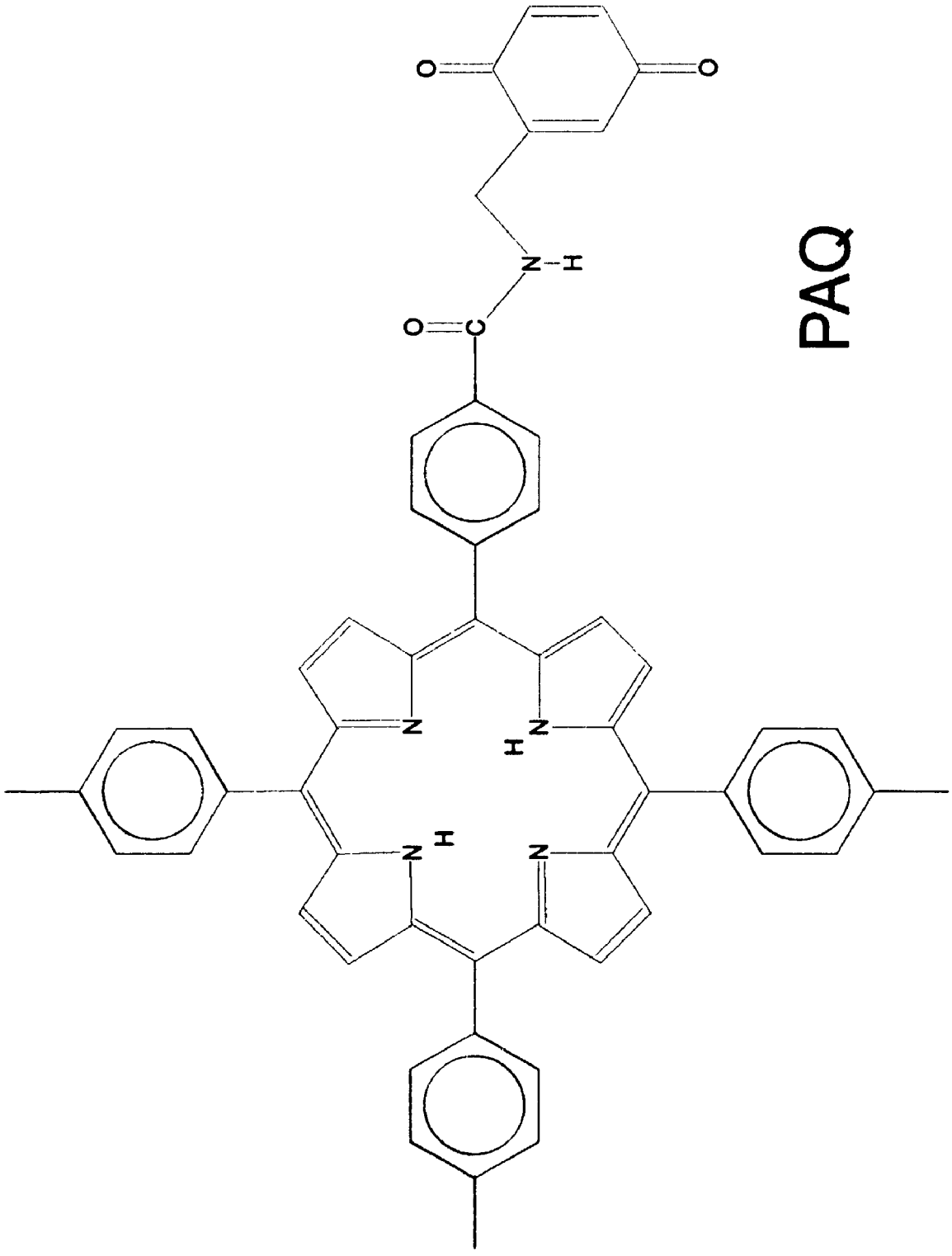

PAQ

exciplex model. Sample preparation, the experimental apparatus, and the method of analysis are described in Chapter 2. Spectral results and a Marcus theory analysis of kinetic results are given in Chapter 3, while Chapter 4 presents an analysis based on the exciplex model.

1.2 Deexcitation processes

After absorbing a photon, a molecule is promoted to an excited singlet state, which may decay by radiationless internal conversion back to the ground state, fluorescence to the ground state, intersystem crossing to an excited triplet state, isomerization, intramolecular energy or electron transfer, dissociation, or collisional deactivation, energy transfer, electron transfer, or chemical reaction with another molecule.[7] The last four processes are bimolecular and the first seven are unimolecular, although they may be enhanced by the presence of other molecules. If the molecule reaches an excited triplet state, most of these same processes can occur from there.

Second-order electron transfer reactions (or any second-order reaction) can be divided into three steps.[8] In the first step the donor and acceptor D and A diffuse together to form a precursor complex $D^{\dagger}A$ (the rate constant for association k_a may approach the diffusion-controlled limit). In the second step, the precursor complex moves to a transition state $(D^{\dagger}A)^{\ddagger}$, where electron transfer occurs, which then moves to a successor complex $D^{\dagger}A$ (second step rate constant k_{ET}). The final step is the dissociation of the successor complex into separate ions (rate constant k_s). In the

first two steps the reverse processes may also happen: dissociation of the precursor complex (rate constant k_d) and reverse electron transfer through the same transition state (rate constant k_{-ET}).

$$D + A \underset{k_d}{\overset{k_a}{\rightleftharpoons}} D|A \underset{k_{-ET}}{\overset{k_{ET}}{\rightleftharpoons}} D^+A^- \xrightarrow{k_s} D^+ + A^- \qquad 1$$

Fast bimolecular rates are usually controlled by diffusion in fluid media, with a rate constant of the order of 10^{10} $M^{-1}s^{-1}$. To ensure that the investigation of the photoinduced electron transfer step is unhindered by diffusion, the donor porphyrin has been covalently attached to a quinone via an amide linkage and the molecule is kept in low concentration. Then only the forward and reverse electron transfer and any other unimolecular decay processes have significant rates. The electron transfer pathway may be blocked by reducing the quinone to a hydroquinone form. The general kinetic scheme for PAQ is shown in Fig. 1.2.

If the initial excitation or a jump between states puts the molecule into a high electronic state ($S_0 \rightarrow S_n$ or $S_1 \rightarrow T_n$), then internal conversion shifts the molecule to the lowest state of that multiplicity ($S_n \rightarrow S_1$ or $T_n \rightarrow T_1$) with a rate constant k_{IC}, which can be very fast (10^{14} s^{-1}) for a vanishingly small energy gap $\Delta E = E(S_n) - E(S_1)$ and which decreases rapidly as this gap widens.[9] Vibrational relaxation follows yielding a thermally equilibrated S_1 or T_1 state within 100 fs to 100 ps.[10] The time for the solvent to follow such a change in the electronic configuration is given by the constant charge dielectric relaxation time τ_l in the range of picoseconds to nanoseconds.[11,12]

Figure 1.2. Gibbs energy diagram showing the energy levels and decay pathways of PAQ. The rate constants are

k_F fluorescence

k_{IC} internal conversion

k^S_{ISC} intersystem crossing from the singlet to the triplet state

k^S_{ET} electron transfer from the singlet state

k^T_{ET} electron transfer from the triplet state

k^T_{-ET} reverse electron transfer in the triplet state

k_{13}, k_{31} spin rephasing between the singlet and triplet radical-ion-pairs

k_P phosphorescence

k^T_{ISC} intersystem crossing from the triplet to the ground state

k^S_R charge recombination from the singlet radical-ion-pair

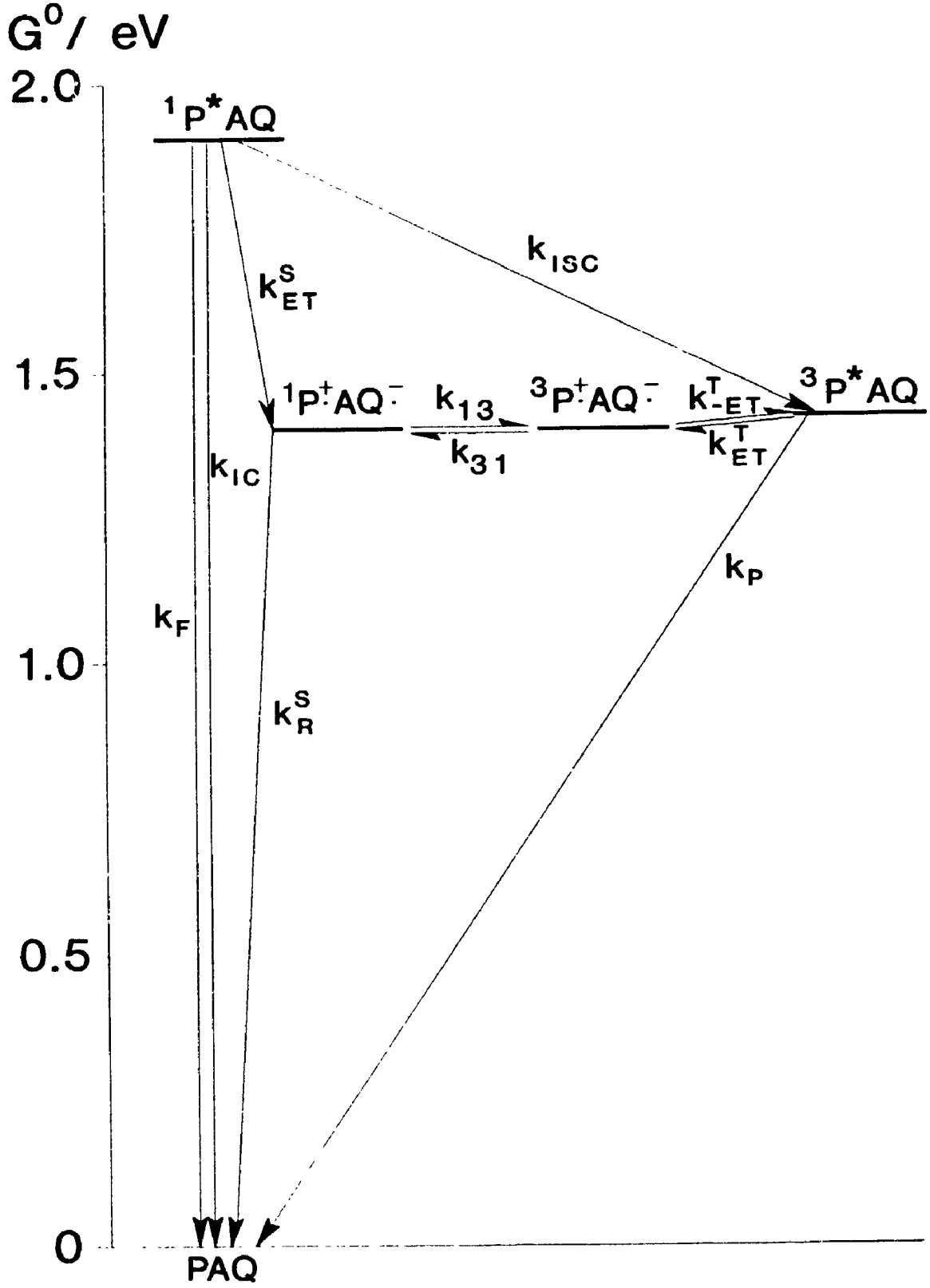
G⁰/ eV
2.0
1.5
1.0
0.5
0
¹P*AQ
³P*AQ
¹P⁺·AQ⁻·
³P⁺·AQ⁻·
PAQ
k_ISC
k^S_ET
k_IC
k_13
k_31
k^T_-ET
k^T_ET
k_P
k_F
k^S_R

The first excited singlet state is usually much longer lived than higher excited singlet states.[9] With the addition of other possible decay processes, it can have a lifetime of picoseconds to microseconds.[13]

Internal conversion and intersystem crossing are similar nonradiative processes; the only difference between them is that intersystem crossing is forbidden by the selection rule that the spin must not change. However, spin-orbit coupling produces a mixing of the states, making the transition weakly allowed. If the states S_n and T_n are identical in every aspect except spin, then the rate constant of intersystem crossing k_{ISC} can be slower than that of internal conversion by a factor of 10^6 to 10^8.[9] In aromatic hydrocarbons k_{ISC} decreases with an increasing gap between the zero-point energies of the source and destination states[14,15]

$$\log k_{ISC} \approx 7.5 - 8.5[\Delta E(T_1,S_0)/20\,000\,\mathrm{cm}^{-1}] \qquad 2$$

where $\Delta E(T_1,S_0)$ is the difference in energies of the triplet and ground states in units of cm^{-1}.

The general form of the Pauli Principle states that *the wave function of a system of electrons must be antisymmetric with respect to the interchange of any two electrons.*[16] This forces the singlet state with an antisymmetric spin function to have a symmetric spatial wavefunction and the triplet state with a symmetric spin function to have an antisymmetric spatial wavefunction. Since singlet pairs of electrons are allowed to be in the same vicinity at the same time, while triplet pairs are not, the former suffer, on average, a larger Coulombic repulsion and hence have a larger

potential energy. To a first approximation, this is the origin of the singlet-triplet splitting in states of the same molecular configuration.

Above the first excited triplet state there may be several higher triplet states that are still lower in energy than the first excited singlet state, permitting a small energy gap and thus an intersystem crossing rate constant of up to 10^8 s^{-1}. In contrast, there is no singlet state between S_0 and S_1 so the energy gap for $T_1 \rightarrow S_0$ is usually large with a correspondingly long lifetime - from microseconds to several seconds.[13] The intersystem crossing rate constants in both directions can be increased by the presence of heavy atoms or paramagnetic species, such as oxygen, which increase the spin-orbit coupling.

The long lifetime, the lower energy, and the multiplicity of the triplet state make it useful for many applications either directly, via triplet energy transfer, or via triplet-triplet annihilation which may create higher energy states.[17,18] It can initiate photochemical reactions in molecules that do not absorb directly in a convenient wavelength range (i.e., the near UV - visible). Triplet energy transfer can populate triplet states not otherwise populated because of low intersystem crossing rates. The long triplet lifetime allows for greater probability of reaction with molecules in low concentrations or to diffuse to molecules at greater distances in a matrix. The triplet multiplicity may involve different pathways in a reaction compared to singlet or ground state reactions.

1.3 Porphyrins

All porphyrins exhibit similar optical spectra due to the inner 16 carbon - 2 nitrogen macrocyle with 18 π electrons[19] (Fig. 1.1). The bare, unsubstituted, and fully conjugated porphyrin is called porphine. The naturally occurring and biologically important porphyrins are unsubstituted at the meso positions and substituted at the eight β-pyrrole positions and most have metal centers. The readily synthesized tetraarylporphyrins have hydrogens at the β-pyrrole positions and aromatic groups at the meso positions. The aromatic substituents have small effects on the spectra since the phenyl groups are twisted out of the porphyrin plane by steric hindrance of the pyrroles.[20] Saturated substituents and unsaturated groups insulated from the ring by alkyl linkages also have little effect[19,21] while unsaturated groups such as vinyl and carbonyl conjugate to the porphyrin ring have a stronger effect.

Reduction of one of the β-pyrrole double bonds to form a chlorin produces the intense far-red band and then a second reduction of the opposite β-pyrrole double bond gives the porphyrin parent of bacteriochlorophyll. In both cases the 18 π electron macrocycle remains intact.

Metalloporphyrins can be separated into two classes according to characteristics of the metal center. 'Regular' metal centers, which may also have axial ligands, contain only closed shells, are diamagnetic, and have only a small variation in optical absorption and emission spectra, which is understood as a small perturbation on the ring π electrons.[19] The metal oxidation states remain stable in

redox reactions of these metalloporphyrins; it is the tetrapyrrole ligand that gains or loses electrons.[22] Magnesium in chlorophyll and zinc in ZnTPP are examples of such regular metals.

The 'irregular' metalloporphyrins have transition metals with unfilled d or f shells in the center (although some of these may behave as the regular metalloporphyrins above). The d and f electrons interact with the ring π-electrons producing much more variability in the absorption and emission spectra. The first oxidation is that of the central metal; subsequent oxidations are of the porphyrin ring. Iron in heme proteins is an important example.[23]

Therefore, freebase (and 'regular' metal) porphyrins are an acceptable model for chlorophyll, bacteriochlorophyll and their pheophytins with respect to their spectral and electrochemical properties.

All porphyrins have narrow bands in the visible region with very large extinction coefficients in the ground state, excited states and ions; there also some broad bands of smaller extinction coefficient. Thus, it is easy to observe very dilute solutions of porphyrins.

When the porphyrin has a metal center or is an acid dication formed by the addition of two protons, PH_2^{2+}, the macrocycle has a D_{4h} symmetry. This porphyrin form exhibits an absorption spectrum consisting of an intense band (called the Soret band) about 370 to 430 nm with $\epsilon \sim 2$ to 5×10^5 $M^{-1}cm^{-1}$, due to excitation to the second excited singlet state and labelled in the Platt notation as B(0,0). Between 480 and 660 nm there are two bands with $\epsilon \sim 1$ to 2×10^4 $M^{-1}cm^{-1}$, due to excitation to

the lowest and second lowest vibrational levels of the first excited singlet state, designated Q(1,0) and Q(0,0).

By removing the metal or two protons from the porphyrin center to form the freebase form, the symmetry is reduced to D_{2h}. Each of the Q bands is split into Q_x and Q_y yielding four bands in all. The Soret band is not split. Both these forms are seen in Fig. 1.3, tetratolylporphyrin (TTP) in methylene chloride and its dication form $TTPH_2^{2+}$, which has D_{4h} symmetry.

Pekkarinen and Linschitz[24] have shown that the triplet-triplet spectra of tetraphenylporhine (TPP), zinc tetraphenylporphine and bacteriochlorophyll all have a strong band just to the red of the Soret band, a weaker band just to the blue of the Soret band, and then a smaller, broad and featureless absorption band extending to the far-red. Yasiuke et al.[25] has shown similar spectra in magnesium, zinc and cadmium *meso*-diphenyltetrabenzoporphyrins. These all give rise to a difference spectrum with an intense band to the red of the Soret band and smaller bands further to the red and to the blue of the Soret band.

The radical cations of regular metalloporphyrins, all have spectra with an intense band just to the blue of the Soret band and a broad region of strong Q bands.[25,26] Distinguishing between the triplet and radical cation forms of the freebase porphyrin on the basis of published spectra[24,27] is difficult although a study of metallotetrabenzoporphyrins[25] showed difference spectra just to the blue of the Soret band that are significantly dissimilar and indicated that the freebase radical cation may have a much longer lifetime than the triplet state.

Figure 1.3. The spectra of tetratolylporphyrin (TTP) and its acid dication form $TTPH_2^{2+}$. The solid line with a peak at 416 nm and the 4 Q bands between 515 and 647 nm (here increased by a factor of 20 for visibility) is the spectrum of TTP in methylene chloride with 2×10^{-4} M imidazole. The dashed line with peaks at 444 and 670 nm is the spectrum of $TTPH_2^{2+}$ in methylene chloride/glacial acetic acid = 1:1 by volume. The steep rises in the UV are due to the solvent cutoffs.

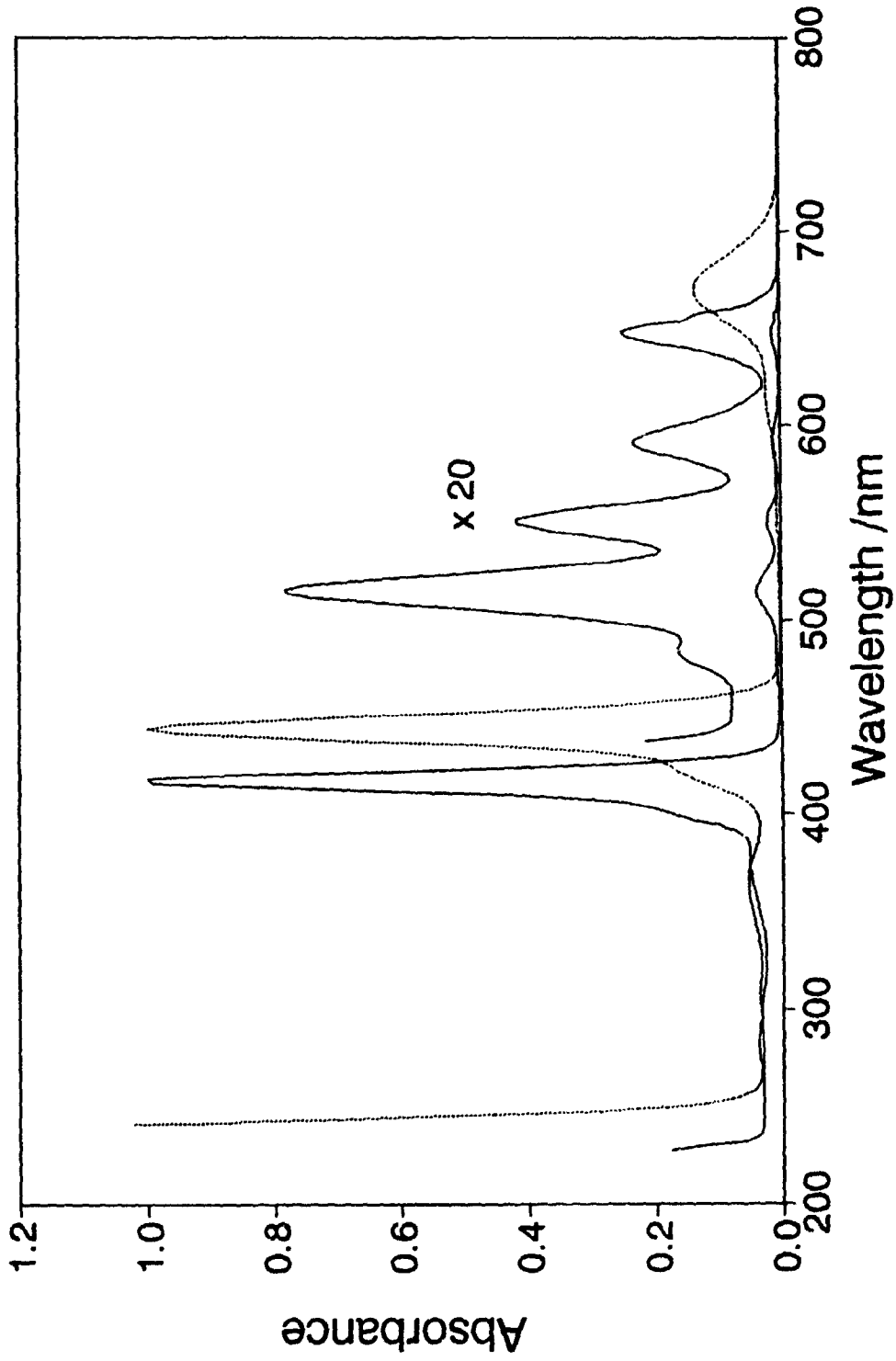
Absorbance
1.2
1.0
0.8
0.6
0.4
0.2
0.0
200
300
400
500
600
700
800
Wavelength /nm
x 20

1.4 Marcus electron transfer theory

By classical transition state theory, the first-order electron transfer rate constant is[28]

$$k_{ET} = \kappa_{el}\nu_n \exp(-\Delta G^{\ddagger}/k_B T) \qquad 3$$

where ν_n is the frequency of passage through the transition state, k_{el} is the electronic transmission coefficient or the probability of electron transfer once at the transition region, and $\Delta G^{\ddagger}$ is the Gibbs energy of activation to reach the transition state, k_B is the Boltzmann constant, and T is the absolute temperature.

The Gibbs energies of the reactant and product are functions of many nuclear coordinates, which yield multi-dimensional Gibbs energy surfaces. In transition-state theory, a reaction coordinate is introduced along the path of the reaction. A projection of the Gibbs energy surfaces onto this path results in one-dimensional surfaces of Gibbs energy as a function of reaction coordinate (Fig. 1.4). These one-dimensional Gibbs energy surfaces of the reactant and the product can be shown to be parabolic with respect to the reaction coordinate to a good approximation.[29]

ΔG^{*} is the theoretical activation energy, derived from the intersection of the reactant and product Gibbs energy parabolas, and should be distinguished from $\Delta G^{\ddagger}$, which is an experimental parameter derived from an Arrhenius analysis. ΔG^{o} is the difference in Gibbs energy between the zero point energies of the product and reactant states.[30]

$$\Delta G^{\circ} = G(\text{product,eqm}) - G(\text{reactant,eqm}) \qquad 4$$

Figure 1.4. Gibbs energy surfaces to show the relationship of energy changes as an electron moves from the reactant to the product surface.

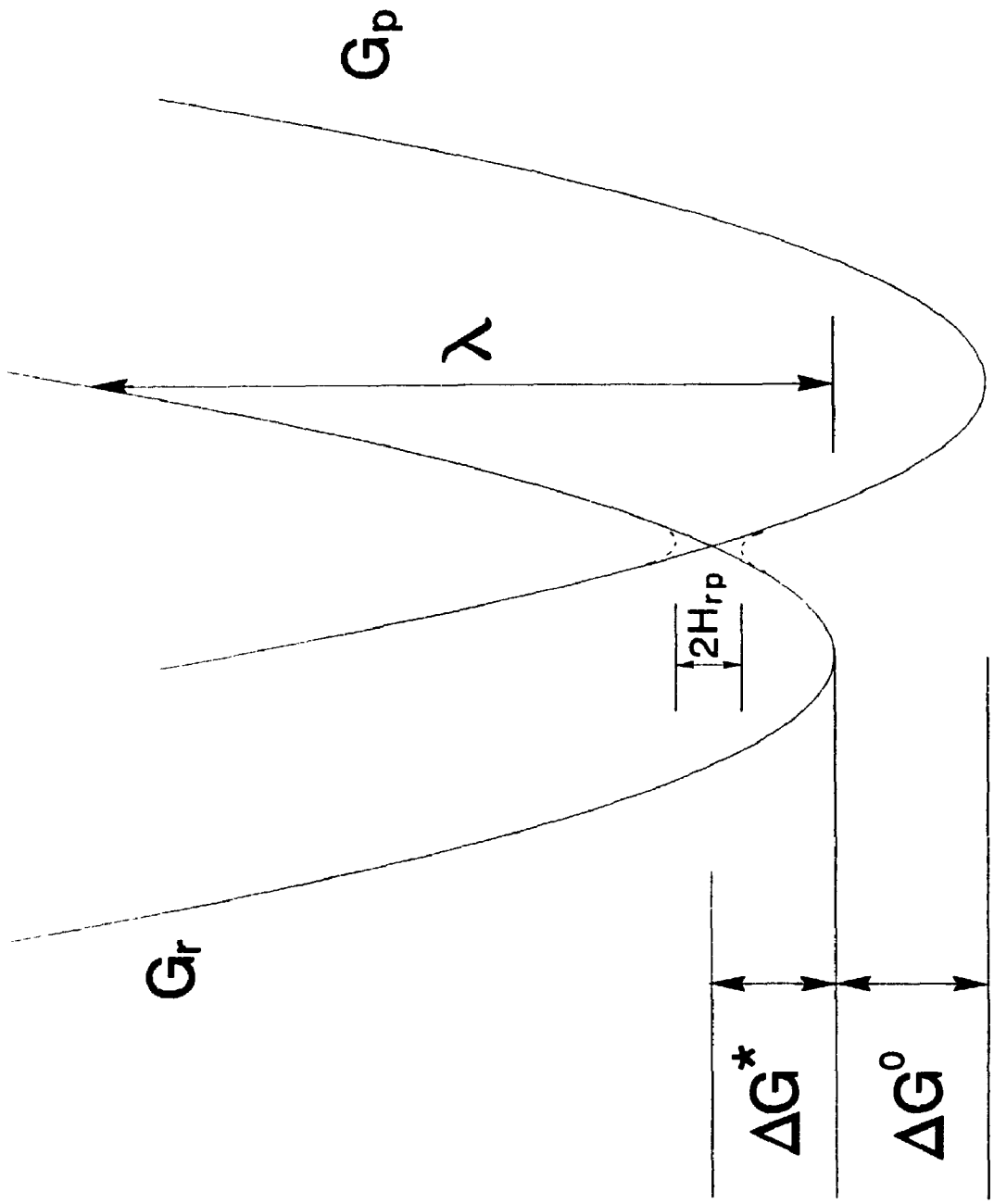
Gp
λ
2Hrp
Gr
ΔG*
ΔG°

The Gibbs energy of the reactant state is approximated by $h\nu_{0,0}$, the energy of the porphyrin excited singlet state, determined by the frequency at which the normalized absorption and fluorescence spectra overlap, or is the energy of the triplet state determined by the frequency of the maximum of the 0-0 phosphorescence band at low temperature.[31] The Gibbs energy of the product state is usually measured as the difference in standard reduction potentials of the D^+ and A plus a Coulombic work term for bringing D^+ and A^- together. The Gibbs energy of the reaction is thus

$$\Delta G^\circ = e(E^\circ_{D^{\cdot}/D} - E^\circ_{A/A^-}) - \frac{e^2}{4\pi\varepsilon_0\varepsilon_s r_{DA}} - h\nu_{0,0} \qquad 5$$

where ε_0 is the permittivity of free space, ε_s is the static dielectric constant of the solvent, and r_{DA} is the distance between the centers of the donor and acceptor.

The curvatures of the parabolas are assumed to be equal.[32] If they are not, the simplest approximation is that the reorganization energy used is the arithmetic mean of the separate reorganization energies found by self-exchange reactions between two reactant molecules and between two product molecules.[33,34] By the properties of parabolas,

$$\Delta G^* = \frac{(\lambda + \Delta G^\circ)^2}{4\lambda} \qquad 6$$

Here, λ is the reorganization energy - the change in Gibbs energy if the reactant state distorts to the equilibrium configuration of the product state without transfer of the electron in the transition region.

The classical Marcus equation for electron transfer then becomes

$$k_{ET} = \kappa_{el}\nu_n \exp\left[-\frac{(\lambda + \Delta G^\circ)^2}{4\lambda k_B T}\right] \qquad 7$$

Equations 6 and 7 indicate that, for endergonic and moderately exergonic reactions, as ΔG° decreases ΔG^* decreases and k_{ET} increases, attaining a maximum value of $\kappa_{el}\nu_n$ when $\Delta G^\circ = -\lambda$ (see Fig. 5). This is called the 'normal region'. The 'inverted region' results when ΔG° becomes more negative, ΔG^* again becomes positive and k_{ET} decreases.

The reorganization energy λ can be divided into two terms

$$\lambda = \lambda_{in} + \lambda_{out} \qquad 8$$

The inner reorganization energy λ_{in} arises from changes in the molecule's internal geometry and is usually treated harmonically so that

$$\lambda_{in} = \frac{1}{2}\sum_j f_j(\Delta q_j)^2 \qquad 9$$

Δq_i is the change in a normal mode coordinate equilibrium value from reactant to product and f_i is a reduced force constant

$$f_j = \frac{2f_j^r f_j^p}{(f_j^r + f_j^p)} \qquad 10$$

λ_{in} is solvent independent and small, probably not more than 0.2 eV.[3,35,36] This value is used as a constant term in subsequent calculations of λ.

The outer reorganization energy λ_{out} arises from the reorganization of the molecule's external solvent environment. Imagining the molecule in a dielectric continuum, then[32]

$$\lambda_{out} = \frac{1}{2}\varepsilon_0\left[\frac{1}{\varepsilon_{op}} - \frac{1}{\varepsilon_s}\right]\int(E^r - E^p)^2 dV \qquad 11$$

ε_{op} is the optical dielectric constant of the solvent, E^r and E^p are the in vacuo electric fields due to the reactant and product states, respectively. Evaluation of the integral depends on the model of the molecule in its reactant and product states. Taking the donor and acceptor to occupy hollow spheres of radii r_D and r_A, respectively, and the distance between them to be $r_{DA} > r_D + r_A$ gives

$$\lambda_{out} = \frac{(\Delta e)^2}{4\pi\varepsilon_0}\left[\frac{1}{2r_D} + \frac{1}{2r_A} - \frac{1}{r_{DA}}\right]\left[\frac{1}{\varepsilon_{op}} - \frac{1}{\varepsilon_s}\right] \qquad 12$$

or

$$\lambda_{out} = B\left[\frac{1}{\varepsilon_{op}} - \frac{1}{\varepsilon_s}\right] \qquad 13$$

where Δe is the charge transferred. In general, other models usually give the same form as eqn. 13 where B incorporates the particulars of the molecular model.

The full quantum mechanical expression for the rate constant comes from Fermi's 'Golden Rule' as

$$k_{et} = \frac{2\pi}{\hbar}\sum_{i}\sum_{j} \langle \Psi_{pj} | \hat{\mathcal{H}}_{el} | \Psi_{ri} \rangle^2 P(\varepsilon_{ri})\delta(\varepsilon_{pj} - \varepsilon_{ri}) \qquad 14$$

The Ψ°_{ri} and Ψ°_{pj} are the vibronic wavefunctions of the reactant state i and the product state j and $\hat{\mathcal{H}}_{el}$ is a Born-Oppenheimer (rigid nucleus) electronic Hamiltonian[28]. $P(\varepsilon_{ri})$ is the Boltzmann probability weight of the reactant state i. This matrix element is then factored into a nuclear overlap integral involving only vibrational wavefunctions and an electronic coupling term H_{rp} between electronic wave functions ψ°_{r} and ψ°_{p}.

$$H_{rp} = \langle \psi^{\circ}_{r} | \hat{\mathcal{H}}_{el} | \psi^{\circ}_{p} \rangle \qquad 15$$

The electron transfer reaction is said to be adiabatic if H_{rp} is relatively large, so that the Gibbs energy surfaces interact to produce an upper and a lower surface. In this case, the reaction always stays on the lower surface and proceeds directly through the transition state so that the electronic transmission coefficient $\kappa_{el} \approx 1$.

If H_{rp} is small, the reactant and product surfaces interact weakly, the electron transfer is said to be nonadiabatic, and the system then proceeds along the reactant surface. There is only an occasional electron transfer by tunnelling mechanisms. The division between adiabatic and nonadiabatic is determined by $H_{rp} \approx 0.025$ eV.[28]

The sums are over all reactant states i and all product states j; these include both molecular and solvent vibrations. However, the solvent modes usually have low

frequencies and are treated classically, yielding the outer reorganization energy calculated in eqns. 11 to 13. Jortner[37] has shown that the reactant and product high frequency modes are usually in a narrow band and so can be averaged to a single mean frequency ω. Miller et al.[38] defined the internal reorganization energy via reduced displacements Δ_i

$$\Delta_l = \frac{\mu_l \omega_l \Delta q_l}{2\hbar} ; \qquad \omega_l = (f_l/\mu_l)^{1/2} \tag{16}$$

so that

$$\lambda_{in} = \sum_l \Delta_l^2 \hbar\omega_l \tag{17}$$

where the sum is over all high frequency modes. Setting $S = \lambda_{in}/\hbar\omega$

$$k_{ET} = \frac{2\pi}{\hbar} \frac{H_{rp}^2}{(4\pi\lambda_{out}k_BT)^{1/2}} \sum_{m=0}^{\infty} \left(\frac{e^{-S}S^m}{m!}\right) \exp\left[-\frac{(\Delta G^\circ + \lambda_{out} + m\hbar\omega)^2}{4\lambda_{out}k_BT}\right] \tag{18}$$

In the 'high temperature limit' $k_BT >> \hbar\omega$ this semiclassical form reduces to

$$k_{ET} = \frac{2\pi}{\hbar} \frac{H_{rp}^2}{(4\pi\lambda k_BT)^{1/2}} \exp\left[-\frac{(\Delta G^\circ + \lambda)^2}{4\lambda k_BT}\right] \tag{19}$$

This is the same as eqn. 7 with the preexponential replaced by

$$\kappa_{el}\nu_n = \frac{2\pi}{\hbar} \frac{H_{rp}^2}{(4\pi\lambda k_BT)^{1/2}} \tag{20}$$

It should be noted that in the 'normal' region ($-\Delta G° < \lambda$) at room temperature, eqn. 19 closely matches eqn. 18 even though the high temperature limit is not valid (see Fig. 1.5). Because of its ease of calculation, and the fact that $\Delta G°$ for electron transfer from ^{3}PAQ is well into the normal region, eqn. 19 is used to analyze the experimental data.

This may be written in the form

$$\ln(k_{et}\lambda^{1/2}) = \ln\left(\frac{2\pi}{\hbar}\frac{H_{rp}^2}{(4\pi k_B T)^{1/2}}\right) - \frac{(\Delta G° + \lambda)^2}{4\lambda k_B T} \qquad 21$$

or

$$Y_1 = C_1 - X \qquad 22$$

where

$$Y_1 = \ln(k_{ET}\lambda^{1/2}) \qquad 23$$

$$C_1 = \ln\left(\frac{2\pi}{\hbar}\frac{H_{rp}^2}{(4\pi k_B T)^{1/2}}\right) \qquad 24$$

and

$$X = \frac{\Delta G^*}{k_B T} = \frac{(\Delta G° + \lambda)^2}{4\lambda k_B T} \qquad 25$$

If the system behaves according to Marcus theory, a plot of Y_1 vs. X should yield a straight line with slope of -1 and intercept C_1.

Figure 1.5. The variation of $\log(k_{ET})$ with the exergonicity ($-\Delta G°$) of the reaction. Curve a was calculated by using the 'high temperature limit' (eqn. 19) of the semiclassical expression. Curves b, c, and d were calculated using the semiclassical expression (eqn. 18) with the averaged internal vibrational frequencies ν = 750, 1500, 2250 cm^{-1}, respectively. λ_{in} = 0.2 eV; λ_{out} = 0.8 eV; H_{rp} = 0.3 meV; and T = 300 K. Note that k_BT = 0.026 eV and the lowest frequency vibration 750 cm^{-1} = 0.093 eV, so the high temperature regime is definitely not in place here. (Taken from J.R. Bolton and M.D. Archer *Direct Conversion of Solar Energy*, to be published.)

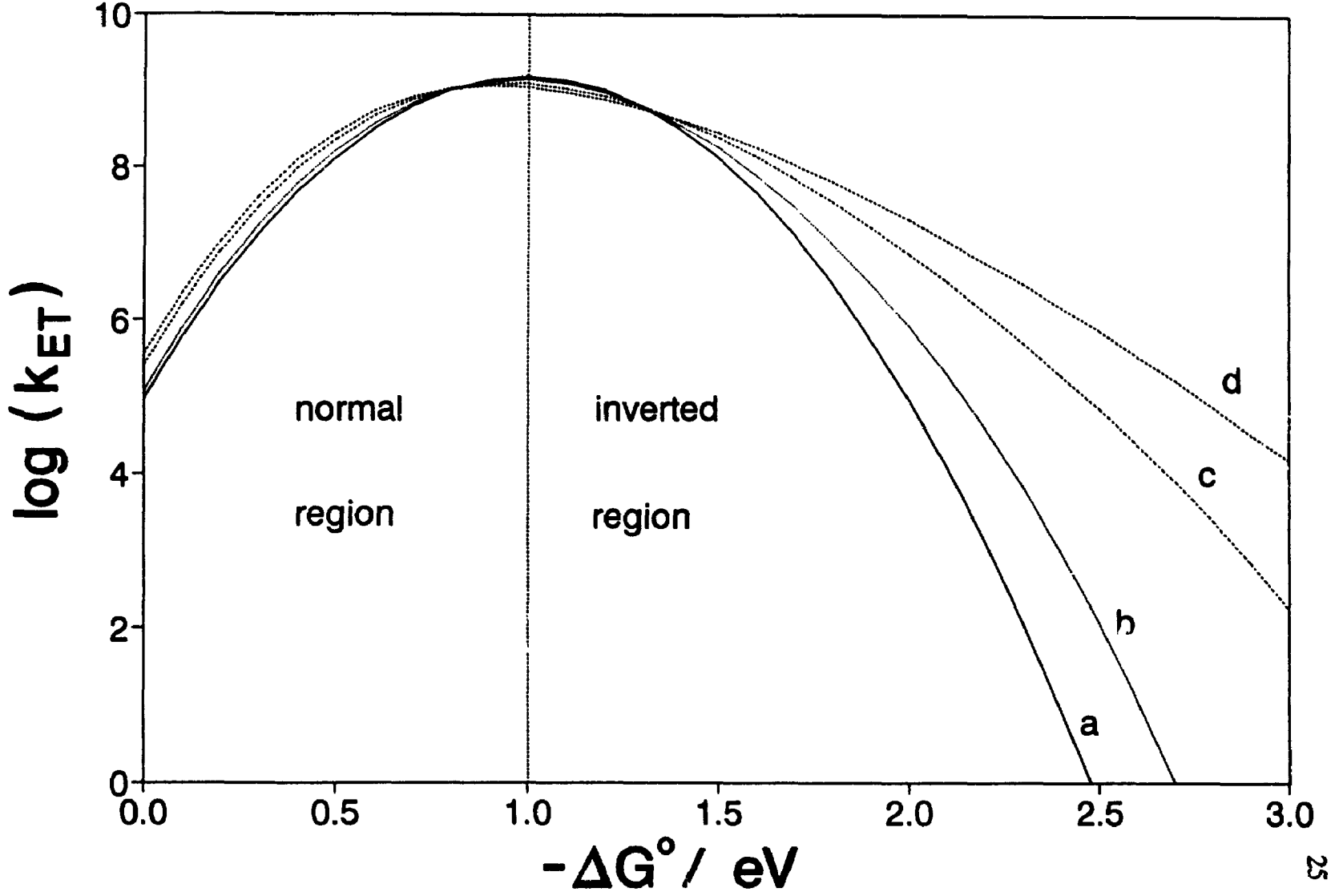
10
8
6
4
2
0
log (k_{ET})
normal
region
inverted
region
d
c
b
a
0.0
0.5
1.0
1.5
2.0
2.5
3.0
$-\Delta G^{\circ}$ / eV

A further test of Marcus theory is to remove the explicit temperature term from the preexponential by combining it with the left hand side of the equation as

$$\ln(k_{ET}(\lambda k_B T)^{1/2}) = \ln\left(\frac{2\pi}{\hbar}\frac{H_{rp}^2}{(4\pi)^{1/2}}\right) - \frac{(\Delta G^\circ + \lambda)^2}{4\lambda k_B T} \qquad 26$$

or

$$Y_2 = C_2 - X \qquad 27$$

where

$$Y_2 = \ln(k_{ET}(\lambda k_B T)^{1/2}) \qquad 28$$

and

$$C_2 = \ln\left(\frac{2\pi}{\hbar}\frac{H_{rp}^2}{(4\pi)^{1/2}}\right) \qquad 29$$

so that H_{rp} can be determined from the intercept. Again the slope of Y_2 vs. X should be -1.

The above expressions have been confirmed experimentally for electron transfer from the singlet state of PAQ.[5,6] Although in polar solvents there is a reasonable correlation of the rate constants of this decay with the predic. ons of Marcus theory in the form of eqn. 21, nonpolar solvents show a large discrepancy (Fig. 1.6). The separation of eqn. 21 was based on the electronic coupling energy H_{rp} being independent of solvent. This term may be calculated from an analysis of the temperature dependence of the electron transfer rate constant. The ^{1}PAQ data showed a linear relationship of Y_2 vs. X in various solvents, but the slopes varied

Figure 1.6. Marcus analysis of the solvent dependence of k_{ET} at 295 K for singlet PAQ[6] using eqn. 21. The solvent key is (1) acetonitrile; (2) proprionitrile; (3) benzonitrile; (4) acetone; (5) *n*-butyl alcohol; (6) 1,2-dichloroethane; (7) methylene chloride; (8) 2-methyltetrahydrofuran; (9) 1,1,1-trichloroethane; (10) 1,2-dimethoxyethane; (11) ethyl acetate; (12) ethyl ether; (13) chlorobenzene; (14) α-chloronaphthalene; (15) chloroform; (16) 1,2-dibromomethane; (17) anisole.

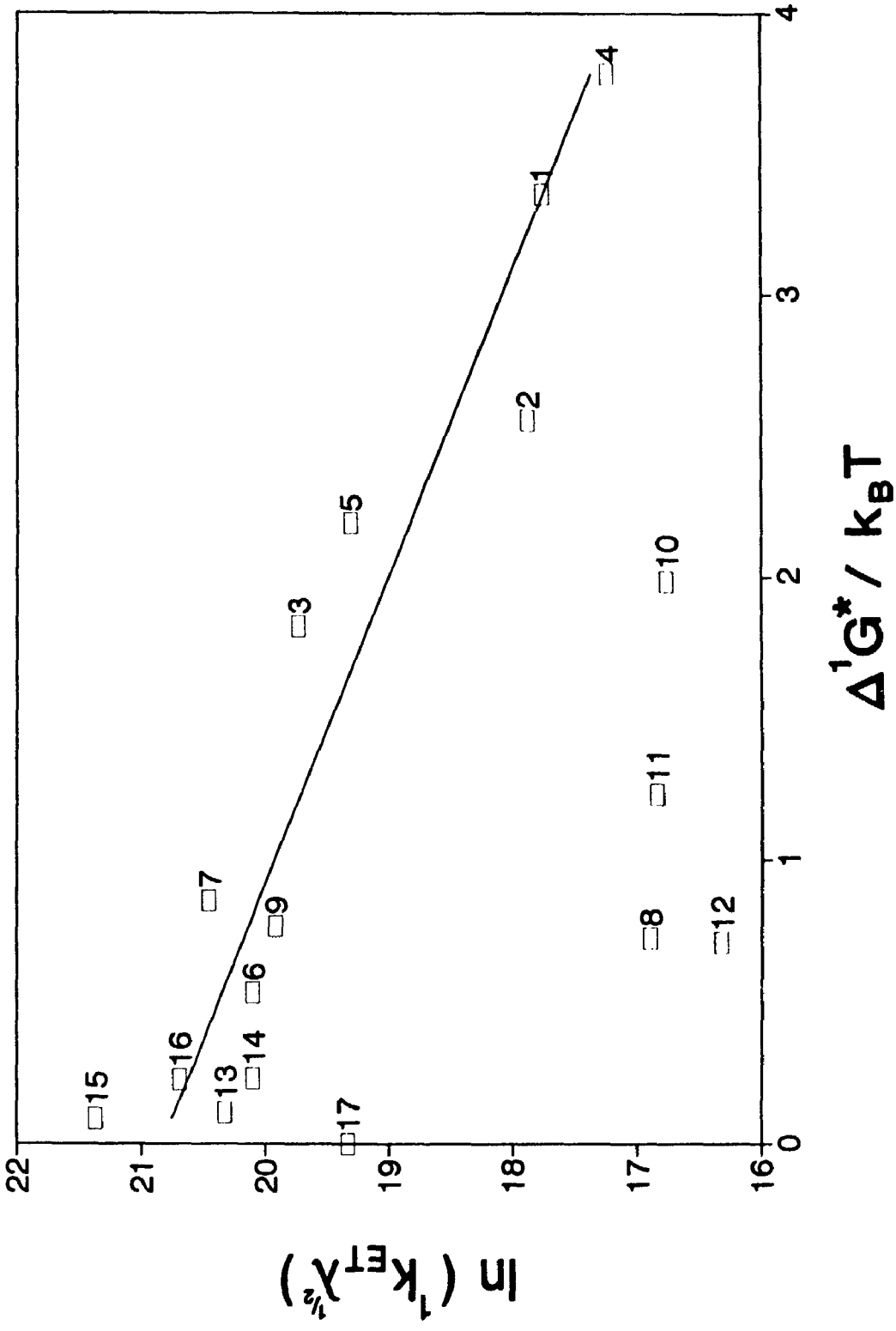
ln ($^1k_{ET}\lambda^{1/2}$)
Δ^1G^* / k_BT
22
21
20
19
18
17
16
0
1
2
3
4
15
16
13
14
6
7
9
17
3
5
2
1
4
10
11
8
12

from -2.1 to -0.8. By calculating $\Delta G°$ at a fixed temperature T_1 from eqn. 5, and then allowing a linear temperature dependence $\Delta G° = \Delta G°(T_1) + K(T-T_1)$, where K is a parameter to be determined separately for each solvent, it is possible to force the slope of Y_2 vs. X to be -1.00. With this treatment, H_{rp} is found to be much smaller in nonpolar solvents than in polar solvents (e.g., H_{rp} is about 4×10^{-5} eV in ethyl ether, ethyl acetate, and 2-methyltetrahydrofuran and is about 3×10^{-4} eV in methylene chloride, acetonitrile, and acetone).

Liu and Bolton[6] have determined, through NMR analysis, that in polar solvents a PAQ analog is in a compact conformation with the quinonoid moiety closer to the porphyrin. Associated with this are higher values of the electronic coupling coefficients H_{rp} for electron transfer between the first singlet excited state and the singlet radical-ion-pair. The molecule porphyrin-amide-dimethoxybenzene ($PAQ(Me)_2$) where methoxy groups replace the oxygens on the quinone, was used because of the possibility of contamination by $PAQH_2$ which would complicate the NMR analysis. Acetyl-*N*-dimethoxybenzylamine (ADB) was chosen as a reference compound in which a methyl group replaces the tetratolylporphyrin group.

Equation 21 can now be reformulated by including the H_{rp} term in the left-hand side as

$$Y_3 = \ln(k_{ET}\lambda^{1/2}H_{rp}^{-2}) \qquad 30$$

and

$$C_3 = \ln\left(\frac{2\pi}{\hbar(4\pi k_B T)^{1/2}}\right) \qquad 31$$

A plot of Y_3 vs. X for PAQ in those solvents in which H_{rp} has been determined now yields a straight line with a slope near -1.00 (Fig. 1.7).

1.5 Electron transfer via an exciplex

The above model of the deexcitation of the triplet state is based on a one-way electron transfer from the reactant state (excited triplet) to the product state (triplet radical-ion-pair). However, as these states are isoergonic, a combination state may be formed which may act as a conduit for electron transfer between the two. The wavefunction $\Psi_{(PAQ)}^*$ of this excited complex (hence exciplex)[39] state may be expressed as[43]

$$\psi_{(PAQ)^*} = a\psi_{(M_1^* M_2)} + b\psi_{(M_1 M_2^*)} + c\psi_{(M_1^+ M_2^-)} + d\psi_{(M_1^- M_2^+)} + e\psi_{M_1 M_2} \qquad 32$$

The contribution of each component is usually determined by the energy of the corresponding state. For exciplexes the ground state term is usually negligible.[43] The energies of the states $M_1^*M_2$ and $M_1M_2^*$ are assumed to be close to those of the respective excited monomers.[44] The energies of the charge transfer states depend on the redox properties of the components.[13] As a first approximation, one therefore usually needs to deal only with two interacting states: a charge transfer state and the lower energy state of the two excited donor-acceptor possibilities.

The lowest singlet state of TPP has an energy of 1.92 eV[14] and its triplet energy is 1.43 eV.[45] ZnTTP has a singlet energy of 2.1 eV and a triplet energy of 1.60 eV.[46] The energy of the lowest singlet $n\pi^*$ state of *p*-benzoquinone in nonpolar

Figure 1.7. Marcus analysis of the solvent dependence of k_{ET} for singlet PAQ with H_{rp} removed from the intercept according to eqns. 30 and 31. The solvent key is the same as for Fig. 1.5. Benzonitrile (3) is discussed in section 3.2. This graph has a slope of -1.07 ± 0.04.

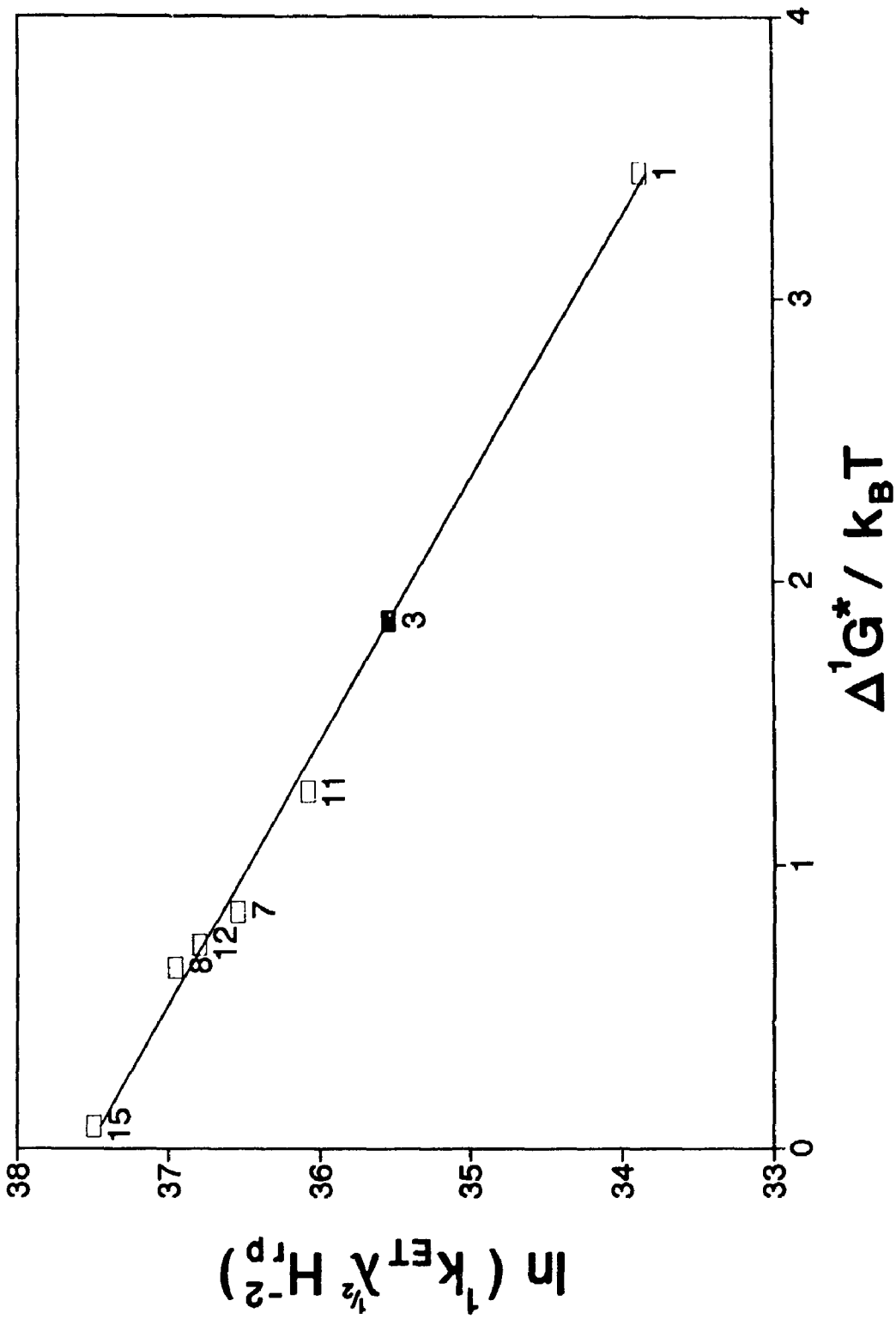
ln ($^1k_{ET}\lambda^{1/2}$ H_{rp}^{-2})
38
37
36
35
34
33
0
1
2
3
4
Δ^1G^* / k_BT
15
8
12
7
11
3
1

solvents is about 2.5 eV and the triplet $n\pi^*$ energy is about 2.3 eV.[47,48] In contrast to the usual absorption blue shift of $n\rightarrow\pi^*$ transitions in polar hydrogen bonding solvents compared to nonpolar solvents,[49] the methylated *p*-benzoquinones show essentially no shift in the wavelength of the $n\rightarrow\pi^*$ absorption peak (e.g., λ_{max} = 433 nm in hexane, 434 nm in ethanol).[50,51] The quinones are easily reduced but not easily oxidized.[46] Thus, the states to be considered for both nonadiabatic and exciplex mediated electron transfer are P^*Q and P^+Q^-.

Inserting such an exciplex into the scheme shown in Fig. 1.2 gives the following mechanism

$$\begin{array}{l} {}^3P^*AQ \underset{k_{-EX}}{\overset{k_{EX}}{\rightleftharpoons}} {}^3(PAQ)^* \underset{k_{-IP}}{\overset{k_{IP}}{\rightleftharpoons}} {}^3(P^+AQ^-) \underset{k_{13}}{\overset{k_{31}}{\rightleftharpoons}} {}^1(P^+AQ^-) \xrightarrow{k_{CR}} PAQ \\ \quad\downarrow k_0 \\ \quad PAQ \end{array} \qquad 33$$

where k_0 is the sum of rate constants for decay of the excited donor without exciplex formation, k_{EX} and k_{-EX} are the rate constants for exciplex formation and decay, k_{IP} and k_{-IP} are the rate constants for forward and reverse formation of a triplet radical-ion-pair from the exciplex, k_{31} and k_{13} are the rate constants for spin rephasing of the radical-ion-pairs, and k_{CR} is the rate constant for charge recombination to the ground state.

1.5.1 Steady-state approximation

The assumption of steady-state conditions for the intermediates yields the following expressions for the observed decay of the initially excited donor component

$$-\frac{d[D^*A]}{dt} = (k_0 + k_Q)[D^*A] \qquad 34$$

where

$$k_Q = \frac{k_{EX}}{1 + \frac{k_{-EX}}{k_{IP}}\left(1 + \frac{k_{-IP}}{k_{31}}\left(1 + \frac{k_{13}}{k_{CR}}\right)\right)} \qquad 35$$

If

$$k_{31}\left(1 + \frac{k_{13}}{k_{CR}}\right)^{-1} \gg k_{-IP} \qquad 36$$

then eqn. 35 reduces to

$$k_Q = \frac{k_{EX}}{1 + \frac{k_{-EX}}{k_{IP}}} \qquad 37$$

corresponding to the scheme

$$\begin{array}{l} {}^3P^*AQ \underset{k_{-EX}}{\overset{k_{EX}}{\rightleftharpoons}} {}^3(PAQ)^* \xrightarrow{k_{IP}} PAQ \\ \quad \Big\downarrow k_0 \\ \quad PAQ \end{array} \qquad 38$$

In benzonitrile, the charge recombination from the PAQ singlet radical-ion-pair decays to the ground state with a lifetime of ca. 6 ns.[4] while in photosynthetic bacterial reaction centers the time of spin rephasing between singlet and triplet

populations of radical-ion-pairs has been measured at ca. 20 ns.[52] Since these two radical-ion-pair states are degenerate in energy, $k_{31} \approx k_{13}$, and the requirement is that $k_{-IP} \ll 4 \times 10^7\ s^{-1}$. If, in addition, $k_{-EX} \gg k_{IP}$ then

$$k_Q \approx \frac{k_{EX}}{k_{-EX}} k_{IP} = K_{EX} k_{IP} \qquad 39$$

1.5.2 Kinetic analysis of exciplex

This expression may also be derived using a kinetic analysis[53] of the scheme shown in eqn 38 (i.e. using the scheme in eqn. 33 with the approximation of eqn. 36.) For a δ-pulse excitation, an initial (t=0) population $[D^*A]_0$ of locally excited molecules is produced. The temporal behaviour of the monomer and exciplex populations are modeled by the coupled differential equations

$$\frac{d[P^*AQ]}{dt} = -(k_0 + k_{EX})[P^*AQ] + k_{-EX}[(PAQ)^*]$$

$$\frac{d[(PAQ)^*]}{dt} = k_{EX}[P^*AQ] - (k_{-EX} + k_{IP})[(PAQ)^*] \qquad 40$$

The solution of these two equations, subject to the boundary conditions $[D^*A] = [D^*A]_0$ and $[(DA)^*] = 0$ at $t = 0$ are

$$[P^*AQ] = c_1 e^{-\lambda_1 t} + c_2 e^{-\lambda_2 t} \qquad 41$$

$$[(PAQ)^*] = c_3\{e^{-\lambda_1 t} - e^{-\lambda_2 t}\} \quad 42$$

where

$$\lambda_{1,2} = \frac{1}{2}\left[(k_0 + k_{EX} + k_{-EX} + k_{IP}) \pm \sqrt{(k_0 + k_{EX} - k_{-EX} - k_{IP})^2 + 4k_{EX}k_{-EX}}\right] \quad 43$$

$$c_1 = \frac{[D^*A]_0}{\lambda_1 - \lambda_2}(k_0 + k_{EX} - \lambda_2) \quad 44$$

$$c_2 = \frac{[D^*A]_0}{\lambda_1 - \lambda_2}(\lambda_1 - (k_0 + k_{EX})) \quad 45$$

$$c_3 = \frac{[D^*A]_0 k_{EX}}{\lambda_1 - \lambda_2} \quad 46$$

If the following approximation is valid

$$\frac{2(k_{EX} - k_{-EX})(k_0 - k_{IP}) + (k_0 - k_{IP})^2}{(k_{EX} + k_{-EX})^2} < 1 \quad 47$$

then

$$\lambda_1 \approx k_{EX} + k_{-EX} + \frac{k_0 k_{EX} + k_{IP}k_{-EX} + \frac{1}{2}(k_0 - k_{IP})^2}{k_{EX} + k_{-EX}} \quad 48$$

and

$$\lambda_2 \approx \frac{k_0 k_{-EX} + k_{IP} k_{EX} - \frac{1}{2}(k_0 - k_{IP})^2}{k_{EX} + k_{-EX}} \quad 49$$

The condition for rapid equilibrium between the locally excited state and the exciplex is that k_{EX}, $k_{-EX} >> k_0$, k_{IP}, in which case

$$\lambda_1 \approx k_{EX} + k_{-EX} \quad 50$$

$$\lambda_2 \approx \frac{k_0 k_{-EX} + k_{IP} k_{EX}}{k_{EX} + k_{-EX}} \quad 51$$

For the exciplex concentration to remain low requires in addition that

$$k_{-EX} > k_{EX} > k_0, k_{IP} \quad 52$$

in which case the above reduce to

$$\lambda_1 \approx k_{-EX} \quad 53$$

$$\lambda_2 \approx k_0 + k_{IP} \frac{k_{EX}}{k_{-EX}} \quad 54$$

$$c_1 \approx [D^*A]_0 \frac{k_{EX}}{k_{-EX}} \quad 55$$

$$c_2 = [D^*A]_0 \qquad 56$$

$$c_3 = [D^*A]_0 \frac{k_{EX}}{k_{-EX}} \qquad 57$$

Under these conditions the amplitudes c_1 and c_3 may be too small to be seen and the rate constant $\lambda_1 \approx k_{-EX}$ may be too fast for the time resolution of the apparatus, so that only the locally excited state is observed with a rate constant $\lambda_2 \approx \lambda_0 + k_{IP}k_{EX}/k_{-EX}$.

1.5.3 Exciplex activation energy

Using the following expression from transition state theory,

$$k = \frac{k_B T}{h} \exp\left(-\frac{\Delta G^{\ddagger}}{k_B T}\right) \qquad 58$$

one gets

$$k_Q = \frac{k_B T}{h} \exp\left(-\frac{\Delta G^{\circ}_{EX} + \Delta G^{\ddagger}_{IP}}{k_B T}\right) \qquad 59$$

The activation energy is defined from an Arrhenius analysis as

$$E_a = -k_B \frac{\partial \ln(k_Q)}{\partial(1/T)} \qquad 60$$

and the pre-exponential factor A by

$$k = A\exp\left(-\frac{E_a}{k_B T}\right) \qquad 61$$

So the activation energy for quenching due to the existence of the exciplex is

$$E_a \approx \Delta H_Q^{\ddagger} + k_B T = \Delta H_{EX}^{o} + \Delta H_{IP}^{\ddagger} + k_B T \qquad 62$$

If the exciplex is strongly bound, the exciplex binding enthalpy ΔH_{EX}° may be sufficiently negative to make the overall activation energy negative.[54] That the activation energy may be negative does not depend on the exciplex being stable, only on the fact that the enthalpy of the rate-limiting activated complex be less than that of the starting materials.[55] This is illustrated in Fig. 1.8.

Based on extensive experimental results with ground state electron donor-acceptor complexes, excimers, hetero-excimers, and charge transfer exciplexes Weller[42,56] has developed a correlation between the excited complex energy and the redox properties of the two components. For exciplexes it is then possible to estimate the exciplex enthalpy of reaction (equal to $-B_e$ where B_e is the binding energy of the exciplex) as

$$\Delta H_{EX}^{o} = E_{EX} - h\nu_{0,0} \qquad 63$$

where E_{EX} is the exciplex enthalpy of formation.

Figure 1.8. Reaction enthalpy scheme leading to an experimental negative activation energy.

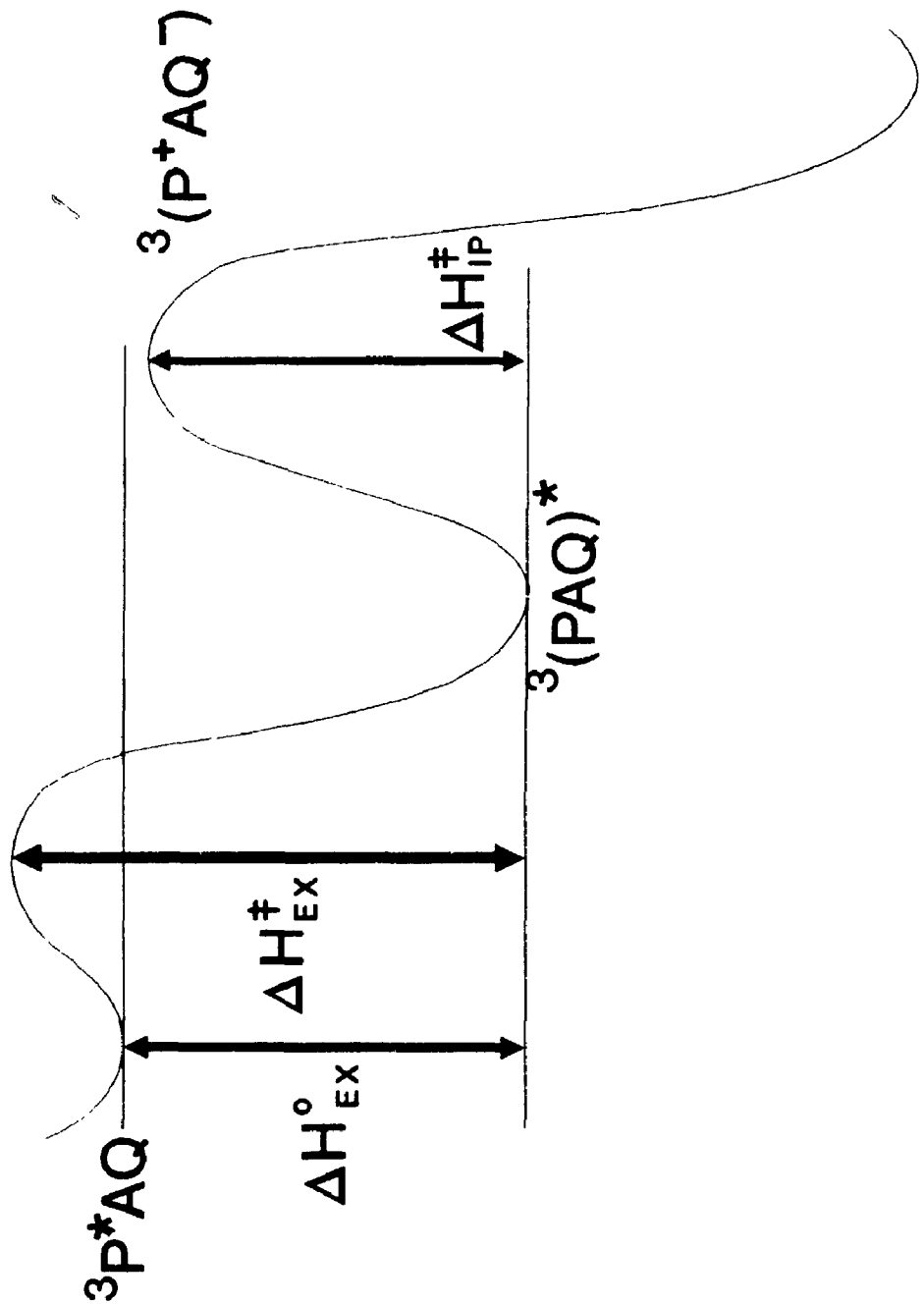
$^3(P^+AQ^-)$
$\Delta H^{\ddagger}_{IP}$
$^3(PAQ)^*$
$\Delta H^{\ddagger}_{EX}$
ΔH°_{EX}
$^3P^*AQ$

For charge transfer exciplexes

$$E_{EX} = e(E^{\circ}_{D^{+}/D} - E^{\circ}_{A/A^{-}}) + (U_{dest} - U_{stab}) - \Delta H^{sol}_{EX} + 0.32\ eV \qquad 64$$

U_{dest} is a destabilization energy of the exciplex due to interaction of the ground states of the two components and is usually nonzero only in complexes which are bound in the ground state. U_{stab} is an energy of stabilization of the exciplex due to interaction of the excited donor-acceptor molecule and the charge transfer state. ΔH_{EX}^{sol} is the enthalpy of solvation of the exciplex.

In triplet exciplexes, U_{stab} is estimated as[42]

$$U_{stab} = \frac{1}{2}\left\{\left((h\nu_{0,0} - E^{\circ}_{CT})^2 + 4\beta^2\right)^{1/2} - (h\nu_{0,0} - E^{\circ}_{CT})\right\} \qquad 65$$

where E°_{CT} is the energy of the unperturbed (i.e., gas phase) charge transfer state

$$E^{\circ}_{CT} = e(E^{\circ}_{D^{+}/D} - E^{\circ}_{A/A^{-}}) + 0.32eV \qquad 66$$

and β is the Hamiltonian matrix element of the interaction between the triplet and ion pair states.

Weller uses the Kirkwood-Onsager dielectric continuum model to calculate the exciplex solvation enthalpy

$$\Delta H^{sol}_{EX} = \frac{\mu^2}{4\pi\varepsilon_0\rho^3}\left(\frac{\varepsilon - 1}{2\varepsilon + 1} - \frac{d\ln\varepsilon}{d\ln T}\frac{3\varepsilon}{(2\varepsilon+1)^2}\right) \qquad 67$$

where μ is the dipole moment of the exciplex, ρ is the equivalent sphere radius, and ε is the static dielectric constant.

In eqns. 64 and 66 the value 0.32 eV has been determined from a plot of measured singlet exciplex formation enthalpies vs the difference in redox energies of the charge transfer components.

1.6 Comparison to photosynthesis

Photosynthesis is the process by which plants, algae, and some bacteria use light energy to synthesize energy-rich carbohydrates. In the chloroplasts of green plants, the light-absorbtion and subsequent electron transfer reactions take place in membrane bound protein complexes.[57] The light is initially absorbed by one of a few hundred 'antenna' chlorophyll and carotenoids which transfer the energy to a reaction center chlorophyll. The excited photosystem II reaction center chlorophyll (labelled P680 for the wavelength of a bleaching due to photoinduced oxidation) transfers an electron to a pheophytin and then to a quinone and further to plastoquinone and a series of other electron acceptors. The positive ion reaction center is in turn reduced by extracting electrons from the oxidation of water to oxygen. Excited photosystem I (labelled P700) similarly transfers an electron to a series of electron acceptors and is reduced by electrons from photosystem II.

In photosynthetic bacteria, the structure of the primary reaction center protein complex has recently been determined by X-ray diffraction.[58,59,60] The light is absorbed by peripheral bacteriochlorophyll or carotenoids and transferred to the

reaction center bacteriochlorophyll dimer. The primary reaction is the electron transfer from this dimer to a bacteriopheophytin, probably via a bacteriochlorophyll monomer, followed by the reduction of a ubiquinone.

Similar series of electron transfers occur in many biological processes in plants, animals and bacteria. There have also been several proposals to use such light-induced electron transfer between donors and acceptors separated by a physical barrier to act as a solar cell.

In photosynthesis the primary electron transfer occurs from the reaction center chlorophyll excited singlet state in picoseconds and the quinone is reduced within nanoseconds. However, if the quinone is already reduced and cannot accept another electron, the chlorophyll may decay directly to the ground state or convert to the triplet state by intersystem crossing. The chlorophyll triplet state may transfer its energy to the triplet ground state of oxygen to produce singlet oxygen which is very reactive and can cause molecular damage.[61] The carotenoids, besides acting as accessory pigments to transfer energy to the reaction center, can accept the triplet energy from chlorophyll and the triplet carotenoid safely decays to its ground state. The carotenoids can also quench singlet oxygen directly.[62,63]

To study the various photophysical aspects of the initial electron transfer in photosynthesis, a variety of electron donors and acceptors have been used with regard to the energies of their excited states and redox potentials. There are several related goals in these studies: 1) to minimize the time to achieve forward electron transfer, while 2) maximizing the duration of the separated charge, and 3) having an

appreciable potential energy incorporated in the separation of charges which may be used to drive other chemical or electrical processes. To this end, several compounds have the driving force $-\Delta G^{\circ}_{ET}$ close to the reorganization energy λ for forward electron transfer so that the activation energy is near zero. For charge recombination, the driving force $-\Delta G^{\circ}_{-ET}$ is desired to be much larger than the reorganization energy so that the system is in the inverted region and electron transfer is much slower.

Rehm and Weller[64] showed that in bimolecular systems the electron transfer rate constant does reach a maximum with increasing driving force, but their study showed that as $-\Delta G^{\circ}$ increased further, the observed electron transfer rate constant remained constant instead of decreasing as indicated by the semiclassical form of the Marcus equation that should be applicable. This discrepancy is believed to arise from the electron transfer rate constant being diffusion limited.

To eliminate diffusion as a factor in experiments, Miller et al.[38] observed the absorbance decay of biphenyl anions (produced by pulse radiolysis) in the presence of various electron acceptors in a frozen glassy matrix of 2-methyltetrahydrofuran. After calculating for the distance dependence of electron transfer to the randomly dispersed acceptors, they found that the electron transfer rate constant at first increased and then decreased as $-\Delta G^{\circ}$ increased. Using biphenyl and similar acceptors linked by a rigid androstane skeleton Miller et al.[65] were the first to see a complete bell-shaped curve in the dependence of $\ln(k_{ET})$ on the driving force in room temperature solution.

Since the above reports, the predicted inverted region behaviour has been observed for charge recombination in other intramolecular systems[35,66,67] and in intermolecular systems (recombination in geminate ion pairs)[68]. All of these reports have been for electron transfer between singlet states. Levin et al.[69] report the complete bell-shaped curve for intersystem charge recombination from geminate triplet radical-ion-pairs.

When the driving force is small, there is the possibility of forming an exciplex. In order for an exciplex (other than pure charge transfer complexes) to exist it is thought that there must be direct orbital overlap (i.e. through space interaction) of the donor and acceptor.[3,70] Such a situation is easily achieved in bimolecular systems, but in intramolecular systems this usually requires a folding of the linkage joining the donor and acceptor. There are some cases of 'exciplex' emission observed in fully extended conformers.[71] However, it is not always clear whether such an exciplex is just a pure charge transfer complex or if there is some direct orbital overlap. Even the term charge transfer is not uniform in the literature, being defined in one report as a state in which electron transfer from the donor to the acceptor is complete[3] and in another report as having an electron shared by both ions.[72]

The aims of this study were to determine if Marcus theory is applicable to the triplet state of PAQ and if so would it be simply a extension of the range of ΔG° already studied for the singlet state of PAQ. There is also the possibility that electron transfer from the triplet state of PAQ may be mediated by the existence of an exciplex.

CHAPTER 2

EXPERIMENTAL

2.1 Sample Preparation

Cuvettes (and some other preparative glassware) were washed in 20% nitric acid and then in 30% ammonia to remove any residual organics. Nitrogen was bubbled through the ammonia in the cuvettes to make sure all acid residue was removed from the corners. After this and for all other glassware, washing consists of soaking in Sparkleen solution, rinsing with distilled water and a final rinse with ethanol before drying in a steam oven.

Distillation of all of the following solvents was carried out while being slowly bubbled with prepurified nitrogen. Benzonitrile (Aldrich HPLC) was distilled twice from phosphorus pentoxide.[73] 1,2-dichloroethane (BDH Omnisolv) was distilled from phosphorus pentoxide. Methylene chloride (BDH Omnisolv) was distilled from phosphorous pentoxide, but this was found to give identical results to undistilled solvent which was used thereafter. Acetonitrile (BDH Omnisolv) was distilled from calcium hydride. Acetone (BDH Omnisolv) was crystallized as $NaI \cdot 3C_3H_6O$ and distilled. 1,1,1-Trichloroethane (BDH Aristar) was used as supplied.

A quantity of lead dioxide was washed several times in methylene chloride and dried under high vacuum for later use.

Imidazole (Aldrich) was twice recrystallized from 3:1 chloroform-hexane and added to the chlorinated hydrocarbon solvents to 0.2 mM to prevent any acid buildup

(Fig. 2.1) during photolysis.[74] Imidazole is an excellent substance for these experiments, being weakly basic and very stable with respect to oxidation and reduction,[75] soluble in polar organic solvents and weakly soluble in nonpolar solvents,[76] and having no noticeable absorbance above 230 nm[77] (the UV cutoff of methylene chloride). The latter is particularly important because there is no interference with the measurement of the quinone peak at 246 nm in methylene chloride. As a test of the inertness in the experiments, a PAQ sample in methylene chloride showed the same fluorescent lifetimes as found by Schmidt et al.[5] who used sodium or potassium carbonate to quench any acidity.

The $PAQH_2$ was synthesized by John Schmidt, a previous graduate student in this lab.[1,2] Thin-layer chromatography (TLC) used nonindicating (zinc-free) silica gel (Machery-Nagel) on plastic sheets. TLC of $PAQH_2$ eluted with 100% methylene chloride and then 2% methanol/methylene chloride showed primarily $PAQH_2$ and some PAQ. PAQ with the same elution showed the same spots with that identified as PAQ being much stronger plus a very weak spot attributed to photodegradation of PAQ.[78]

All samples were handled under reduced lighting because such porphyrin-quinone compounds can be photochemically unstable.[79,80] $PAQH_2$ samples in each solvent were prepared by adding $PAQH_2$ directly to the solvent, pipetting some of this solution into the freeze-pump-thaw cell, adding enough solvent to obtain 0.10 O.D. at the $Q_y(1,0)$ maximum (ca. 516 nm), and then degassing by 4 or 5 freeze-pump-thaw cycles to achieve a vacuum of less than 2×10^{-4} mbar for an estimated O_2

Figure 2.1 The spectra of $PAQH_2$ and PAQ in methylene chloride. Both spectra have been normalized to 0.1 at 516 nm. PAQ has a peak at 246 nm and $PAQH_2$ a peak at 300 nm. The methylene chloride UV cutoff is about 230 nm.

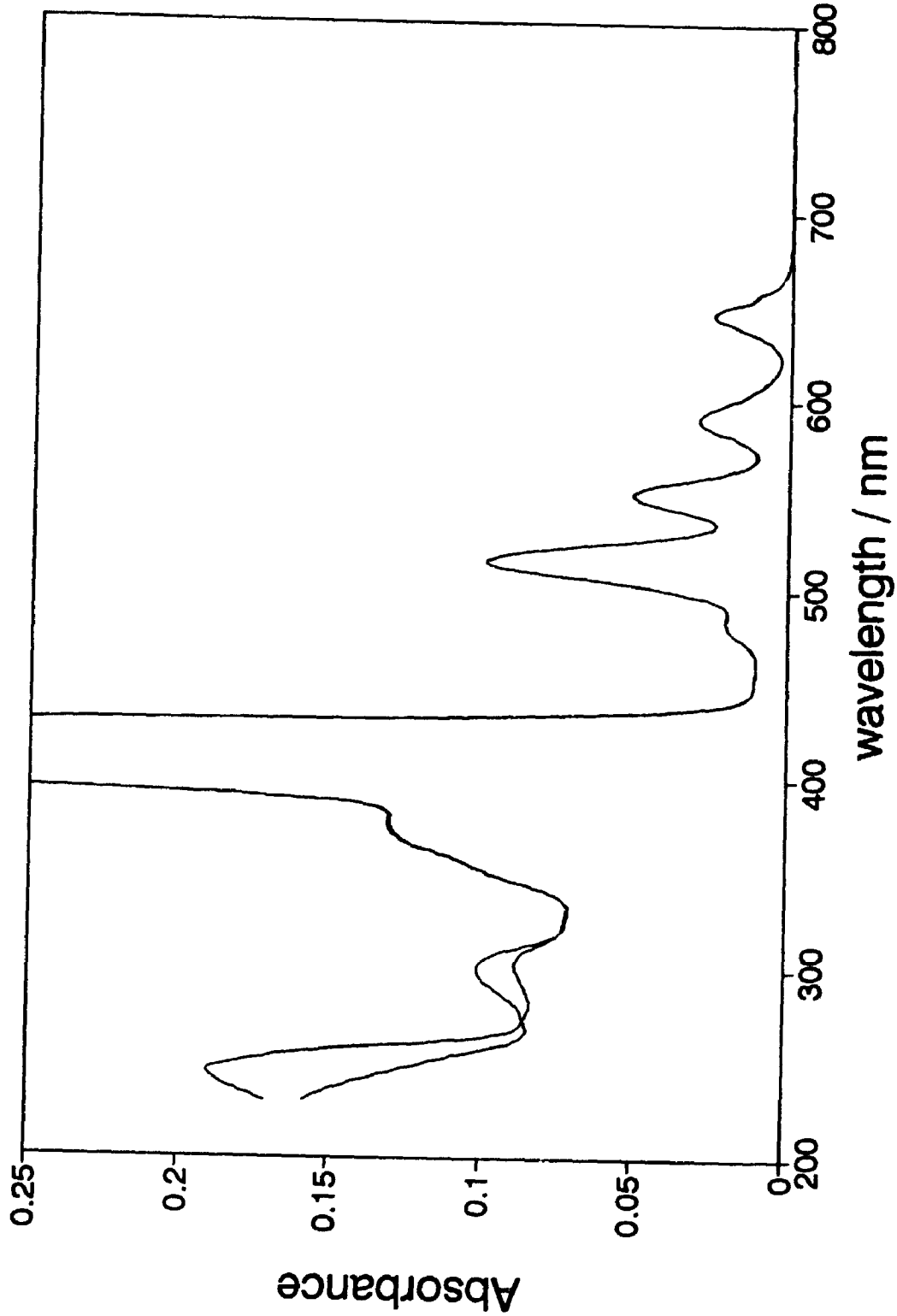
Absorbance
0.25
0.2
0.15
0.1
0.05
0
200
300
400
500
600
700
800
wavelength / nm

concentration of less than 6×10^{-10} M. For $PAQH_2$ in benzonitrile, this gave a first order decay constant about three times smaller than that which could be achieved by 1 to 2 hours bubbling with prepurified nitrogen; there was no significant difference in $PAQH_2$ kinetics from 4, 5, or 6 freeze-pump-thaw cycles. Absorption spectra of the methylene chloride blank, the solvent blank, when the $PAQH_2$ was at final dilution, when the PAQ was freshly oxidized by the lead dioxide, after the freeze-pump-thaw procedure, and after the laser flash photolysis experiments were taken on a HP8450A spectrophotometer and stored on computer. The cuvettes both in the freeze-pump-thaw cell and for preparative work were 1.0 cm quartz SUPRASIL (Hellma).

The results of 1,1,1-trichloroethane, 1,2-dichloroethane, and acetone samples are from preliminary experiments in which the PAQ solutions were degassed by bubbling the sample with prepurified nitrogen (Canox, < 3 ppm oxygen). 4 ml of solution were placed in a long-necked cuvette capped with a rubber septum. The nitrogen entered the solution through a 10 cm 20 gauge hypodermic needle and was allowed out through a 2 cm 24 gauge needle at a rate of 10 ml min^{-1} for at least one hour before the flash photolysis and at 4 ml min^{-1} during the flash photolysis. Although these kinetics were stable over repeated runs in the same day, this technique was abandoned in favour of freeze-pump-thaw for all samples because the more volatile solvents (especially methylene chloride) tended to be carried away with the dry nitrogen gas stream, even if a gas bubbling flask was used as a prebubbler to wet the nitrogen.

The freeze-pump-thaw cell went through several changes ending with the final configuration shown in Fig. 2.2. In this design an Ace 8195-21 stopcock was fitted with a Teflon O-ring as the primary seal, the stopcock barrel is straight, and both the ampule and stopcock arms are tilted up from the cuvette arm. When the cuvette was heated above room temperature, solvent would vaporize and then condense in the cooler arms outside the insulated cell holder and run back into the cuvette. When the cell was first designed these arms were perpendicular to the cuvette arm, allowing a significant amount of solvent to condense in the ampule and in the stopcock bulb, thus concentrating the sample.

PAQ samples were prepared by adding $PAQH_2$ to methylene chloride (containing about 2×10^{-4} M imidazole), adding lead dioxide[80], shaking in a SuperMixer at maximum speed for 5 minutes, and filtering through a glass fibre filter (Millipore AP40) stuffed in a Pasteur pipette. An absorbance ratio of A_{246}/A_{516} of about 2.0 (Fig. 2.1) indicated nearly complete quinone oxidation[2] although as indicated by the TLC and by the fluorescent lifetime data of other workers[5,81] there is usually some residual $PAQH_2$.

For other solvents, some of the PAQ/methylene chloride solution was transferred to a cuvette and the methylene chloride evaporated under a stream of nitrogen. New solvent was then added to redissolve the PAQ. Some of this solution was transferred to the freeze-pump-thaw cell and more solvent added to achieve an absorbance of 0.10 O.D at the $Q_y(1,0)$ maximum. With an extinction coefficient of about 2.0×10^4 $M^{-1}cm^{-1}$, this corresponds to 5×10^{-6} M PAQ or $PAQH_2$ in solution.

Figure 2.2 The freeze-pump-thaw cell.

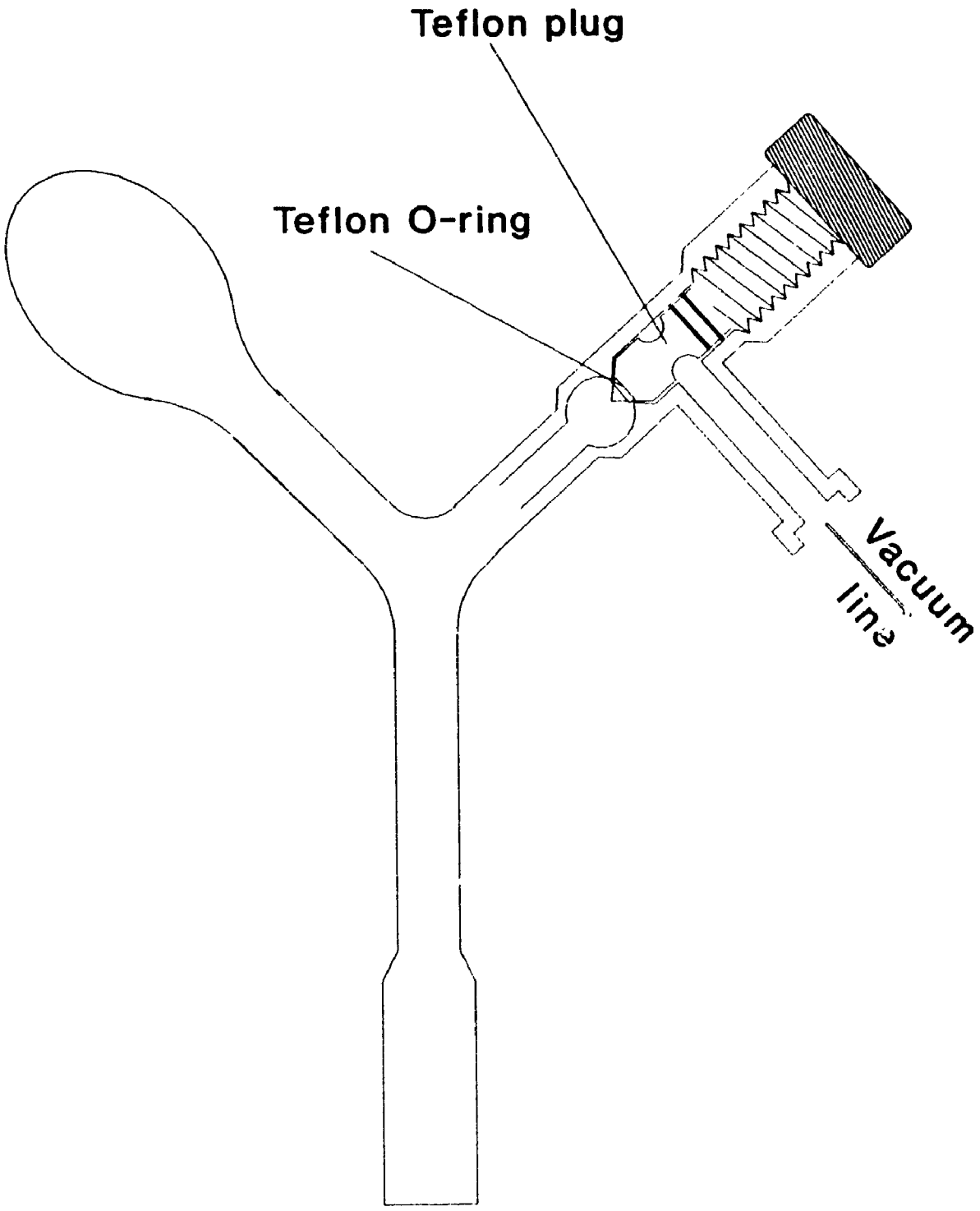
Teflon plug
Teflon O-ring
Vacuum line

2.2 Apparatus

The experimental setup is shown in Fig. 2.3. A PRA International LN1000 N_2 laser (337 nm, pulse width 800 ps) pumps a PRA LN102 dye laser using 1.0×10^{-2} M Coumarin 500 in ethanol (~516 nm) for a pulse duration of 100-700 ps. The dye laser beam is focused and directed through a hole in a mirror and then through a 1.6 mm (1/16") hole in a polished aluminum cone. That part of the laser beam which passes through the cone and then into the sample cuvette constitutes the excitation beam. The monitoring beam from a PTI Model LPS-220 150 W Xe arc lamp operated near 120 W is passed through a Bausch & Lomb 0.25 m monochromator (catalogue number 33-86-40-02) and focused onto the opposite face of the cuvette. The monitoring beam, colinear with the laser beam, exits from the hole in the cone and diverges enough by the time it hits the mirror with the hole that most of it is reflected and then focused onto the entrance slit of a Model 82-415 Jarrell-Ash 0.25 m monochromator.[82]

The purpose of the cone is to reflect to the side (rather than back to the mirror) that portion of the laser beam that lies outside the entrance hole. The cell holder is rotated by about 4° so that any specular reflection of the laser beam off the cell surface misses the mirror. This lengthens the sample path by only 0.2%.

After the excitation beam passes through the sample cell, part of it is reflected from a microscope cover glass slide to a Clairex CL 705HL CdS photoconductivity cell in series with 50 Ω load resistor and a 1.5 V battery. The leading edge of this signal is faster than the digitizer resolution and is used as a stop trigger. The N_2 and

Figure 2.3 Laser flash photolysis apparatus.

PC = photoconductivity circuit; -H.V. = Pacific Photometric Instruments Model 203 negative high voltage power supply; Amp = Comlinear CLC 100 amplifier;

The lenses are Ealing laboratory quality Crown Glass:

L_1 = 36 cm focal length, 5 cm diameter (cat.# 30-8445)

L_2 = 10 cm focal length, 5 cm diameter (cat.# 23-8923)

L_3 = 17.5 cm focal length, 7.5 cm diameter (cat.# 30-8304)

D = iris diaphragm

BS = beam splitter (microscope cover glass slide)

F = Corning glass filter

Let the exit port of the dye laser = 0.0 cm, then the optical components are placed approximately at L_1 13.5 cm, D 18.5 cm, Mirror 24 cm, center of sample cuvette 63.5 cm, BS 72 cm, L_2 84 cm, exit slit of B&L monochromator 100 cm. The Xe lamp front cover is 21 cm from the Bausch & Lomb monochromator entrance slit. From the mirror, the distance to L_3 is 14.5 cm and 40 cm to the Jarrell-Ash monochromator entrance slit. The angle between the monitoring beam before and after it is reflected by the mirror is about 65°.

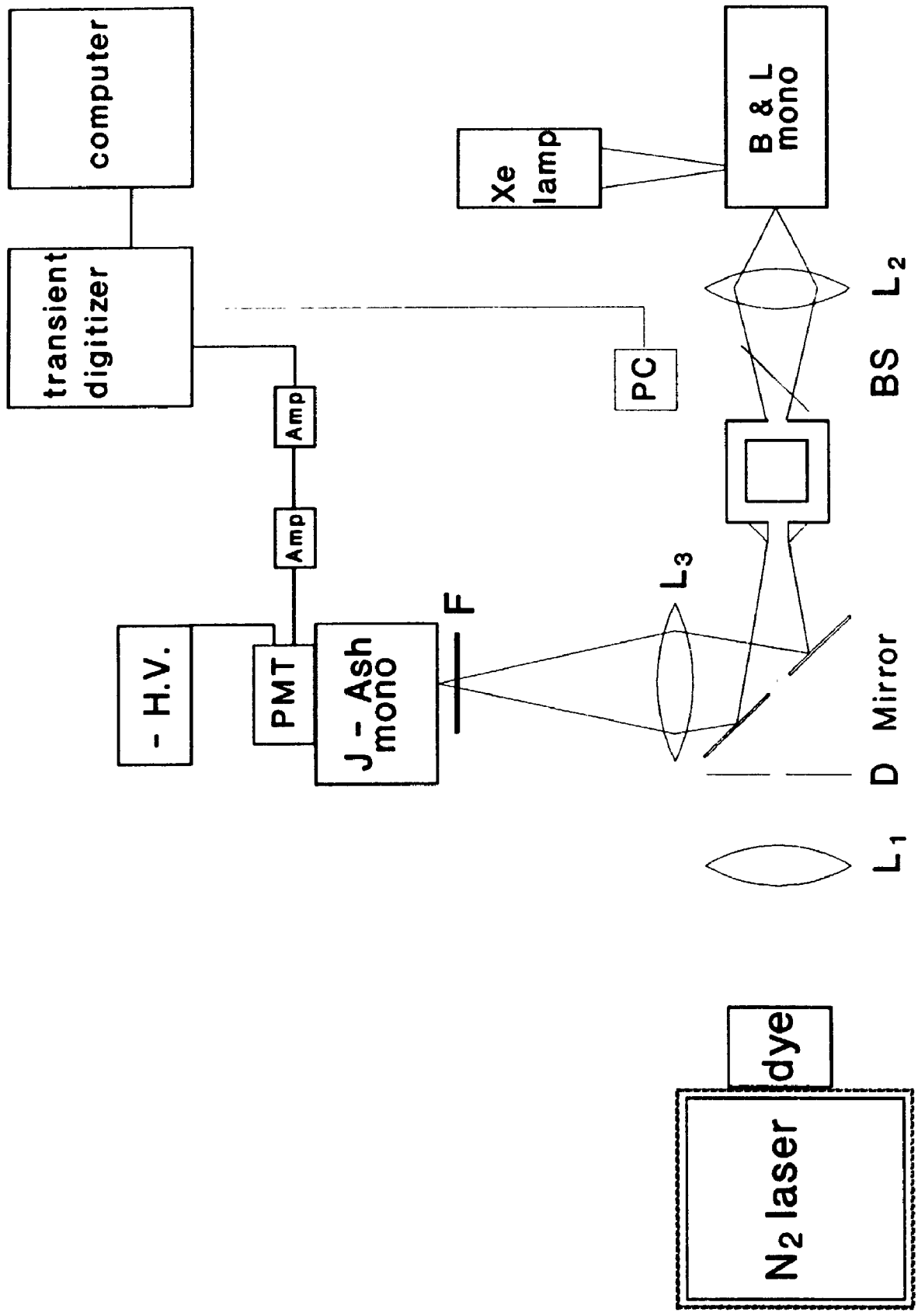
computer
transient digitizer
Amp
Amp
- H.V.
PMT
J - Ash mono
F
PC
Xe lamp
B & L mono
L3
L2
BS
D
Mirror
L1
N2 laser
dye

dye lasers are optimized for energy and stability by monitoring the laser pulse energy with a Molectron J3-02DW Pyroelectric Joulemeter placed where the monitoring beam focusing lens sits. The stop trigger threshold is then set to accept only laser pulses within 5% of the maximum pulse energy. The rejected fraction varies from 1 to 30% depending on how well the laser is tuned. As measured by the Joulemeter when set to run at ~16.8 kV at a 5 Hz pulse rate the N_2 laser output is about 1.1 mJ and the dye laser energy detected after it passes through the empty cell holder is a maximum of 30 μJ.

To reduce the electromagnetic interference from the laser's spark gaps, the laser is enclosed in a Faraday cage with a power line isolator, a beryllium-copper sawtooth gasket (Instrument Specialties, Inc.) on the cage door, and the power line from the isolator is plugged into a surge suppressor that is separate from the one powering the measuring devices. Still, there is a decaying ripple that lasts up to 500 μs. Fortunately, most of this is reproducible in both the transient and light-off signals and is subtracted out in the calculation of the transient absorbance (Fig. 2.4).

The Bausch & Lomb monochromator was used instead of a color filter to restrict the amount and wavelengths of steady light hitting the sample to lessen any degradation of the samples. The Jarrell-Ash monochromator has 0.54 mm slits for a spectral bandwidth of 1.8 nm, sufficient to resolve the porphyrin triplet-triplet spectra.[83] For most experiments, the sample was monitored near 444 nm as this wavelength is near a maximum in the triplet-triplet absorption spectrum (see Fig. 3.1). A Corning CS 7-59 glass filter was placed at the Jarrell-Ash entrance slit

Figure 2.4. Reduction of electromagnetic interference in the signal.

a) A light-on signal showing excessive ripple; b) the corresponding light-off signal with ripple; c) the transient absorbance and fit to the sum of two exponentials of the above signals. Note the reduction in the ripple; d) the residuals of the fit in Fig. 2.4c.

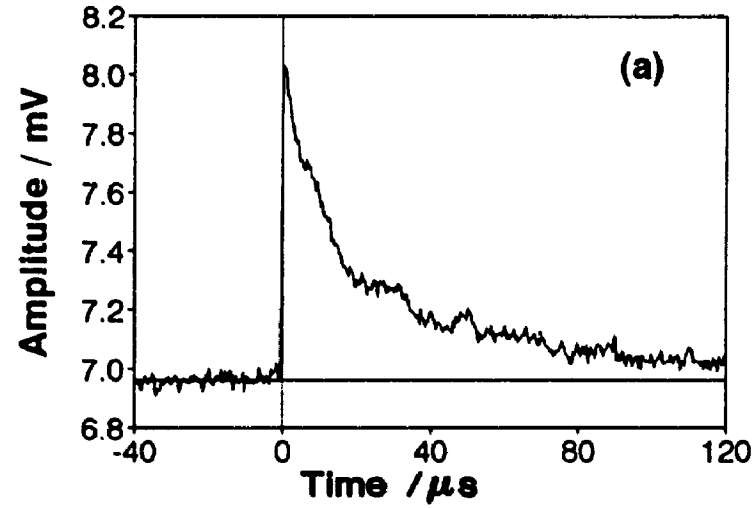
(a)
Amplitude / mV
8.2
8.0
7.8
7.6
7.4
7.2
7.0
6.8
-40
0
40
80
120
Time /μs

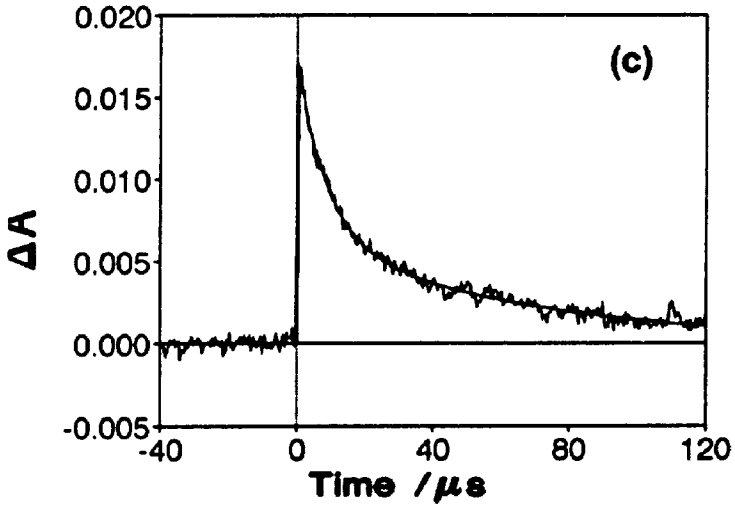
(c)
ΔA
0.020
0.015
0.010
0.005
0.000
-0.005
-40
0
40
80
120
Time /μs

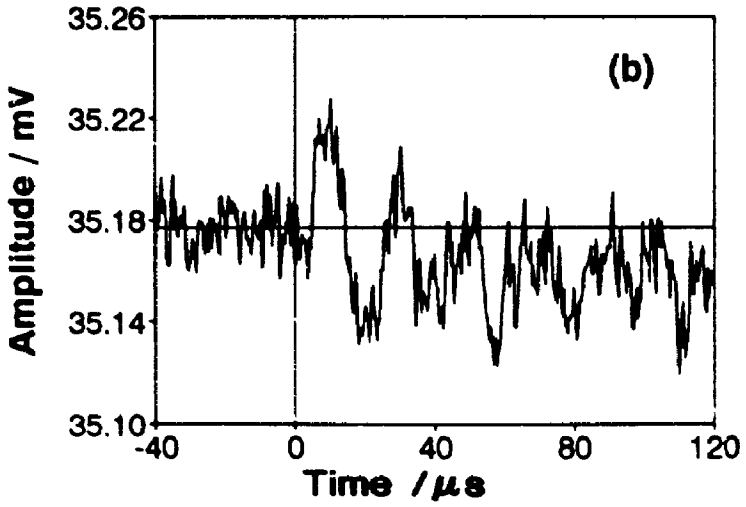
(b)
Amplitude / mV
35.26
35.22
35.18
35.14
35.10
-40
0
40
80
120
Time /μs

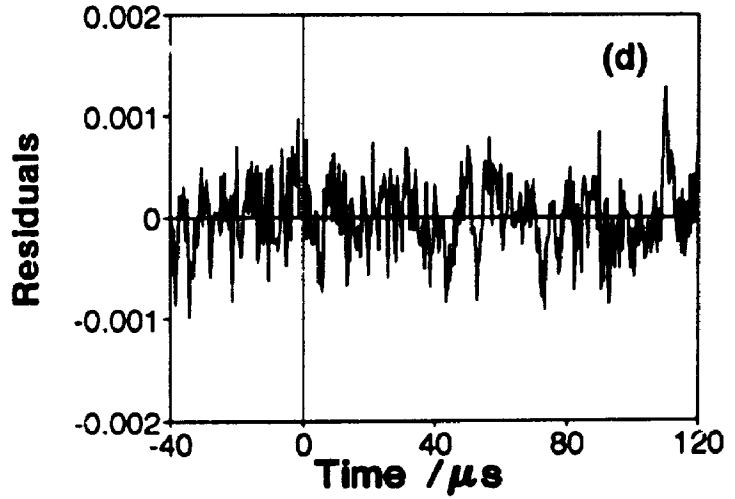
(d)
Residuals
0.002
0.001
0
-0.001
-0.002
-40
0
40
80
120
Time /μs

to help remove scattered dye laser light. Other Corning glass filters were used during the determination of the PAQ and $PAQH_2$ spectra (noted in the captions for Figs. 3.1 and 3.3). The monochromators were calibrated for wavelength by observing the sharp peaks of a 100 W mercury arc lamp at 334, 406, 436, and 546 nm and a He-Ne laser at 633 nm. The Jarrell-Ash monochromator was uniformly off by 2.1 nm and this correction was used for all wavelength data. The Bausch & Lomb monochromator was off by 7 nm at 334 nm to 4 nm at 633 nm. For spectral measurements, the Bausch & Lomb was adjusted first, a blank solvent cell was put into the holder, and the Jarrell-Ash was adjusted to obtain a maximum signal, the wavelength being read then and the sample put in place.

The light exiting from the Jarrell-Ash monochromator hits a Hamamatsu R928 photomultiplier whose signal is amplified by two Comlinear CLC 100 amplifiers (DC to 500 MHz) before reaching a LeCroy TR8828D 200 MHz transient digitizer. The photomultiplier uses a Hamamatsu E715-05 socket (3.3 MΩ dynode chain) and was operated at -400 V with a 50 Ω load resistor. The light-on anode current was kept to one-tenth the dynode chain current. The amplifiers and the transient digitizer all have matching 50 Ω impedances, giving a light-on signal of about 30 mV. Under these conditions the DC signal was found to be linear up to a signal of at least 50 mV. The time base and linearity of the transient digitizer and the two CLC amplifiers were checked with the signal from a Wavetek 114 Function Generator fed in parallel to a Tektronix 2213A 60 Mhz analog oscilloscope and a Nicolet 4094

digital oscilloscope with a Model 4180 200 MHz module. Square-wave and triangular-wave signals were not distorted on any of the digitizer timebases.

The difference between the pretransients of the monitoring light-on and light-off signals is about 30 mV and the peak transient signal is about 6 mV or less (Fig. 2.5). The difference of the pretransient signals $V_o = V_{o,\text{light-off}} - V_{o,\text{light-on}}$ is proportional to the light transmitted I_o by the ground state molecules in solution. The difference of the transient signals $V(t) = V(t)_{\text{light-off}} - V(t)_{\text{light-on}}$ is similarly proportional to the light transmitted I(t) by the mixture of excited and remaining ground state molecules in solution I(t). If I_{inc} is the incident light intensity, then the change in absorbance due to the transient population is

$$\Delta A(t) = A(t) - A_0 = \log\left[\frac{I_{inc}}{I(t)}\right] - \log\left[\frac{I_{inc}}{I_o}\right] = \log\left[\frac{I_o}{I(t)}\right]$$

$$= \log\left[\frac{V_o}{V(t)}\right] \approx \frac{\Delta V(t)}{2.303 V_o} \qquad 69$$

and so I_{inc} need not be measured. The approximation involving $\Delta V(t) = V(t)_{\text{light-on}} - V_{o,\text{light-on}}$ is valid if $\Delta V(t)/V_o << 1$ (the maximum value of $\Delta V(t)/V_o$ in these experiments was about 0.1). This approximation was not used for measurements, but only for a quick estimate of the absorbance change when viewing the Waveform-Catalyst display.

The Soret and Q-band extinction coefficients do not change significantly on oxidation of $PAQH_2$ to PAQ since these bands arise solely from the porphyrin; only

Figure 2.5. The calculation of the transient absorbance.

a) Plot showing the signal averages of light-off and light-on signals received at the transient digitizer input. These are averages of 4000 sweeps each, further averaged by 20 channels per point. b) The transient absorbance and fit to combined first- and second-order kinetics of the above signals.

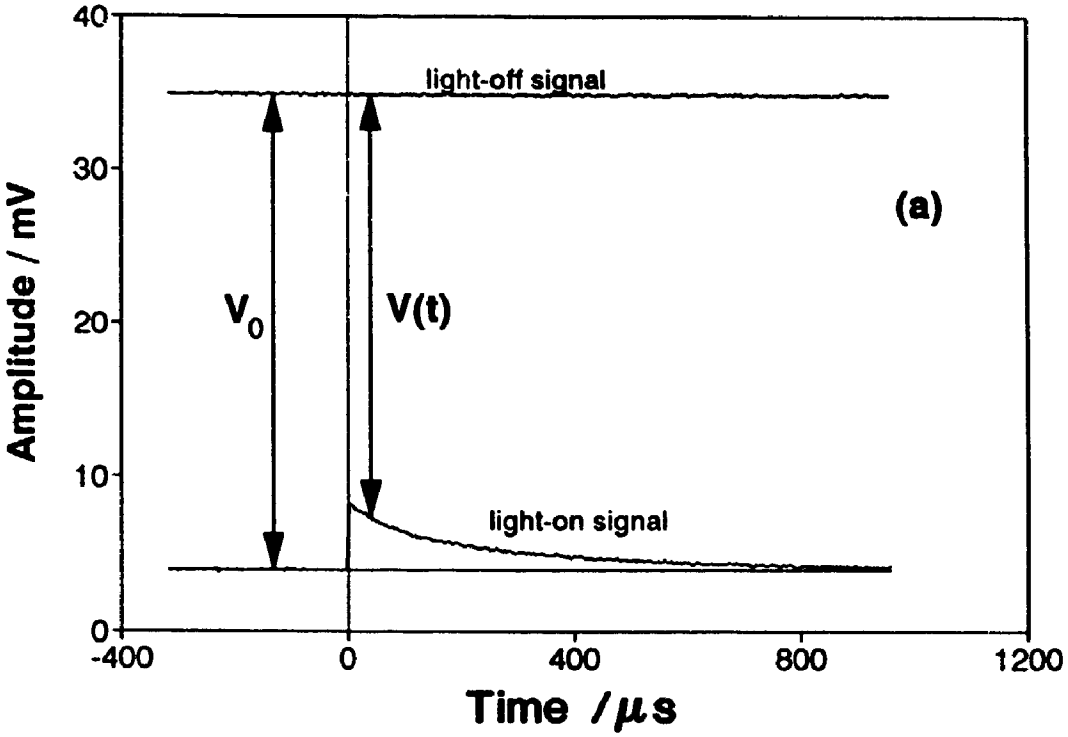
40
30
20
10
0
Amplitude / mV
light-off signal
V_0
V(t)
(a)
light-on signal
-400
0
400
800
1200
Time /μs

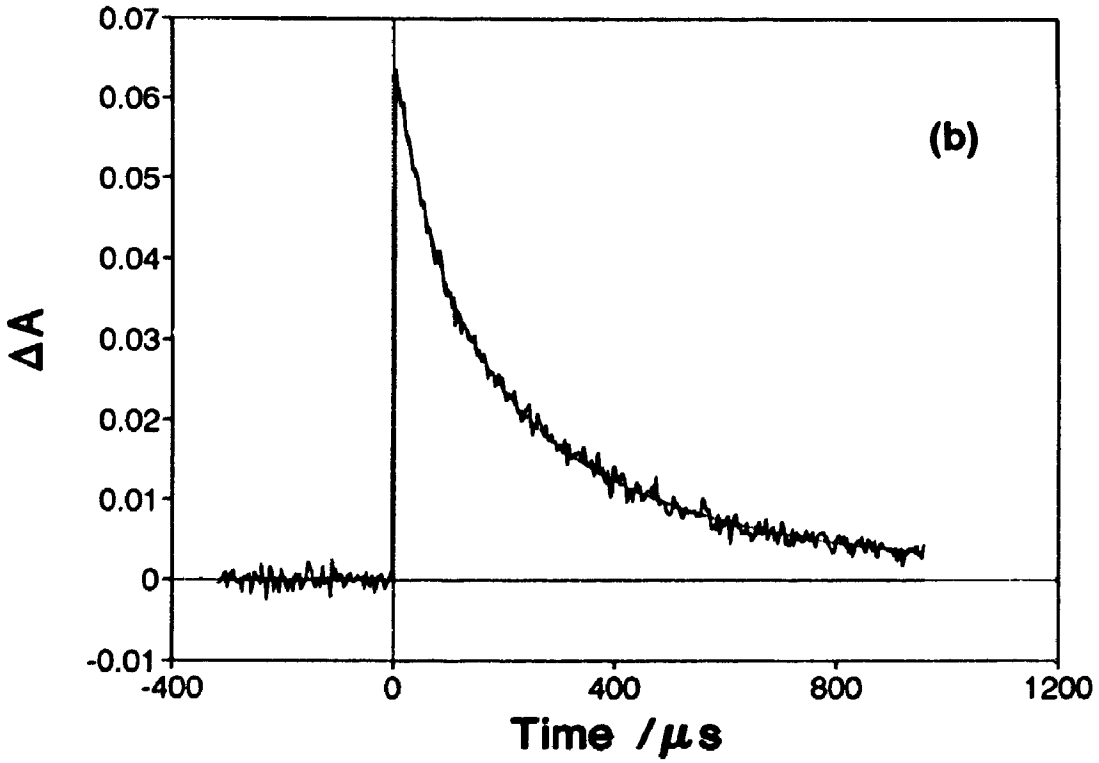
0.07
0.06
0.05
0.04
0.03
0.02
0.01
0
-0.01
ΔA
(b)
-400
0
400
800
1200
Time /μs

the quinone absorbance in the UV changes.[79] Similarly, the triplet-triplet absorption spectrum is expected to arise only from the porphyrin.[2] Thus, it is assumed that any change in absorbance at the monitoring wavelength of 444 nm arises from the ground state porphyrins being excited to the triplet state. Therefore,

$$\Delta A(t) = [\epsilon_T c_T(t) + \epsilon_G c_G(t) - \epsilon_G c_0]\ell \qquad 70$$

where ε_T and ε_G are the extinction coefficients of the porphyrin triplet and ground states, c_T and c_G are the respective concentrations, and c_o is the ground state concentration with no excitation. The excited triplet state eventually decays back to the ground state; there is no spectroscopic evidence of degradation of the sample or of other products. Thus,

$$c_0 = c_T(t) + c_G(t) \qquad 71$$

giving

$$\Delta A(t) = (\varepsilon_T - \varepsilon_G)c_T(t)\ell \qquad 72$$

so that the observed absorbance transients directly reflect the concentrations of the triplet species.

All samples were made up so that the absorbance at the $Q_y(1,0)$ band maxima, 512 - 518 nm, was about 0.10. This was to achieve a compromise between concentrations too high for some fluorescence lifetime measurements and so low that transient absorbance measurements would take too long.

For first- or second-order reactions Boag[84] has calculated the deviation of the rate constant away from a true value due to certain models of variation of the transient concentration along and across the monitoring beam. In the present case such a variation would be due to poor overlap of the excitation laser beam with the monitoring beam or a possible "hot-spot" in the laser beam profile. There is no change in a first-order rate constant due to any change in concentration along the beam. If the absorption of the excitation laser beam causes an exponential decrease of the excited state concentration along the beam path (Fig. 2.6), then it is possible to calculate that the ratio of the apparent second-order rate constant k′ to the true value k would have a maximum at time 0 of

$$\frac{k'}{k} \approx 1 + \frac{(2.3A_{exc})^2}{12} \qquad 73$$

For an excitation O.D. of 0.1 this yields a difference of only 0.4%. For an extreme case of variation across a monitoring beam of rectangular cross section with zero transient absorbance at the sides rising linearly to a value ΔA_0 in the center (Fig. 2.6), Boag calculates for the first-order rate constant,

$$\frac{k'}{k} = 1 - \frac{(2.3A_0)}{12} \qquad 74$$

In this system ΔA_0 never exceeded 0.12, so a first-order rate constant of the transient decay would not be more than 2 % in error. However, an experimental second-order rate constant could have much more severe error, being double the true value for the case where only half the sample in the monitoring beam has been excited.

Figure 2.6. Variation in concentration along and across the monitoring beam path for a hypothetical square cross-section.

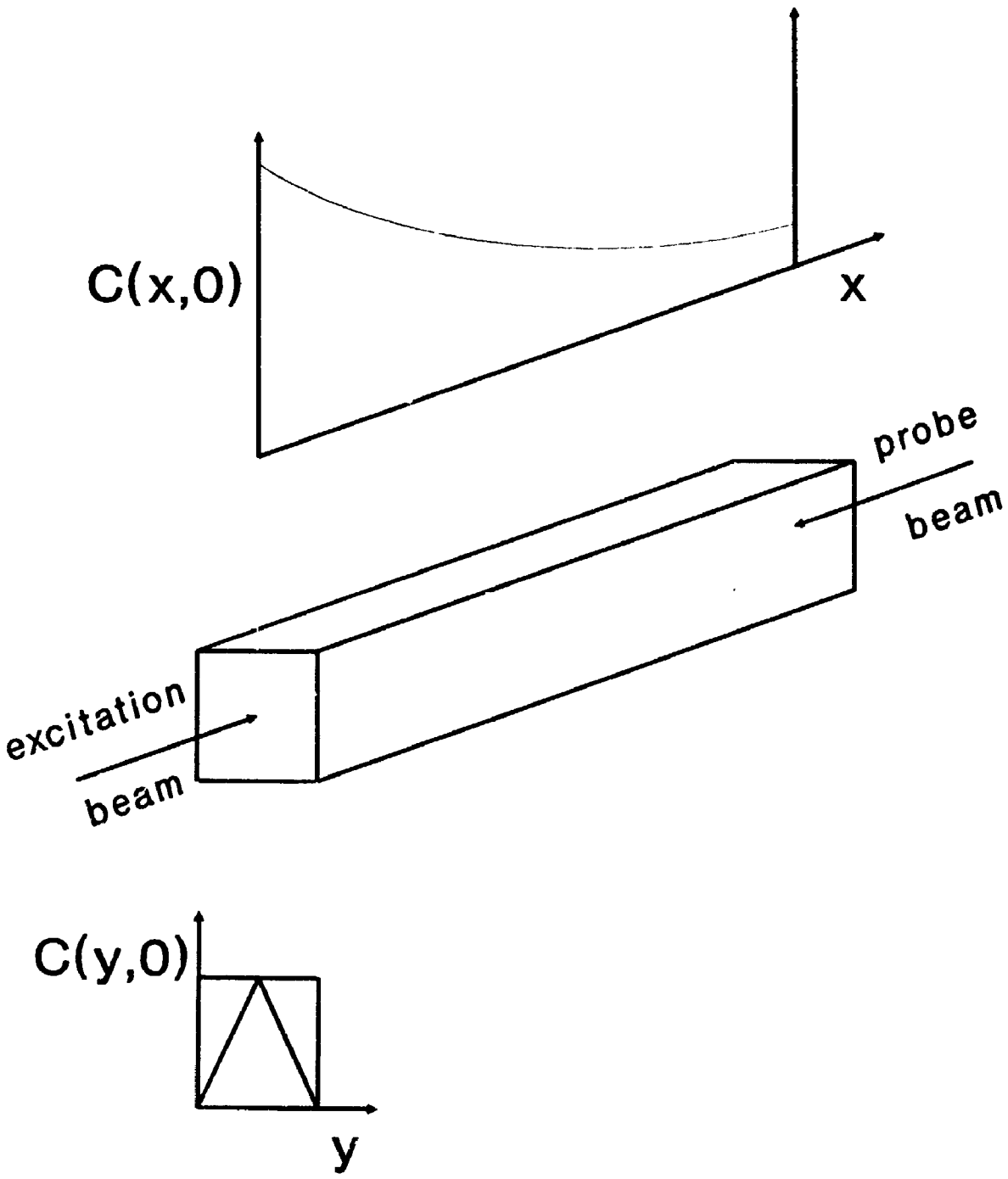
C(x,0)
x
probe
beam
excitation
beam
C(y,0)
y

It is believed that overlap of the monitoring and laser beams was not a problem since the calculated rate constants and initial absorbances did not change when the size of the monitoring beam entrance pinhole was reduced.[82]

Unless otherwise stated, the optical components and positioning pieces in this paragraph were manufactured by Ealing Electro-Optics. The 3 lenses and the cuvette holder are held by vertical and transverse slides mounted on triangular bench carrier bases with locking pinions which moved along a 1 meter cast iron triangular optical bench and a 1/4 meter bench for that portion from the mirror to the Jarrell-Ash monochromator. The beam splitter was glued to a post in a pillar mount. The mirror was made by drilling a 0.6 cm hole in a 6 cm × 6 cm plate of glass and then evaporating several layers of aluminum onto it in an Edwards Model 306 Vacuum Coater. The mirror was glued to the face of a Oriel 17500 2" adjustable mirror mount with elastomer springs which was mounted on a carrier base with transverse slide only.

The optical components were initially aligned by directing the dye laser beam along the triangular bench at a constant height and then moving lenses into position so that this beam was undeviated. To align the Bausch & Lomb monochromator a He-Ne laser beam was sent into the entrance slit and the monochromator was manoeuvred until the He-Ne beam was colinear with the dye laser beam. After this the Xe arc lamp was shone into the Bausch & Lomb monochromator and the light beam focused by lens L_2 onto the pinhole and through a cuvette filled with a solvent. The light exiting the cone was reflected by the mirror to lens L_3 and through the

Jarrell-Ash monochromator to the photomultiplier tube. All optical components were then adjusted to give a maximum signal as displayed on the Tektronix analog oscilloscope.

The cuvette holder is an aluminum block (3.5 cm × 4 cm × 8 cm) with a copper tube wrapped around it to act as a heat exchanger. The entire block is covered with 3 to 5 cm of foam rubber for insulation (except holes for the light beams and the cuvette top). A 1:1 ethylene glycol:water mixture was pumped through the copper tube via insulated plastic tubing to a heat exchange coil in a thick walled plastic dewar or plastic pail. Dewar temperatures colder than room temperature were maintained with ice water or cold tap water, while hotter temperatures were maintained by an immersion heater in the plastic pail.

The temperature of the outside of the cell was monitored by an unshielded YSI 44202 thermistor probe (manufacturer's specifications: ± 0.15°C over range -5 to 45°C; operational range -80 to 120°C Yellow Springs Instrument Co. Inc.) attached to a digital readout. Two probes of this type matched a thermometer within 1.0°C over the range -5 to 50°C; they were then compared to each other when one was placed in water in a long-necked cuvette and the other below the cuvette and on top of a layer of foam plastic in the bottom of the cuvette holder. As long as the first probe was inside the body of the cuvette the readings agreed within 0.5°C. The probe under the cuvette was used for all temperature measurements.

In those experiments where the temperature was varied the cell holder and cell were first brought to the highest or the lowest temperature and maintained there

while several signals were taken. The dewar temperature was then changed by about 10° and the cell and holder reached this new temperature in about fifteen minutes. A further five minutes were allowed to be certain of the cell temperature stability which was kept within one-half a degree. These experiments were done in order of both increasing and decreasing temperature to ensure that there was not some deterioration due to the high temperatures.

Under the control of the LeCroy data acquisition software, Waveform Catalyst 3.03, the digitizer is set to average the signals, 250 to 16,000 sweeps per run, with the monitoring light unblocked and a second run with the light blocked. These two signals are stored on the computer hard disk in files of 8160 data channels each. A computer program written in GAUSS 2.0[85] CAT8WCBK (Appendix A) takes the light-on signal, and looks for the starting channel of the transient. It finds the laser spike or initial transient by calculating the noise as the standard deviation of the pretransient data channels, then finding the first channel that is six standard deviations away from the pretransient, and finally finding the first channel that is more than 70 % of this difference. If the data has a very low signal-to-noise and the transient start position cannot be found by this method it is set to an average value determined from many other signals. Taking this channel to be time zero, 20 channels are averaged into one data point giving 100 pre-transient and 300 transient points. The light-off signal is similarly averaged using the same start channel. The transient absorbance change is calculated and stored on disk.

A second program CATGRDBK calculates a best fit to the integrated forms of single or double exponential, second-order or combined first- and second-order decay. The non-linear least squares convergence to a fit follows the Marquardt algorithm[86] and uses analytical gradients of the above decay functions. Noise for the fit results is recalculated as the standard deviation of 100 pretrigger points. Because the ΔA is so small, the noise does not vary over the range of ΔA and is used as a constant weighting term in the analysis. Within the fitting procedure MARQCALC the rate constants are in units of μs^{-1} so that the gradient moment matrices are not singular due to ill-conditioning.

The reduced chi-square is calculated as[86]

$$\chi_\nu^2 = \frac{1}{N-\nu-1}\sum_{i=1}^{N}\frac{1}{\sigma_i^2}[y_i - y(x_i)]^2 \qquad 75$$

where N is the number of data points, ν is the number of parameters to be fit, σ_i is the noise associated with the i^{th} data point, y_i is the data, $y(x_i)$ is the fit to the data, and the sum is over transient points only. If the data has a normal random distribution about the fitted function, and the discrepancy is entirely due to the inherent noise in the data as described by σ_i, then the reduced chi-square should approach 1.0 in the limit of an infinite sample size. If χ_ν^2 is significantly different from 1.0 but the plot of the residuals (a plot of $y_i - y(x_i)$ vs. x_i) appears random, then the σ_i are not a good representation of the real noise in the data. If the residuals

show a trend away from being random, then the fitted function is not a good approximation of the true relationship between x and y.

For all fitting schemes the initial guesses were made based on a subset of the data. The first transient point less than or equal to zero and subsequent points were excluded. A linear least squares fit of the natural logarithm of this non-zero transient data vs time gave the initial guess for the single-exponential fit. A linear least squares fit of the inverse of this transient data vs time gave the initial guess for the second-order fit. For the double-exponential fit, the transient subset was divided into quarters. A fit to the last quarter gave the initial guess for the slow rate constant. This fit was extrapolated and subtracted from the first quarter of the data which was then fit to give the initial guess for the fast rate constant. Also, various multiples of the results of the single exponential fit rate constant were tried. The fits of these different trials were compared and that with the lowest chi-squared value was chosen as the best double-exponential fit. The initial guess for the competing first- and second-order fit used the results of the single-exponential fit for ΔA_0 and k_1' and let k_2' equal zero.[87]

In many cases, the best fit kinetic scheme could not be decided on the basis of the reduced chi-square, since two or more schemes had values near 1.0; however, only one of these schemes would have consistent and reproducible trends in experiments when repeated on different days. An example of an unambiguous fit is shown in Fig. 2.7 in which only a two exponential decay is an adequate match to the data. In those solvents where k_{ET} was the slowest (e.g., acetonitrile), a two

Figure 2.7. A comparison of two fitting schemes with a significant difference between the two. The signal is the average of 4000 traces of $\Delta A(t)$ of ^3PAQ in methylene chloride at 5°C. (a) The data and the two fits. (b) The residuals to a two exponential decay. $\chi^2_\nu = 0.84$, $a_f = 0.00592(26)$, $k_f = 2.95(19) \times 10^5\ s^{-1}$, $a_s = 0.00402(6)$, $k_s = 9.84(22) \times 10^3\ s^{-1}$. (c) The residuals to a competing first- and second-order decay. $\chi^2_\nu = 1.87$, $\Delta A_0 = 0.00713(17)$, $k_1' = -8.5(12) \times 10^3\ s^{-1}$, $k_2' = 9.06(50) \times 10^6\ s^{-1}$, $\Delta A_0 k_2' = 6.46(46) \times 10^4\ s^{-1}$. (single exponential fit $\chi^2_\nu = 3.60$, second-order fit $\chi^2_\nu = 2.12$)

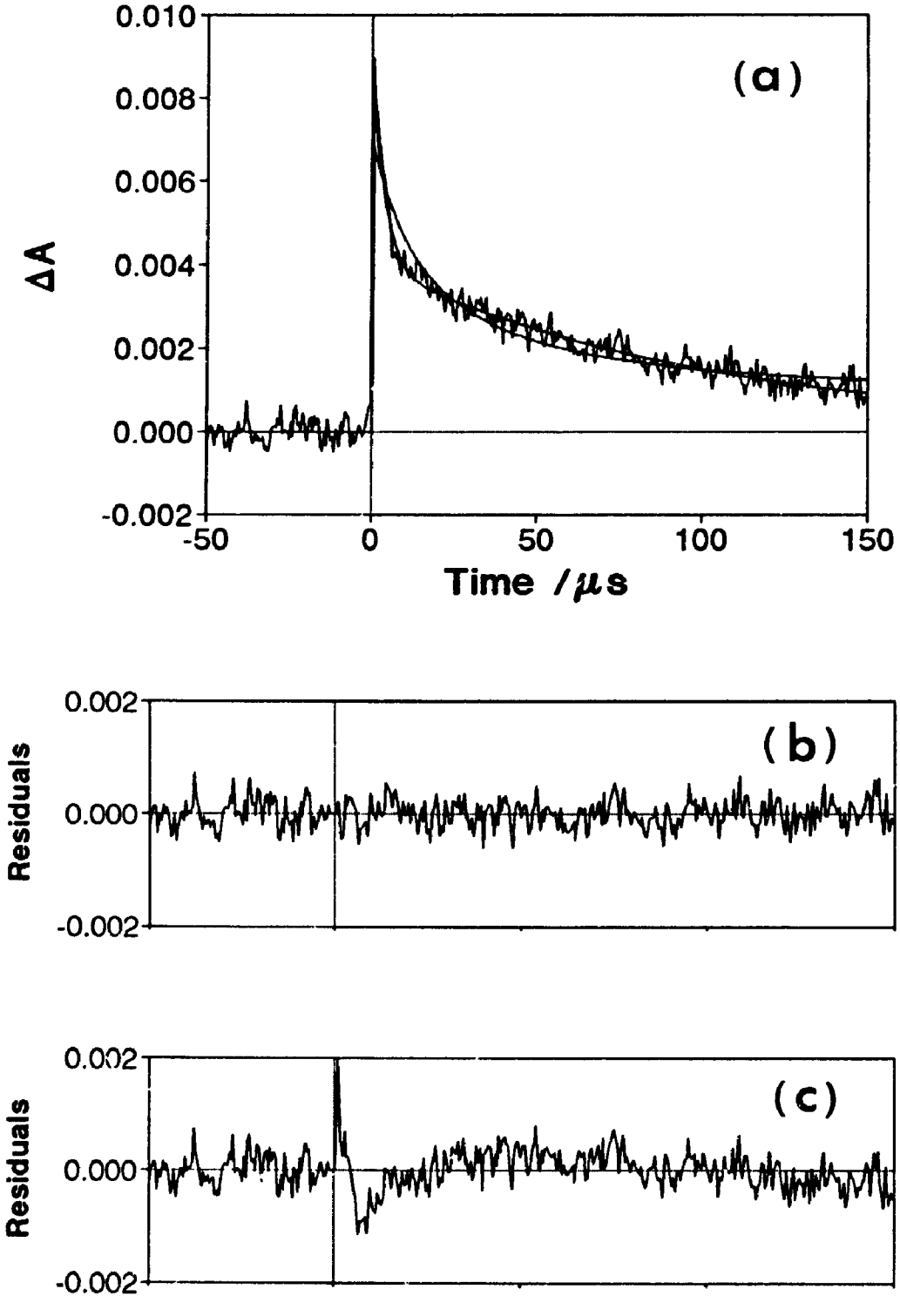
0.010
0.008
0.006
0.004
0.002
0.000
-0.002
ΔA
(a)
-50
0
50
100
150
Time /μs
0.002
0.000
-0.002
Residuals
(b)
0.002
0.000
-0.002
Residuals
(c)

exponential decay was not immediately obvious from the signal trace (Figs. 2.8 and 2.9). In the former plot the residuals indicate that a two exponential decay is the better fit, while in the latter, the residuals do not show a significant preference between the two exponential fit and the competing first- and second-order fit.

The single-exponential, second-order and competing first- and second-order fits always would converge to give some parameters even if they were inadequate (such as the best fit being double-exponential). However, the double exponential fit would sometimes yield an inadequate fit - most often converging too slowly, or trapped in a local minimum. It was possible to run another program with user-input initial guesses of parameters to see if a better fit would result.

Simulation studies were done by producing a 6000 channel decay curve and then adding normally distributed random noise to the signal and then running this through the fitting programs. The most difficult resolution was for a two exponential fit with the fast component at a fraction $a_f/(a_f+a_s) < 0.25$, the fast rate constant ten times value of the slow rate constant, with the fast component lifetime equal to 200 channels, and the signal-to-noise at a level of 1.0. The program resolved the parameters to within 20% in one-half of the trials. Therefore, all signals (with the exception of small signals during the taking of difference spectra) were accumulated until the Waveform-Catalyst display showed an averaged per channel signal-to-noise of more than 3.

The $^3PAQH_2$ transients are best described by combined first- and second-order kinetics according to the following mechanism[83,87,88]

Figure 2.8. A comparison of two fits that are not easily distinguished. The signal is the average of 1000 traces of $\Delta A(t)$ of ^3PAQ in acetonitrile at 5°C. (a) The data and the two fits. (b) The residuals to a two exponential decay. $\chi^2_\nu = 1.22$, $a_f = 0.02678(60)$, $k_f = 1.18(34) \times 10^4\ s^{-1}$, $a_s = 0.00250(66)$, $k_s = 0.228(56) \times 10^4\ s^{-1}$. (c) The residuals to a competing first- and second-order decay. $\chi^2_\nu = 1.64$, $\Delta A_0 = 0.03037(26)$, $k_1' = 6.81(18) \times 10^3\ s^{-1}$, $k_2' = 2.30(15) \times 10^5\ s^{-1}$, $\Delta A_0 k_2' = 6.99(52) \times 10^3\ s^{-1}$. (single exponential fit $\chi^2_\nu = 2.65$, second-order fit $\chi^2_\nu = 13.5$)

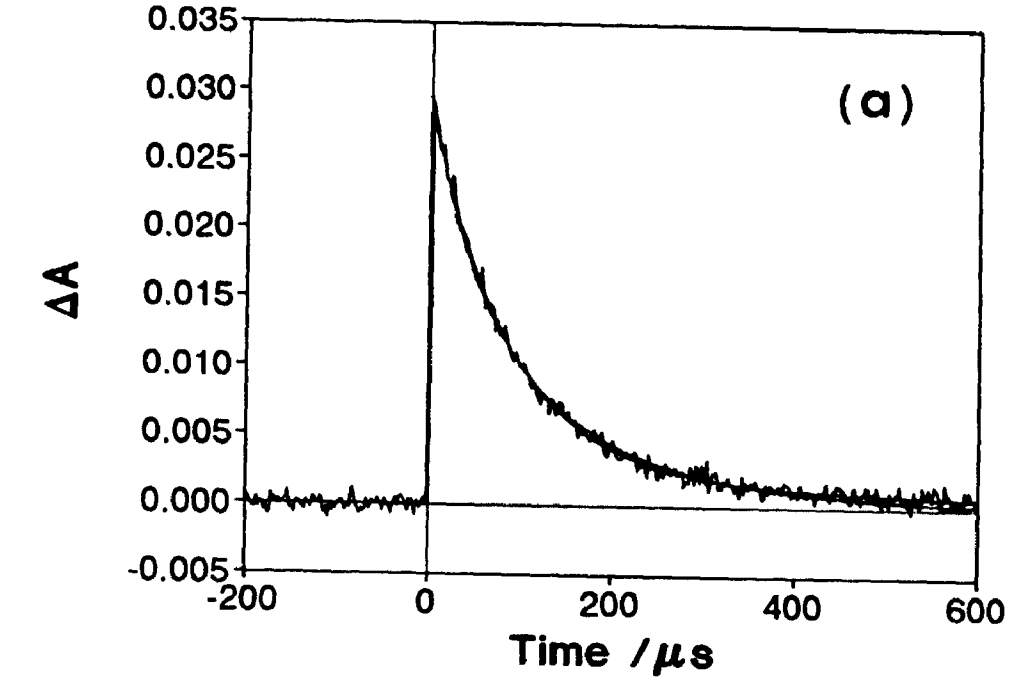
0.035
0.030
0.025
0.020
0.015
0.010
0.005
0.000
-0.005
ΔA
(a)
-200
0
200
400
600
Time /μs

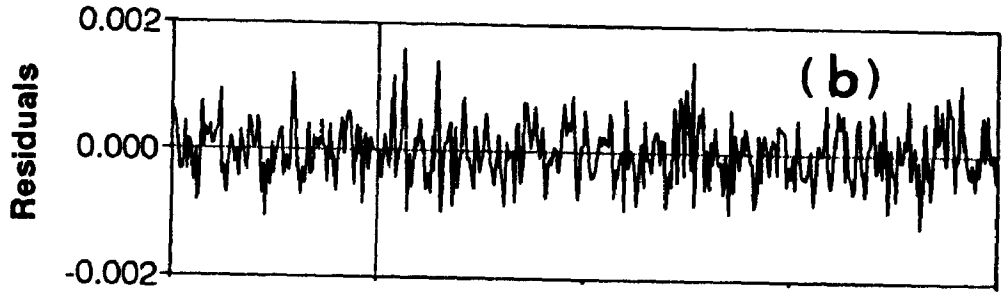
0.002
0.000
-0.002
Residuals
(b)

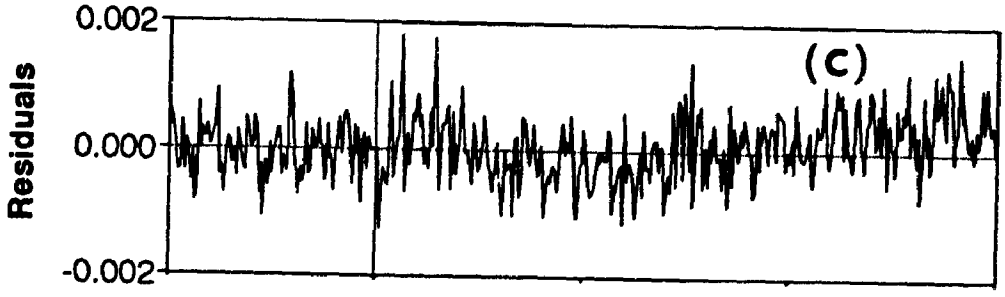
0.002
0.000
-0.002
Residuals
(c)

Figure 2.9. A comparison of two fits that do not show a difference. The signal is the average of 1000 traces of $\Delta A(t)$ of ^3PAQ in acetonitrile at 5°C. (a) The data and the two fits. (b) The residuals to a two exponential decay. $\chi^2_\nu = 0.93$, $a_f = 0.0141(26)$, $k_f = 1.07(11) \times 10^4\ s^{-1}$, $a_s = 0.0072(26)$, $k_s = 0.430(68) \times 10^4\ s^{-1}$. (c) The residuals to a competing first- and second-order decay. $\chi^2_\nu = 0.95$, $\Delta A_0 = 0.02168(18)$, $k_1' = 5.44(15) \times 10^3\ s^{-1}$, $k_2' = 1.97(17) \times 10^5\ s^{-1}$, $\Delta A_0 k_2' = 4.26(38) \times 10^3\ s^{-1}$. (single exponential fit $\chi^2_\nu = 1.35$, second-order fit $\chi^2_\nu = 6.8$)

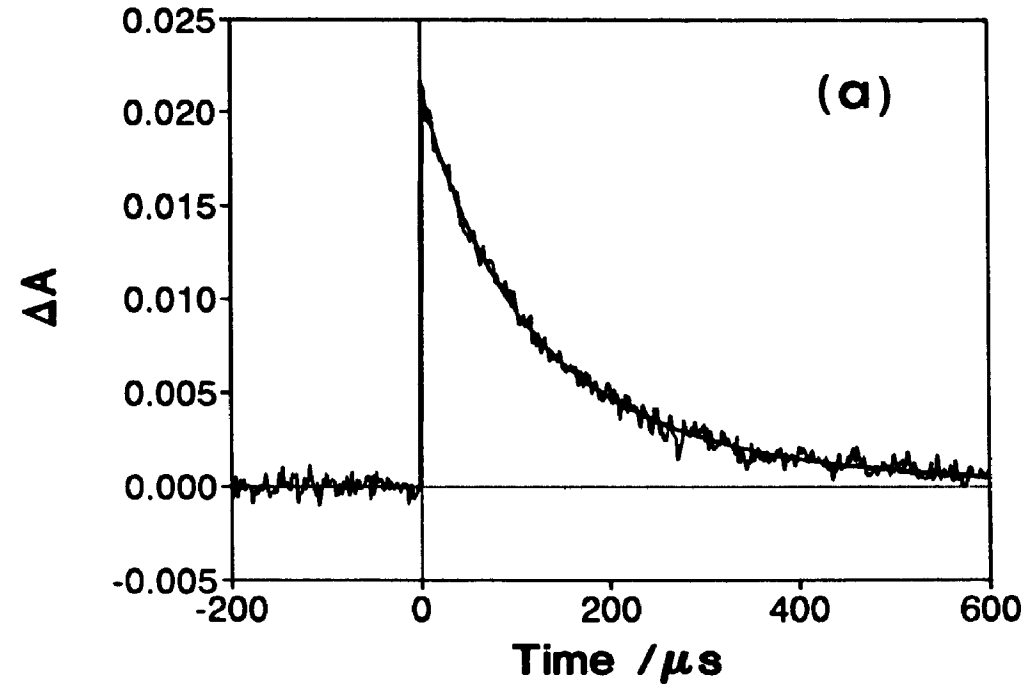
0.025
0.020
0.015
0.010
0.005
0.000
-0.005
ΔA
(a)
-200
0
200
400
600
Time /μs

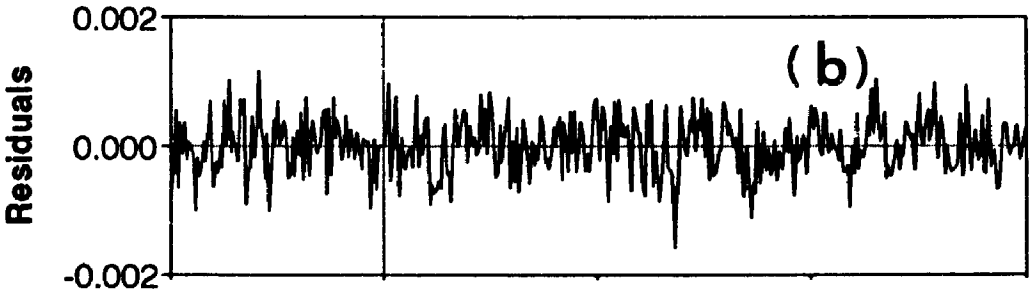
0.002
0.000
-0.002
Residuals
(b)

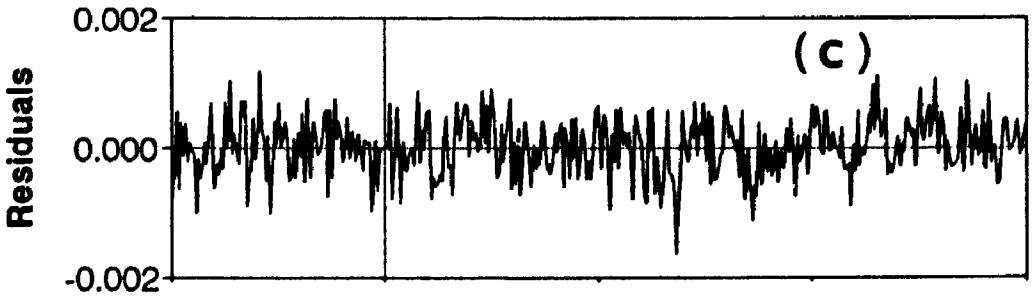
0.002
0.000
-0.002
Residuals
(c)

$$T_1 \xrightarrow{k_1} S_o$$

$$T_1 + T_1 \xrightarrow{k_2} 2S_o$$

$$T_1 + S_o \xrightarrow{k_3} 2S_o$$

$$T_1 + M_i \xrightarrow{k_{4i}} S_o + M_i$$

76

where T_1 represents a lowest triplet state, S_o the ground state, and M_i any of a variety of quenching impurities. In the triplet-triplet quenching step above, k_2 is the rate constant for the disappearance of triplets. Statistically, the excited intermediate in this step would have a probability of 1/9 of being an excited singlet, 3/9 of being an excited triplet, and 5/9 of being an excited quintet. The excited quintet is the lowest energy state of the set[10] and thus cannot undergo internal conversion and intersystem crossing is a spin-forbidden process. Thus, it must revert back to two triplets on dissociation of the triplet collision dimer. If the doubly excited intermediate is a triplet, then rapid internal conversion to a singly excited triplet occurs, and dissociation to a triplet and a ground state molecule follows. Similarly, internal conversion and dissociation reduces the excited singlet intermediate to an excited singlet and a ground state molecule. Thus, of 9 collisions involving 18 triplets, only 5 triplets are quenched. This does not take into account the quantum yield of intersystem crossing of the excited singlet molecule which has a probability of ϕ_{ISC} for recreating one of the triplets that was lost in the interaction. Thus the actual number of quenched triplets is 5 - ϕ_{ISC}.

The rate law for decay becomes

$$-\frac{dc_T}{dt} = k_1 c_T + k_2 c_T^2 + k_3 c_T c_G + \sum_i k_{qi} M_i c_T \qquad 77$$

with eqns. 71 and 72

$$-\frac{d\Delta A}{dt} = (k_1 + k_3 c_0 + \sum_i k_{qi} M_i)\Delta A + \frac{(k_2 - k_3)}{(\varepsilon_T - \varepsilon_G)}\Delta A^2 \qquad 78$$

$$= k_1'\Delta A + k_2'\Delta A^2 \qquad 79$$

where

$$k_1' = k_1 + k_3 c_0 + \sum_i k_{qi} M_i \qquad 80$$

and

$$k_2' = \frac{(k_2 - k_3)}{(\varepsilon_T - \varepsilon_G)} \qquad 81$$

which yields the integrated form

$$\Delta A(t) = \left[\left(\frac{1}{\Delta A_0} + \frac{k_2'}{k_1'}\right)\exp(k_1' t) - \frac{k_2'}{k_1'}\right]^{-1} \qquad 82$$

where ΔA_0 is the value of ΔA at $t = 0$.

The ^{3}PAQ transient decay fits best to the sum of two first-order decays

$$\Delta A(t) = a_f \exp(-k_f t) + a_s \exp(-k_s t) \qquad 83$$

where the fast component is attributed to ^3PAQ and the slow one to unoxidized $^3PAQH_2$. ^3PAQ has an extra decay mechanism available

$$PAQ \xrightarrow{k_{ET}} P^{\cdot+}AQ^{\cdot-} \qquad 84$$

which makes the overall first order rate constant

$$k_f = k_1 + k_3c_0 + \sum_i k_{4i}M_i + k_{ET} \qquad 85$$

When the absorbing species is in low concentration, the electron transfer rate constant is usually large enough to deplete the triplet population in a much faster time than any significant decay due to triplet-triplet quenching. The latter rate is then neglected in the above approximation (eqn. 83).

From eqns. 80 and 85 k_{ET} can be evaluated as the difference of the fast rate constant from the PAQ decay, k_f, and the first-order rate constant from the $PAQH_2$ decay, k_1'.

$$k_{ET} = k_f - k_1' \qquad 86$$

The slower rate constant, k_s, was not very useful for quantitative comparison to k_f because it either had such a small contribution to the ^3PAQ decay (indeed, it was desired to produce as much oxidized form via lead dioxide as possible) that it was difficult to reproduce or it was of the same size as the term $\Delta A_0 k_2'$, the dominant term in the $PAQH_2$ decays. Compared to an upper limit for k_1' of 150 s^{-1} for

tetraphenylporphine (TPP) in pyridine[88] the data indicates considerable quenching by impurities in the samples. To test whether treatment with lead dioxide added any extra quenching impurities, a comparison was made of tetratolylporphyrin (TTP) plus imidazole in methylene chloride without and with lead dioxide treatment. The latter did not show any significant increase in the decay rate.

Since it was suspected that some residual $PAQH_2$ contaminated the PAQ samples, a determination of both components in the sample was attempted. Because ^3PAQ and $^3PAQH_2$ can quench each other via triplet-triplet annihilation and both can also be quenched by either ground state, a coupled system was considered. Let $Q = \Delta A_{PAQ}$ and $H = \Delta A_{PAQH}$. Then with the same rate constants defined above and c_0 in k_1' now equal to the pre-excitation ground state concentration of PAQ and $PAQH_2$

$$-\frac{dH}{dt} = k_1'H + k_2'QH + k_2'H^2 \qquad 87$$

$$-\frac{dQ}{dt} = (k_1' + k_{ET})Q + k_2'QH + k_2'Q^2 \qquad 88$$

These are then added together to be fit to the data since the extinction coefficients of the two components are equal.

$$-\frac{d(Q+H)}{dt} = k_1'(Q+H) + k_2'(Q+H)^2 + k_{ET}Q \qquad 89$$

This system had to be solved by numeric generation of the curves for every increment in the Marquardt procedure. Whereas the procedure MARQCALC (Appendix A) was able to solve a two exponential fit in at most 20 seconds (up to 20 iterations with 5 curves per iteration), a program written for the coupled system following the Bulirsch-Stoer method[89] took 5 minutes just to generate the first curve in the first iteration, so this approach was abandoned. With the noise level present in the data, the latter method might have just led to overdetermination of the system since for PAQ samples a four parameter fit already gave chi-square values near one.

CHAPTER 3

SPECTRAL RESULTS AND ANALYSIS OF THE MARCUS MODEL

3.1 Spectral Results

The decay kinetics of a solution of $PAQH_2$ in methylene chloride were observed at various wavelengths from 355 to 460 nm. The results of fitting these decays to the integrated form of combined first- and second-order kinetics are shown in Table 3.1 and the plot of ΔA_o vs. wavelength is given in Fig. 3.1. If only one transient species is present, both k_1' and $\Delta A_o k_2'$ should be independent of the wavelength. This is seen to be the case in Table 3.1.

A calculation of the initial triplet state concentration $[T]_0$ (eqn. 72) and the value of k_2 - k_3 (eqn. 81) shows a discrepancy between the regions under the Soret band and those to the blue and red of it (Table 3.2). This may be attributed to assuming (incorrectly) that the triplet-triplet absorption spectrum of TPP[24] is identical to that of $PAQH_2$. As seen by a comparison of the Q bands of TPP in toluene[24] vs $PAQH_2$ in benzonitrile[4] such an assumption is not valid; although the positions of peaks and troughs in the difference spectrum are in agreement, their amplitudes are not. To achieve a better match of these amplitudes, the $PAQH_2$ triplet-triplet extinction coefficient to the red of the Soret band would have to be larger than that of TPP, decreasing the value of $[T]_0$. A more accurate estimate of $[T]_0$ is found from the Soret region where ground state depletion dominates the absorbance change and the magnitude of ε_T is less important. In the region 398 to 414 nm $\varepsilon_G \gg \varepsilon_T$; the

Table 3.1. Analysis of the $^3PAQH_2$ decay in methylene chloride at various wavelengths[a]

λ[b] /nm	χ_v^2[c]	ΔA_0[d]	k_1'[e] /10^3 s^{-1}	k_2'[f] /10^5 s^{-1}	$\Delta A_0 k_2'$[g] /10^3 s^{-1}
355.5	0.78	0.0178	1.83	3.11	5.54
360.5	1.16	0.0153	1.83	2.97	4.52
364.5	0.71	0.0159	2.01	3.10	4.92
368.6	1.19	0.0178	1.58	3.45	6.15
373.6	1.11	0.0188	1.93	2.47	4.65
378.0	1.05	0.0196	1.81	2.85	5.60
383.0	1.03	0.0192	1.59	2.85	5.48
388.5	0.74	0.0134	1.47	4.28(53)	5.74(85)
393.0	1.34	-0.0046	4.1(11)	-0.9(51)	0.4(24)
397.8	1.02	-0.0325	2.11(12)	-1.59(10)	5.18(37)
403.2	1.20	-0.0545	1.93(8)	-1.22(4)	6.64(29)
408.3	1.13	-0.1191	2.32	-0.365	4.35
414.0	1.28	-0.2711	1.98	-0.167	4.53
419.7	0.72	-0.3975	2.12	-0.110	4.38
424.3	1.30	-0.1721	2.29	-0.277	4.77
429.0	0.91	-0.0243	2.80(35)	-7.65(57)	18.6(18)
433.9	1.37	0.0362	1.99(15)	0.94(10)	3.41(41)
438.8	0.88	0.0555	1.65	0.89	4.96
443.0	1.04	0.0661	1.73	0.87	5.74
443.8	1.04	0.0656	1.51	0.95	6.24
445.0	1.10	0.0619	1.59	0.92	5.71
447.8	1.38	0.0662	1.71	0.90	5.97

459.8	0.84	0.0627	1.64	0.99	6.19
450.5	0.95	0.0565	1.64	0.98	5.53
452.5	1.02	0.0538	1.57	1.07	5.76
455.0	1.11	0.0481	1.58	1.14	5.47
457.0	1.24	0.0529	1.72	1.13	5.99
459.5	1.03	0.0429	1.57	1.33	5.70

a Experiment carried out at 296 K. All fits are to a competing first- and second-order reaction. ΔA_0, k_1', and k_2' are defined by eqns. 80 to 82.

All errors are one standard deviation. Where indicated by parentheses, errors have the units of the least significant digit of the accompanying value, otherwise they are given below.

b A Corning CS 7-59 filter was used except under the Soret peak, 408.3 to 424.3 nm where no filter was in front of the Jarrell-Ash monochromator.

c Reduced chi-square for the fit.[86]

d Error = ± 0.0005

e Error = ± 0.20×10^3 s^{-1} in the region 355.5 to 388.5 nm

± 0.05×10^3 s^{-1} in the region 408.3 to 459.5 nm

f Error = ± 0.30×10^5 s^{-1} in the region 355.5 to 383.0 nm

± 0.005×10^5 s^{-1} in the region 408.3 to 424.3 nm

± 0.03×10^5 s^{-1} in the region 438.8 to 459.5 nm

g Error = ± 0.7×10^3 s^{-1} in the region 355.5 to 383.0 nm

± 0.09×10^3 s^{-1} in the region 408.3 to 424.3 nm

± 0.16×10^3 s^{-1} in the region 438.8 to 459.5 nm

Figure 3.1. The difference spectrum of $^3PAQH_2$ in methylene chloride.

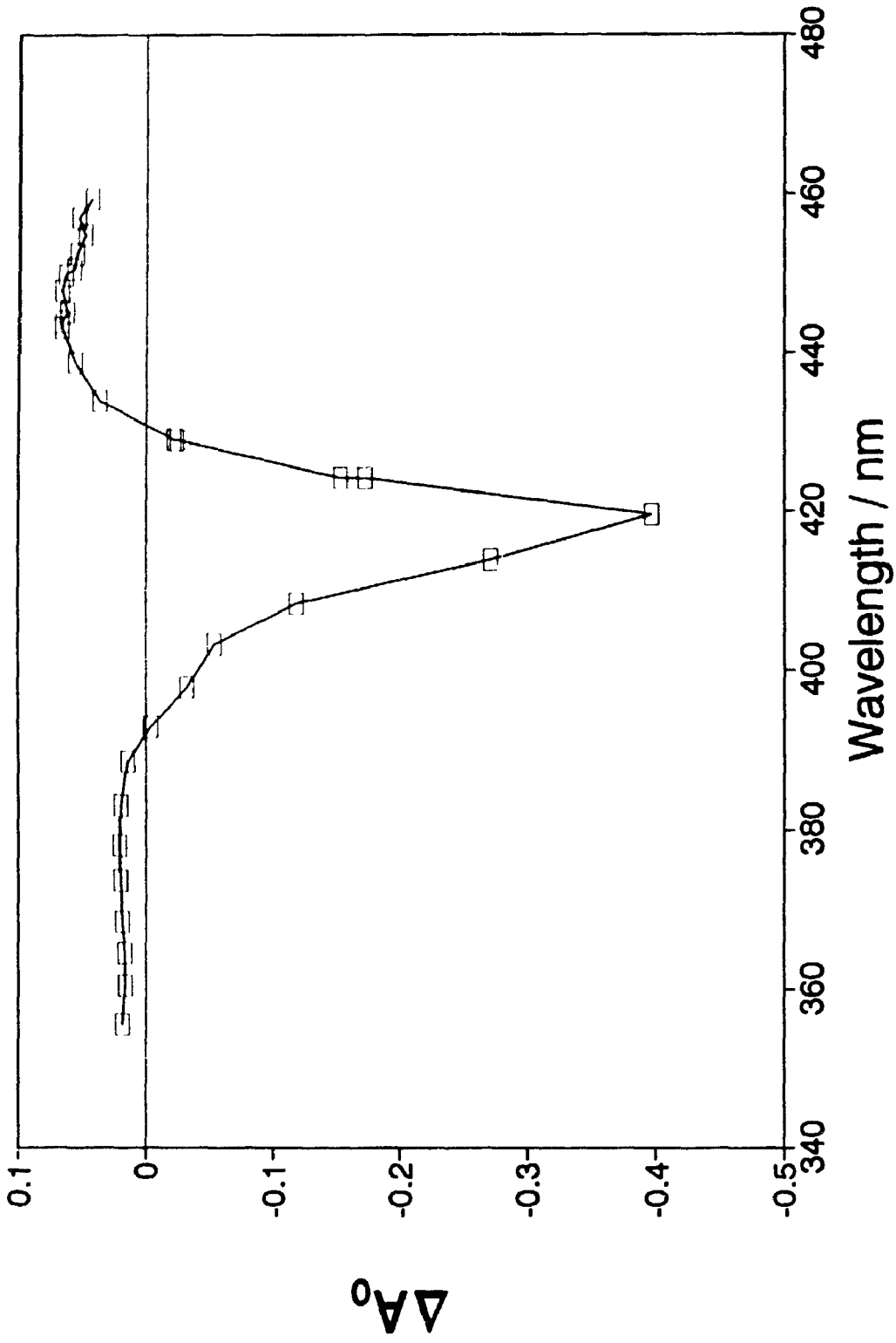
ΔA0
0.1
0
-0.1
-0.2
-0.3
-0.4
-0.5
340
360
380
400
420
440
460
480
Wavelength / nm

Table 3.2. Estimated values of the initial $^3PAQH_2$ concentration and the triplet-triplet annihilation rate constant k_2 in methylene chloride.

λ[a] /nm	Abs[b]	ε_G[c] /10^4 $M^{-1}cm^{-1}$	ε_T[d]	ΔA_0[a]	$[T]_0$[e] /μM	k_2'[a] /10^5 s^{-1}	k_2[f] /10^9 $M^{-1}s^{-1}$
355.5	0.0948	2.22	3.3	0.0178	1.7	3.1	3.3
360.5	0.1028	2.41	3.3	0.0153	1.7	3.0	2.6
364.5	0.1107	2.60	3.4	0.0159	2.0	3.2	2.5
368.6	0.1166	2.74	3.5	0.0178	2.3	3.5	2.6
373.6	0.1207	2.83	3.8	0.0188	1.9	2.5	2.3
378.0	0.1227	2.88	4.0	0.0196	1.7	2.9	3.2
383.0	0.1247	2.93	4.1	0.0194	1.6	2.8	3.3
388.5	0.1429	3.35	4.2	0.0134	1.6	4.3	3.6(12)
393.0	0.2023	4.75	4.0	-0.0046	0.6	-0.93	0.6(35)
397.8	0.3260	7.65	3.8	-0.0325	0.84	-1.59	6.1
403.2	0.4687	11.00	3.3	-0.0545	0.71	-1.22	9.3
408.3	0.7200	16.89	3.3	-0.1191	0.88	-0.36	4.9
414.0	1.6155	37.90	3.3	-0.2711	0.78	-0.167	5.7
419.7	1.9880	46.64	3.3	-0.3975	0.92	-0.110	4.7
429.0	0.4150	9.74	8.3	-0.0243	1.7	-7.7	10.9(34)
433.9	0.1410	3.31	7.9	0.0362	0.79	0.94	4.3(5)
438.8	0.0595	1.40	6.7	0.0555	1.05	0.89	4.7
443.0	0.0357	0.84	6.4	0.0659	1.18	0.87	4.8
443.8	0.0328	0.77	6.3	0.0656	1.19	0.95	5.2

445.0	0.0295	0.69	6.1	0.0619	1.14	0.92	4.9
447.8	0.0238	0.56	5.6	0.0662	1.31	0.90	4.5
449.8	0.0213	0.50	5.2	0.0627	1.33	0.99	4.6
450.5	0.0205	0.48	5.2	0.0565	1.20	0.98	4.6
452.5	0.0187	0.44	5.0	0.0539	1.18	1.07	4.8
455.0	0.0168	0.39	4.7	0.0481	1.12	1.14	4.8
457.0	0.0156	0.37	4.5	0.0529	1.28	1.13	4.6
459.5	0.0145	0.34	4.2	0.0429	1.11	1.33	5.1

a Data from Table 3.1.

b Ground state absorbance of $PAQH_2$ in methylene chloride, ± 0.15%.[90]

c Calculated from $\varepsilon(PAQH_2)_{max,418} = 4.90 \times 10^5 \pm 4\%$[91]

d Estimated from the extinction coefficients of TPP in toluene,[24] error ± 0.2

e $[^3PAQH_2]_0 = \Delta A_0/(\varepsilon_T - \varepsilon_G)\ell$

Error = ± 0.45 μM for the region 355.5 to 393.0 nm and 429.0 nm;

± 0.050 μM for the region 397.8 to 459.5 nm.

f $k_2 = k_2'(\varepsilon_T - \varepsilon_G)\ell + k_3$. $k_3 = 5 \times 10^7\ M^{-1}s^{-1}$ [24]

Error = ± $0.7 \times 10^9\ M^{-1}s^{-1}$ for the region 355.5 to 403.2 nm,

± $0.3 \times 10^9\ M^{-1}s^{-1}$ for the region 408.3 to 459.5 nm.

average estimate of $[T]_0$ is 0.78 ± 0.02 μM. This agrees with 0.79 ± 0.05 μM calculated from the absorbed excitation, assuming negligible scattering of light[92]

$$\langle [T]_0 \rangle = \phi_{ISC} 2.303 \varepsilon_G c_G \frac{\langle N_p \rangle}{A N_A} = \phi_{ISC} 2.303 \frac{A_\lambda}{\ell} \frac{\langle N_p \rangle}{A N_A} \qquad 90$$

Here ϕ_{ISC} is the quantum yield for intersystem crossing (0.67±0.02)[4,93], ε_G is the extinction coefficient at the exciting wavelength (513 nm), A_λ is the ground state absorbance at the exciting wavelength (usually set to 0.10 O.D.), A is the beam cross sectional area determined by the cone (2.0 mm^2), N_A is Avogadro's constant, and $\langle N_p \rangle$ is the average number of photons in the excitation beam assuming that the excitation beam loses intensity in accordance with Beer's Law[92]

$$N_p(x) = N_p^\circ 10^{-\varepsilon_g c_0 x} = \frac{E\lambda}{hc} \exp(-\ln 10 \varepsilon_g c_0 x) \qquad 91$$

so that

$$\langle N_p \rangle = N_p^\circ \frac{1}{\ell} \int_0^\ell \exp(-\ln 10 \varepsilon_g c_0 x) = \frac{E\lambda}{hc} \frac{[1 - \exp(-2.303 A_\lambda)]}{2.303 A_\lambda} \qquad 92$$

where E is the pulse energy of 30 μJ ± 5% and the ground state absorbance is *ca.* 0.088.

Using $k_3 = 5 \times 10^7$ $M^{-1}s^{-1}$, the value for TPP in toluene, yields a triplet-triplet annihilation rate constant k_2 of about 7×10^9 $M^{-1}s^{-1}$. This is multiplied by a factor of $9/(5-\phi_{ISC})$ (see page 81 and reference 94) to give 15×10^9 $M^{-1}s^{-1}$ which can be

compared to the diffusion controlled rate constant. The latter is calculated from the Debye equation[17]

$$k_{DIFF} = \frac{8RT}{3\eta} \qquad 93$$

where η is the viscosity. In methylene chloride at 25°C η = 0.41 mN s m^{-2}, giving $k_{DIFF} = 16 \times 10^9\ M^{-1}s^{-1}$.

The kinetic fit parameters for PAQ in methylene chloride at three different wavelengths in the Soret region are shown in Table 3.3. A fit to two exponentials gives consistent values of the rate constants. A fit to competing first- and second-order kinetics yields inconsistent values of k_1' but consistent values of $\Delta A_0 k_2'$, although the latter is much larger and dominates the decay. Also, a fit to competing first- and second-order kinetics yields a minimum value of k_2 of $2.8 \times 10^{11}\ M^{-1}s^{-1}$ (Table 3.4), much larger than the diffusion controlled limit.

The quantum yields for intersystem crossing in PAQ and $PAQH_2$ in a given solvent are

$$\Phi_{ISC,PAQ} = \frac{k_{ISC}}{k_{ISC} + k_F + k_{IC} + k_{ET}} = k_{ISC}\tau_{F,PAQ} \qquad 94$$

and

$$\Phi_{ISC,PAQH_2} = \frac{k_{ISC}}{k_{ISC} + k_F + k_{IC}} = k_{ISC}\tau_{F,PAQH_2} \qquad 95$$

giving the ratio

$$\frac{\Phi_{ISC,PAQ}}{\Phi_{ISC,PAQH_2}} = \frac{\tau_{F,PAQ}}{\tau_{F,PAQH_2}} \qquad 96$$

Table 3.3. Fit parameters in the analysis of the ^{3}PAQ decay in methylene chloride at various wavelengths[a]

Two exponential fit[b]

λ /nm	χ^2_ν	a_f	k_f /10^4 s^{-1}	a_s	k_s /10^4 s^{-1}
407.7	1.35	-0.01070(17)	12.9(4)	-0.00715(15)	1.52(4)
420.5	1.20	-0.04809(76)	12.2(4)	-0.02766(71)	1.54(4)
444.3	1.13	0.01082(17)	11.4(4)	0.00643(16)	1.49(4)

Competing first- and second-order fit

λ /nm	χ^2_ν	ΔA_0	k'_1 /10^4 s^{-1}	k'_2 /10^6 s^{-1}	$\Delta A_0 k'_2$ /10^4 s^{-1}
407.7	1.35	-0.01791(15)	.02(5)	-5.19(10)	9.31(24)
420.5	1.05	-0.07777(63)	.16(5)	-1.30(2)	10.14(24)
444.3	1.13	0.01767(14)	.20(5)	5.25(9)	9.28(23)

a Experiment carried out at 296 K.

b a_f, k_f, a_s, k_s are defined by eqn. 83

c ΔA_0, k'_1, and k'_2 are defined by eqns. 80 to 82.

Table 3.4. Estimated values of the initial ^{3}PAQ concentration in methylene chloride as derived from the fit parameters shown in Table 3.3

				2 exponential fit		Competing first- and second-order			
λ[a] /nm	Abs[b]	ε_G[c] /10^4 $M^{-1}cm^{-1}$	ε_T[d]	a_f[a]	$[^3PAQ]_0$[e] /μM	ΔA_0[a]	$[^3PAQH]_0$[f] /μM	k_2'[a] /10^6 s^{-1}	k_2[g] /10^9 $M^{-1}s$
407.7	0.7280	17.08	3.3	-0.0104	0.076(4)	-0.0175	0.127(7)	-5.19	712(40)
420.5	1.9630	46.06	3.3	-0.0481	0.112(5)	-0.0778	0.182(8)	-1.30	557(26)
444.3	0.0333	0.78	6.2	0.0108	0.200(8)	0.0177	0.330(12)	5.25	284(12)

a Data from Table 3.3.

b Ground state absorbance of PAQ in methylene chloride, ± 0.15%.[90]

c Calculated from $\varepsilon(PAQH_2)_{max,418} = 4.90 \times 10^5 \pm 4\%$[91]

d Estimated from the extinction coefficients of TPP in toluene,[24] error ± 0.2

e $[^3PAQ]_0 = a_f/(\varepsilon_T - \varepsilon_G)\ell$

f $[^3PAQH_2]_0 = \Delta A_0/(\varepsilon_T - \varepsilon_G)\ell$

g $k_2 = k_2'(\varepsilon_T - \varepsilon_G)\ell + k_3$ $\quad k_3 = 5 \times 10^7$ $M^{-1}s^{-1}$ [24]

Using the value of 0.78 μM for $[T_{PAQH_2}]_0$ calculated above and the ratio $\Phi_{ISC,PAQ}/\Phi_{ISC,PAQH_2} = 0.121 \pm 0.011$ calculated from the fluorescence lifetimes shown in Schmidt et al.[5] produces an estimate of $[T_{PAQ}]_0$ of 0.094 ± 0.009 μM close to that determined by singlet depletion of the fast component at 420 nm. As is the case for $PAQH_2$, the triplet PAQ concentrations calculated from the amplitudes of the fast component do not agree with each other, again indicating that the values of the TPP triplet-triplet extinction coefficients are not the same as those for PAQ.

The decay of PAQ in benzonitrile sampled over various time scales gave consistent two exponential fits but inconsistent competing first- and second-order fits (Table 3.5 and Fig. 3.2).

Guided by the above results, all PAQ decays were analyzed by a two exponential fit.

The decay of PAQ in benzonitrile was observed over the range 440 to 575 nm and fit to two exponentials (Table 3.6). Although there is a large error in several of the fast rate constants, they tend to an average value, as do the slow rate constants. By fixing these two rate constants to the weighted average values (e.g., $\langle k_f \rangle = [\Sigma\{k_f/(\delta k_f)^2\}]/[\Sigma\{1/(\delta k_f)^2\}]$[86]) a linear least squares fit of the amplitudes was produced and is shown in Fig. 3.3. The spectrum of the fast component, when normalized to the slow component amplitude by the weighted average of the relative fraction f_1 ($f = a_f/(a_f+a_s)$. The average value $\langle f \rangle$ is found in the same manner as k_f above. The normalization factor is then $1/\langle f \rangle - 1$), shows that the two components are the same spectral species, attributed to the triplet porphyrin.

Table 3.5. Fit parameters in the analysis of the ^{3}PAQ decay in benzonitrile at various sampling rates[a]

Two exponential fit

DW[b] / ns	χ^2_ν	a_f[c]	k_f[c] / 10^4 s^{-1}	a_s[c]	k_s[c] / 10^4 s^{-1}
25	1.03	0.0039(2)	7.4(9)	0.00897(16)	0.148(18)
50	0.90	0.0050(3)	8.1(9)	0.00883(10)	0.163(7)
100	0.93	0.0039(4)	6.5(10)	0.00898(9)	0.169(4)
200	0.93	0.0060(12)	9.8(20)	0.00905(9)	0.162(2)
400	0.95	0.0014(5)	2.5(14)	0.00872(16)	0.167(3)

Competing first- and second-order fit

DW[b] / ns	χ^2_ν	ΔA_0[d]	k'_1 / 10^3 s^{-1}	k'_2 / 10^5 s^{-1}	$\Delta A_0 k'_2$ / 10^3 s^{-1}
25	1.10	0.01243(18)	-25.3(19)	34.2(24)	42.5(34)
50	1.23	0.01157(19)	-7.85(76)	14.1(11)	16.3(14)
100	1.25	0.01018(14)	0.32(24)	2.60(40)	2.65(42)
200	1.11	0.00992(14)	1.13(10)	1.17(20)	1.16(22)
400	0.96	0.00934(15)	1.51(7)	0.56(18)	0.52(18)

a Experiment carried out at 296 K.

b Dwell time = time per channel of data acquisition

c a_f, k_f, a_s, k_s are defined by eqn. 83

d ΔA_0, k'_1, and k'_2 are defined by eqns. 80 to 82.

Figure 3.2. The absorbance decay of ^{3}PAQ in benzonitrile and its fit to two exponentials over various time scales. The fit coefficients are shown in Table 3.5. (a) Time per channel = 50 ns. (b) Time per channel = 200 ns.

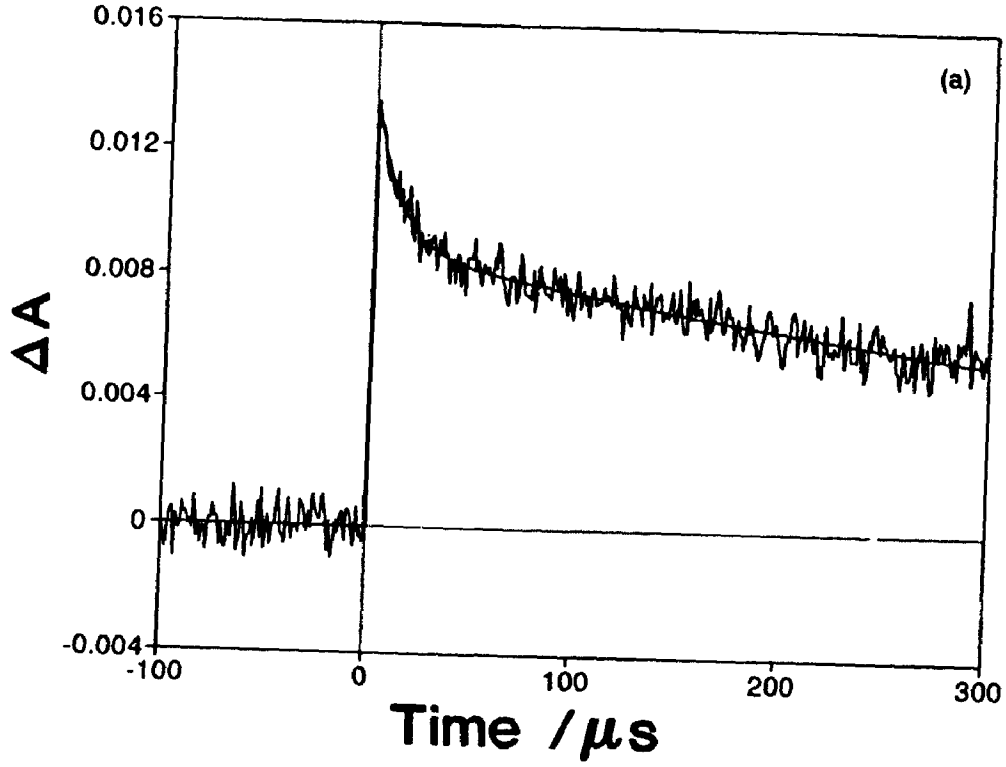
0.016
0.012
0.008
0.004
0
-0.004
ΔA
(a)
-100
0
100
200
300
Time /μs

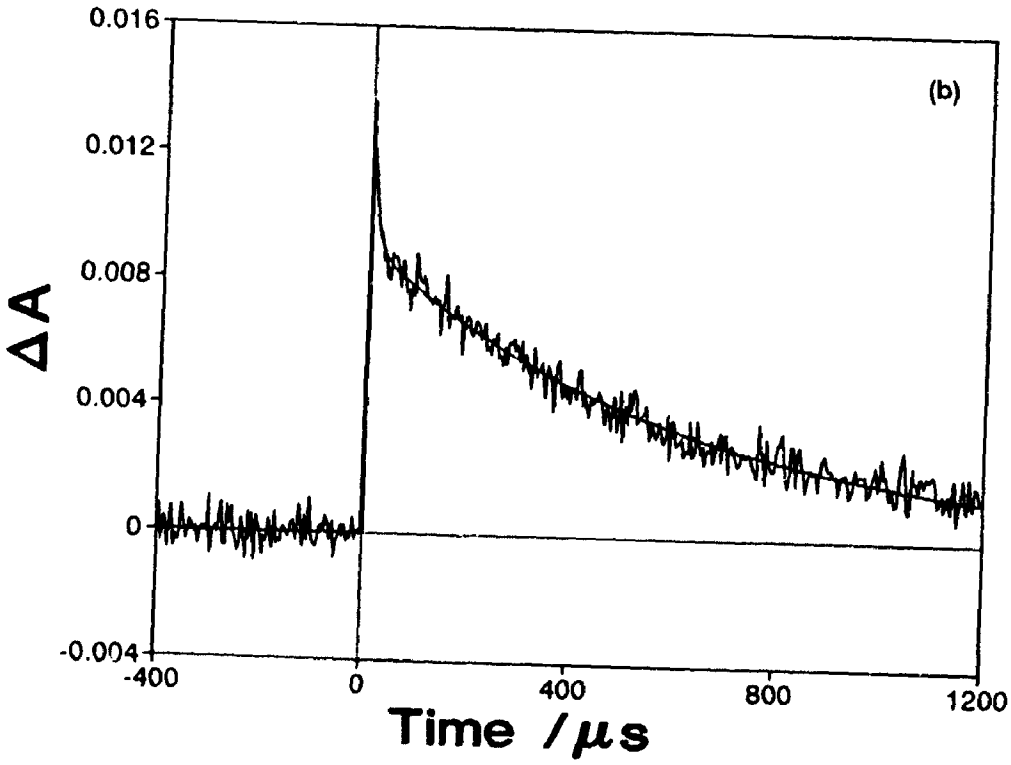
0.016
0.012
0.008
0.004
0
-0.004
ΔA
(b)
-400
0
400
800
1200
Time /μs

Table 3.6. Analysis of the ^{3}PAQ decay in benzonitrile at various wavelengths[a]

λ[b] /nm	χ_ν^2	a_f[c,d]	k_f[c] /10^4 s^{-1}	a_s[c,e]	k_s[c] /10^4 s^{-1}
444	1.06	0.00332	8.2(7)	0.01073	0.331(4)
450	1.19	0.00347	8.4(11)	0.01060	0.329(6)
454	1.06	0.00348	11.5(15)	0.01014	0.325(5)
460	0.90	0.00244	9.0(17)	0.00762	0.329(8)
466	1.15	0.00146	8.2(24)	0.00560	0.333(11)
473	0.96	0.00127	5.1(16)	0.00395	0.304(18)
483	0.99	0.00124	12.6(52)	0.00313	0.320(16)
492	1.24	0.00096	6.1(28)	0.00244	0.309(28)
502	1.41	0.00048	8.0(80)	0.00145	0.406(50)
513	1.10	-0.00038	9.7(96)	-0.00038	0.28(13)
538	1.14	0.00068	10.5(42)	0.00147	0.317(26)
543	0.89	0.00026	10.(12)	0.00089	0.263(40)
556[f]	-	-	-	-	-
564	0.82	0.00056	7.7(40)	0.00089	0.314(46)
573	0.86	0.00045	13.0(94)	0.00133	0.309(24)

a Experiment carried out at 296 K.

b Corning CS filters used: 444-460 nm 7-59; 460-483 nm 5-60; 492-513 nm 5-57; 538 nm 3-70; 543 nm 3-68; 556-573 nm 3-67.

c a_f, k_f, a_s, k_s are defined by eqn. 83

d Error = $\pm$ 0.00025

e Error = $\pm$ 0.00008

f Due to a very small signal this trace could not be resolved.

Figure 3.3. The difference spectrum of ^{3}PAQ in benzonitrile.

□ a_f, ▲ a_s, the unmarked solid line is a_f normalized to a_s.

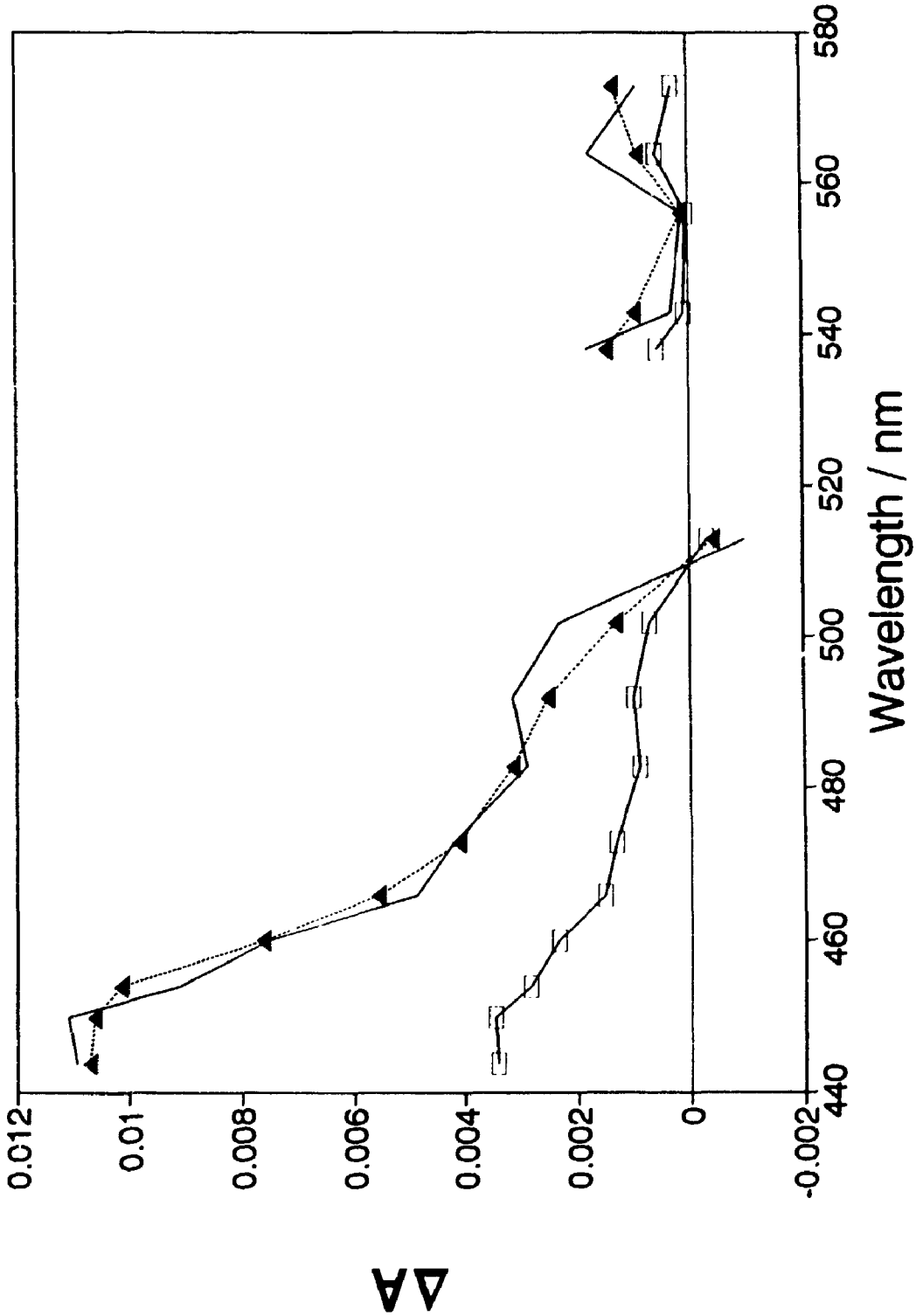
ΔA
0.012
0.01
0.008
0.006
0.004
0.002
0
-0.002
440
460
480
500
520
540
560
580
Wavelength / nm

3.2 Marcus Analysis of the Kinetic Results

3.2.1 Solvent Dependence

The previous studies in this series were on electron transfer from the excited singlet state to the singlet radical-ion-pair state.[4,5,6] Because both those and this work considered reactions involving no change in spin, the hypothesis to be tested is that the triplet state reactions should only differ from the singlet state reactions according to the change in $\Delta G°$ for the respective electron transfers, i.e, that H_{rp} and λ should be the same in any given solvent. This also implies that there is no significant change in molecular geometry between the singlet and triplet states.

In order to apply eqn. 19 to the k_{ET} data some assumptions are made about the energy $\Delta G°$ calculated by eqn. 5. The energy of the triplet state is assumed to be fairly insensitive to solvent.[5] There is a 0.02 eV change in the peak of the low-temperature phosphorescence maximum in going from methylcyclohexane to EPA (ethyl ether:isopentane:ethanol in volume ratio of 5:5:2).[45,14] This transition is $\pi^* \rightarrow \pi$ and any spectral shift should therefore have a similar magnitude to $\pi \rightarrow \pi^*$ transitions in other porphyrins. A study in which the visible spectra of chlorophyll a was recorded in 40 solvents showed that the red band peak absorbance varied by 0.04 eV (660 to 675 nm) with the variation in 30 of the solvents being only 0.02 eV.[95]

The second assumption is that the energy of the radical-ion-pair, calculated as the first two terms on the right hand side of eqn. 5 needs no further correction

due to its triplet character. Wasielewski et al.[52] have shown that the initially formed radical pair in photosynthetic bacteria is formed with a charge separation distance of about 8 Å and has a very small electron-electron exchange interaction resulting in a singlet-triplet splitting very near zero. The amide-methylene linkage in PAQ, although not completely rigid, restricts the approach of the quinone to the porphyrin to greater than 12 Å so that they cannot have direct orbital overlap.[4] Thus a singlet-triplet spitting $\Delta G^{\circ}_{13} = 0$ between the two radical-ion-pair states is assumed.

The reorganization energies are calculated using $r_D = 7$ Å, $r_A = 4$ Å, and $r_{DA} = 14$ Å, giving B = 1.80 eV and $\lambda_{in} = 0.2$ eV.[5]

Laser flash photolysis experiments on solutions of $PAQH_2$ and PAQ were first carried out at room temperature to see if the resulting values of Y_1 follow the predictions of Marcus electron transfer theory (Tables 3.7 and 3.8 and Fig. 3.4). The expected Y_1 values for acetonitrile and methylene chloride were calculated from eqn. 21 using experimental values of H_{rp}.[6] Although the temperature dependence of k_{ET} for ^{1}PAQ in benzonitrile is unknown, a value of $H_{rp} = 3.7 \times 10^{-4}$ eV can be estimated by assuming that Y_3 for ^{1}PAQ in benzonitrile falls on the same line Y_3 vs. X determined experimentally for other solvents (see Fig. 1.6).

Figure 3.4 indicates that the experimental values do not show a uniform trend among the solvents and that the value of Y_1 in most solvents is well below the values predicted in polar solvents. The value of k_{ET} for ^{3}PAQ in benzonitrile

Table 3.7. The energetics of triplet state electron transfer in PAQ in various solvents[a]

solvent[b]	n[c]	ϵ_s[d]	λ[e] /eV	$\Delta E°$[f] /V	$\Delta^3G°$[g] /eV	H_{rp}[h] /meV
BzCN	1.5494	25.40	0.879	1.45	-0.02	0.369(40)
MeCl	1.4288	9.05	0.883	1.40	-0.14	0.269(4)
MeCN	1.3496	36.30	1.139	1.41	-0.05	0.332(15)
Acet	1.3560	20.56	1.09	1.51	0.03	-
DCE	1.4421	10.37	0.89	1.33	-0.20	-
TCE	1.4359	7.25	0.82	1.46	-0.10	-

a Experiments carried out at 296 K.

b BzCN: benzonitrile, MeCl: methylene chloride, MeCN: acetonitrile, Acet: acetone, DCE: 1,2-dichloroethane, TCE: 1,1,1-trichloroethane.

c Index of refraction at 296 K.[96]

d Static dielectric constant at 296 K.[97]

e Reorganization energy. Calculated from eqns. 8 and 13.

f $\Delta E° = E°_{P/P^+} - E°_{Q^-/Q}$. Error = ± 0.040 V.[5]

g $\Delta G°$ for the triplet state electron transfer from eqn. 5. Error = ± 0.04 eV.

h Electronic coupling coefficient. From ref. 6 for MeCl and MeCN and calculated from Fig. 1.6 for BzCN.

Table 3.8. The experimental kinetics of triplet state electron transfer in PAQ in various solvents

solvent	k_f[a]	k_1'[b]	$^3k_{ET}$[c]	$^3Y_1$[d]	^3X[e]	$^3Y_1$[f]	$^3k_{ET}$[g]
	----------	/10^4 s^{-1}	----------	exptl		calc	calc
BzCN	7.62	0.090	7.53(41)	11.17	8.18	12.89	42
MeCl[h]	21.83	0.180	21.65(54)	12.22	6.07	14.52	210
MeCl[i]	17.93	0.180	17.75(52)	12.02	6.07	"	"
MeCN	1.53	0.280	1.25(7)	9.50	10.14	10.56	3.6
MeCN[i]	1.36	0.280	1.08(7)	9.35	10.14	"	"
Acet	2.50	0.106	2.39(39)	10.13	11.22	-	-
DCE	3.23	0.140	3.09(29)	10.28	5.23	-	-
TCE	2.02	0.280	1.74(24)	9.67	6.20	-	-

a Fast rate constant of two exponential fit to PAQ kinetics.

b Pseudo first-order rate constant from competing first- and second-order fit to $PAQH_2$ decay kinetics.

c $k_{ET} = k_f - k_1'$.

d $Y_{1,exptl} = \ln(k_{ET}\lambda^{1/2}/eV^{1/2}\ s^{-1})$ for the triplet state. Error = ± 0.10.

e $X = \Delta G^*/k_BT$. Error = ± 0.4.

f $Y_{1,calc} = C_1 - X$; C_1 calculated from singlet H_{rp} values. See Table 3.7.

g $^3k_{ET,calc}/10^4\ s^{-1}$

h Increasing temperature

i Decreasing temperature

Figure 3.4. Marcus analysis of the solvent dependence of k_{ET} using equation 21.

DCE: 1,2-dichloroethane; TCE: 1,1,1-trichloroethane; BzCN: benzonitrile;

Acet: acetone; MeCl: methylene chloride; MeCN: acetonitrile.

The latter two show values determined from increasing and decreasing

temperature experiments and indicate the spread at any one particular solvent.

□ experiments using freeze-pump-thaw for degassing

▲ earlier experiments using prepurified nitrogen for degassing

* expected values of Y_1: see table 3.8

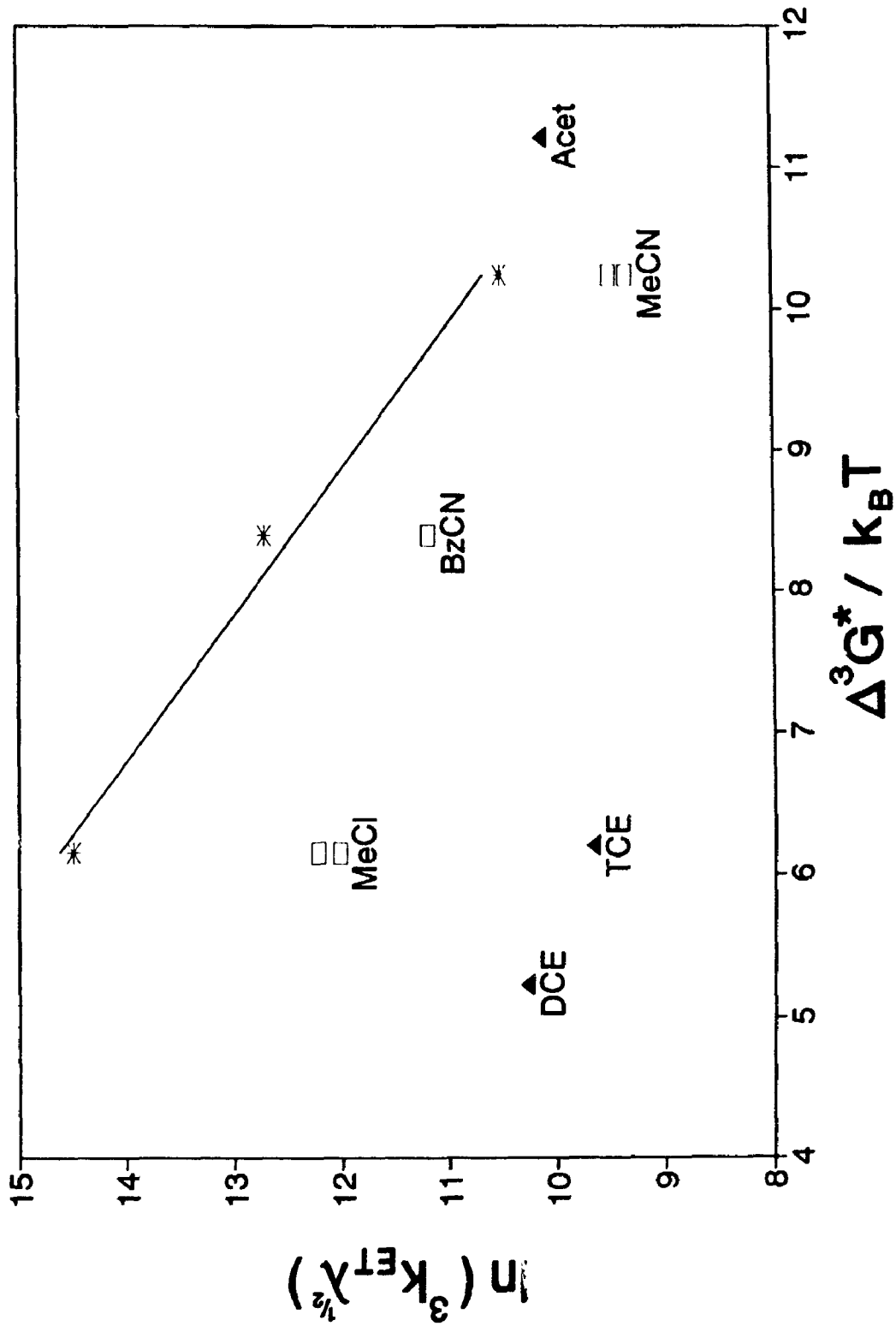
ln ($^3k_{ET}\lambda^{1/2}$)
Δ^3G^* / k_BT
15
14
13
12
11
10
9
8
4
5
6
7
8
9
10
11
12
MeCl
BzCN
MeCN
Acet
DCE
TCE

at room temperature obtained by Schmidt et al.[4], 4.6 (± 0.2) × 10^4 s^{-1}, is even lower than that determined in this lab, 7.5 (± 0.4) × 10^4 s^{-1}.

3.2.2 Temperature Dependence

To determine if, analogous to the case of singlet electron transfer rate constants,[6] the values of H_{rp} vary between solvents and are different than the singlet values, the temperature dependence of the triplet decays was studied. λ was calculated from eqns. 8 and 13 using values of the index of refraction n and the static dielectric constant ε_s vs temperature interpolated from literature values[96,97] and showed an increase with increasing temperature in acetonitrile and benzonitrile, but a decrease in methylene chloride. The temperature dependence of $\Delta G°$ was dependent on the variation of the static dielectric constant in eqn. 5, assuming all the other terms in that equation are independent of temperature.

The value of Y_2 in both methylene chloride and benzonitrile increased with increasing X while decreasing with increasing X in acetonitrile (Tables 3.9 to 3.11 and Fig. 3.5). All these trends were very weak; k_{ET} increased by less than a factor of two for a 30°C temperature change. This shows that the high temperature limit of Marcus electron transfer theory (eqn. 19) definitely does not work in the cases of PAQ in methylene chloride and in benzonitrile, since for the values of λ and $\Delta G°$ used it predicts a decrease in Y_2 with increasing X. In acetonitrile, Y_2 is much smaller than, and changes much less rapidly than predicted. A summary of the results of the temperature dependence analyses is shown in Table 3.12.

Notes for tables 3.9 to 3.11

a The symbols in Tables 3.9 to 3.11 all have the same definition. See text for a discussion of errors in these tables.

b Error ± 0.5°C.

c Index of refraction, interpolated from the literature values.[96]

d Static dielectric constant, interpolated from the literature values.[97]

e Reorganization energy, calculated from eqns. 8 and 13.

f ΔG° for the electron transfer reaction, calculated from eqn. 5.

g $X = \Delta G^*/k_BT$. Error = ± 0.17%.

h $k_{ET} = k_f - k_1'$. Error = ± 0.91×10^4 s^{-1} for benzonitrile, ± 1.1×10^4 s^{-1} for methylene chloride, ± 0.07×10^4 s^{-1} for acetonitrile.

i $Y_2 = \ln(k_{ET}(\lambda k_BT)^{1/2}/eV\ s^{-1})$. Error = ± 0.12 for benzonitrile, ± 0.054 for methylene chloride, ± 0.071 for acetonitrile.

j The decay of $^3PAQH_2$ in methylene chloride did not show a temperature dependence. $k_1' = 1800\ s^{-1}$.

k The decay of $^3PAQH_2$ in acetonitrile did not show a temperature dependence. $k_1' = 2800\ s^{-1}$.

Table 3.9. Triplet state electron transfer in PAQ in benzonitrile at various temperatures[a]

temp[b] /°C	n[c]	ε_s[d]	λ[e] /eV	$\Delta^3G°$[f] /eV	^3X[g] /eV	k_f /10^4 s^{-1}	k_1' /10^4 s^{-1}	k_{ET}[h] /10^4 s^{-1}	$^3Y_2$[i] /eV
4.4	1.5584	27.14	0.8748	-0.0171	8.79	9.76	0.06	9.697	9.549
13.0	1.5543	26.30	0.8767	-0.0183	8.52	8.49	0.08	8.411	9.423
22.8	1.5494	25.40	0.8789	-0.0197	8.23	7.62	0.09	7.531	9.330
33.3	1.5443	24.53	0.8814	-0.0211	7.95	6.81	0.10	6.706	9.233
43.8	1.5392	23.74	0.8840	-0.0225	7.69	5.96	0.12	5.842	9.114

Table 3.10. Triplet state kinetics in PAQ in methylene chloride at various temperatures

temp /°C	n	ε_s	λ /eV	$\Delta^3G°$ /eV	^3X	k_1 /10^4 s^{-1}	k_{ET}^j /10^4 s^{-1}	$^3Y_2$
Increasing temperature								
4.7	1.4387	9.85	0.8869	-0.1291	6.76	27.99	27.8	10.610
12.9	1.4342	9.52	0.8860	-0.1328	6.50	23.18	23.0	10.434
22.2	1.4290	9.07	0.8830	-0.1381	6.17	21.83	21.6	10.387
33.1	1.4230	8.46	0.8760	-0.1463	5.76	15.66	15.5	10.066
Decreasing temperature								
4.9	1.4386	9.84	0.8869	-0.1292	6.76	27.3	27.2	10.586
14.7	1.4332	9.44	0.8856	-0.1337	6.43	21.98	21.8	10.383
22.6	1.4288	9.05	0.8828	-0.1383	6.16	17.93	17.7	10.189
31.1	1.4242	8.58	0.8777	-0.1446	5.84	15.23	15.1	10.036
38.8	1.4199	8.10	0.8705	-0.1517	5.52	15.19	15.0	10.042

Table 3.11. Triplet state kinetics in PAQ in acetonitrile at various temperatures

temp /°C	n	ϵ_s	λ	$\Delta^3G°$	^3X	k_f	$k_{ET}{}^k$	$^3Y_2$
			---------- /eV ----------			------- /10^4 s^{-1} -------		
Increasing temperature								
4.1	1.3580	39.39	1.1304	-0.0475	10.85	1.21	0.93	7.332
13.3	1.3538	37.83	1.1345	-0.0486	10.52	1.37	1.09	7.511
23.1	1.3494	36.25	1.1389	-0.0498	10.20	1.53	1.25	7.666
32.8	1.3450	34.77	1.1432	-0.0510	9.89	1.67	1.39	7.786
43.6	1.3402	33.23	1.1480	-0.0523	9.58	1.72	1.44	7.843
53.6	1.3357	31.90	1.1525	-0.0536	9.30	1.77	1.49	7.893
Decreasing temperature								
4.8	1.3577	39.28	1.1307	-0.0476	10.83	1.09	0.81	7.198
14.1	1.3535	37.69	1.1349	-0.0487	10.50	1.22	0.94	7.366
22.8	1.3496	36.30	1.1387	-0.0497	10.21	1.36	1.08	7.520
33.5	1.3447	34.66	1.1435	-0.0511	9.87	1.47	1.19	7.631
43.5	1.3403	33.25	1.1479	-0.0523	9.58	1.43	1.15	7.619
53.1	1.3359	31.96	1.1523	-0.0536	9.32	1.50	1.22	7.694

Figure 3.5. Marcus analysis of the temperature dependence of k_{ET} in methylene chloride, benzonitrile, and acetonitrile. The error bar represents one standard deviation. The unmarked solid line shows the expected dependence using H_{rp} = 3.3×10^{-4} eV for benzonitrile and values from singlet data for methylene chloride and acetonitrile.

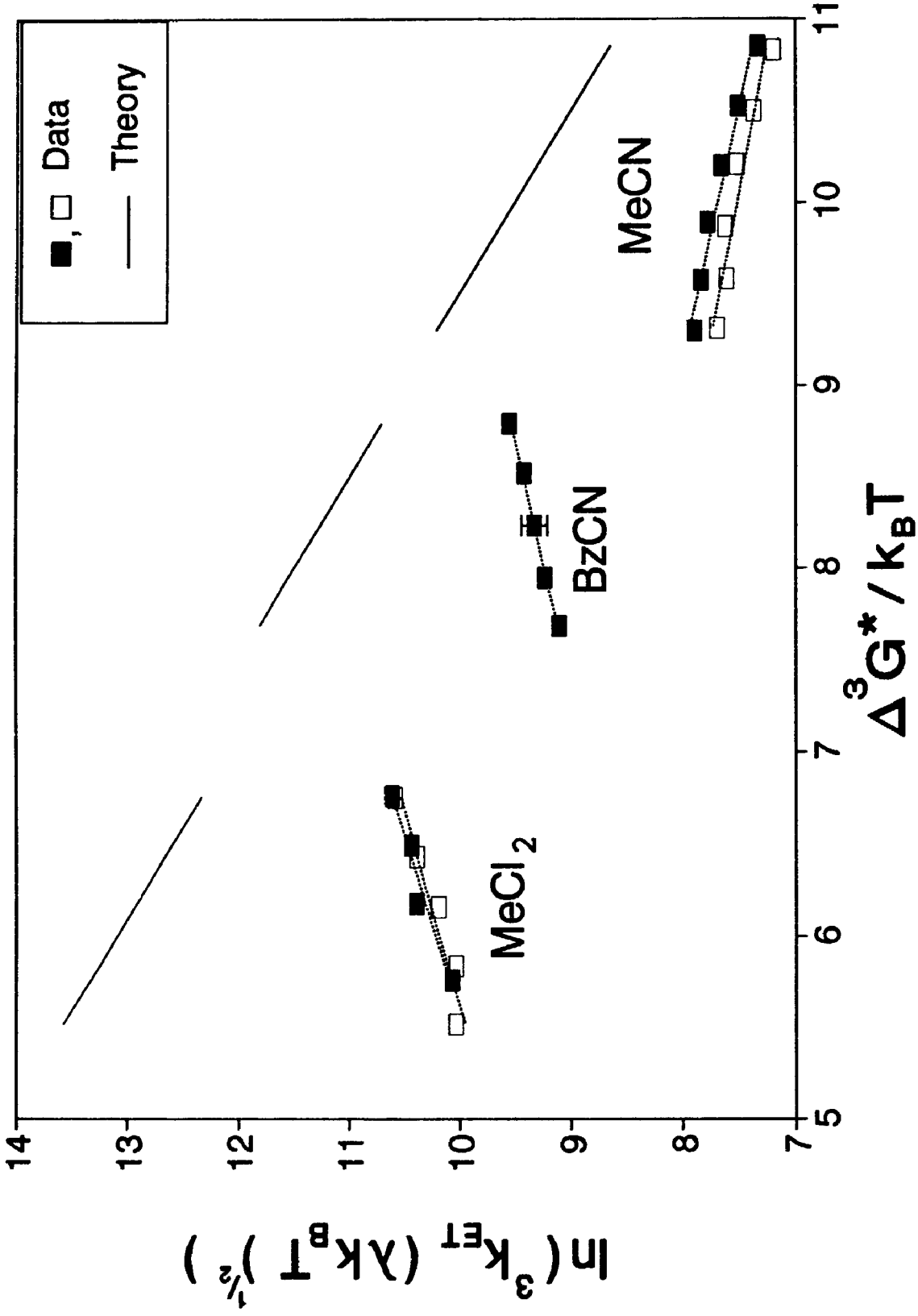
Data
Theory
MeCN
BzCN
$MeCl_2$
$\ln({}^3k_{ET}(\lambda k_B T)^{1/2})$
$\Delta^3 G^* / k_B T$
14
13
12
11
10
9
8
7
5
6
7
8
9
10
11

Table 3.12. Marcus analysis of the temperature dependence of k_{ET} of ^{3}PAQ in three solvents[a]

solvent[b]	slope	intercept	r[c]
BzCN	0.38(2)	6.20(1)	0.998
$MeCl_2$,inc	0.51(9)	7.17(7)	0.971
" dec	0.47(8)	7.39(8)	0.956
MeCN,inc	-0.36(4)	11.30(5)	-0.977
" " d	-0.29(3)	10.57(5)	-0.977
" dec	-0.32(5)	10.68(6)	-0.954
" " d	-0.25(4)	10.03(6)	-0.955

a Except for the linear variation of $\Delta G°$ with temperature (note d below) these results are from the plots of Fig. 3.5.

b inc or dec refer to increasing or decreasing temperature experiments, respectively.

c Correlation coefficient.

d Temperature dependent $\Delta G° = -0.05 - 0.00056(T-293)$ eV.[6]

In order to force the slope of the plot of Y_2 vs X for ^{1}PAQ data to -1.00, Liu and Bolton[6] assigned a linear temperature dependence to $\Delta G°$. Considering Table 3.12, if the same temperature dependence would be applied to the data of ^{3}PAQ in acetonitrile, then such a variation in $\Delta G°$ with temperature becomes larger than that due to the dielectric constant in the Coulombic work term. Over the temperature domain of 4 to 54°C, $\Delta G°$ would then vary from -0.041 to -0.069, and X would have the wider range from 10.98 to 9.04, respectively, lowering the slope of Y_2 vs X.

The error in λ is mainly due to the uncertainty in λ_{in} of $\pm$ 0.1 eV and the error in $\Delta E°$ of $\pm$ 0.04 V.[5] However, the λ_{in} is a fixed quantity for a given molecular system; hence, the $\pm$ 0.1 eV is a systematic error in the Marcus analysis of the solvent dependence of k_{ET} for PAQ (eqn. 21). Changing λ_{in} mainly pushes all the data to higher or lower values of X and thus this would not significantly affect the slope, an effect which can be seen in ref. 5. For a particular plot of Y_2 vs X in one solvent, the error in $\Delta E°$ is an additional systematic error with the same effect as stated for a plot of Y_1 vs. X.

The largest instrumental errors contributing to these plots were the error in $\Delta E°$ [5], the variation of $\pm$ 0.5°C during temperature controlled runs, and the noise in the light-on and light-off signals. The latter contributes the largest error to the values of k_{ET} and hence to Y_1 or Y_2. In the plot of Y_1 vs. X, the error in $\Delta E°$ is the major factor in the error in X, while for the plot of Y_2 vs. X, although

the temperature error would introduce a small error in λ and $\Delta G°$, the dominant effect would be in the explicit temperature term in X giving X $\pm$ 0.2%.

The ^{3}PAQ k_{ET} data and the predictions of Marcus theory in the form of eqn. 19 do not agree when both the solvent dependence and the temperature dependence are considered. An alternative, the exciplex model is examined in Chapter 4.

CHAPTER 4

ARRHENIUS ANALYSIS OF THE EXCIPLEX MODEL

A comparison of eqns. 34 and 86 shows that the rate constant for quenching of ^{3}PAQ due to the possible existence of an exciplex k_Q is numerically equal to the rate constant for the otherwise postulated electron transfer k_{ET}. That the calculated activation energies E_a for quenching in benzonitrile and in methylene chloride (Fig. 4.1 and Table 4.1) are negative indicates that a fast equilibrium between triplet porphyrin and a triplet exciplex might precede ion pair formation.

Consider the mechanism of ^{3}PAQ decay without the presence of an exciplex.

$$\begin{array}{l} {}^3P^*AQ \underset{k_{-IP}}{\overset{k_{IP}}{\rightleftharpoons}} {}^3(P^+AQ^-) \underset{k_{13}}{\overset{k_{31}}{\rightleftharpoons}} {}^1(P^+AQ^-) \xrightarrow{k_{CR}} PAQ \\ \quad \Big\downarrow k_0 \\ \quad PAQ \end{array} \qquad 97$$

The rate constant $k_{-IP} \approx k_{IP}$ because $\Delta G°$ for this elementary step ≈ 0 eV. The value of k_{IP} predicted by Marcus theory ($= {}^3k_{ET,calc}$ shown in Table 3.8) ranges from 3.6×10^4 s^{-1} in acetonitrile to 210×10^4 s^{-1} in methylene chloride. Using this and the values of k_{31}, k_{13}, and k_{CR} cited in section 1.5 shows that in the above mechanism the initial radical-ion-pair production step is rate limiting. A kinetic analysis along the lines of section 1.5.2 produces only one rate constant $\lambda \approx k_0 + k_{IP}$. Such a quenching rate constant $k_Q \approx k_{IP}$ cannot yield a negative activation energy.

Figure 4.1. Arrhenius analysis of k_Q from eqn. 60.

+, methylene chloride increasing temperature; *, methylene chloride decreasing temperature; ■, benzonitrile; □, acetonitrile increasing temperature; ▲, acetonitrile decreasing temperature.

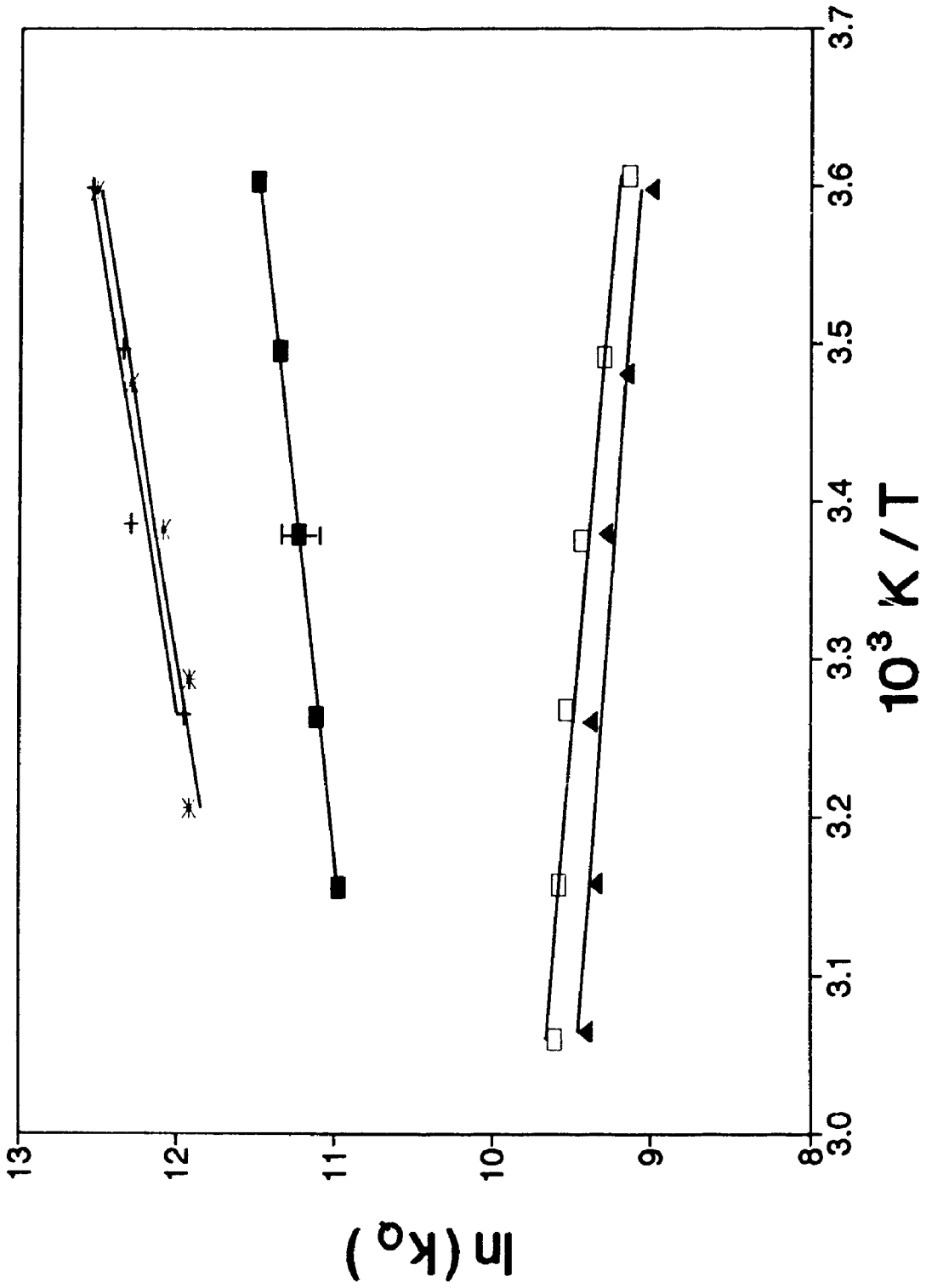
ln (k$_o$)
13
12
11
10
9
8
3.0
3.1
3.2
3.3
3.4
3.5
3.6
3.7
10^3 K / T

Table 4.1. Arrhenius analysis of the exciplex model

solvent[a]	A^a / s^{-1}	$E_a{}^b$ / eV	r^c
BzCN	1827(24)	-0.0948(32)	-0.998
$MeCl_2$,inc	756(57)	-0.142(26)	-0.967
" dec	772(48)	-0.140(18)	-0.977
MeCN,inc	$2.17(11)\times10^5$	0.074(10)	0.970
" dec	$1.19(7)\times10^5$	0.063(12)	0.932

a Increasing or decreasing temperature experiments.

b Arrhenius pre-exponential factor defined by eqn. 61.

c Arrhenius activation energy calculated from eqn. 60.

d Correlation coefficient.

For an exciplex to exist there must be a state with enthalpy low enough that the enthalpy of the transition state to the ion pair is less than that of the initial triplet. In a review of several studies, Kapinus[44] states that triplet exciplexes of porphyrins seem to be almost entirely locally excited triplet porphyrin in character, with a weak binding energy, but stabilized greatly by a large positive entropy of formation from the triplet state. Using a suggestion of Schmidt et al.[1] of a 2 D dipole moment for the excited singlet state of PAQ and assuming that the excited triplet state has a similar dipole moment, then ΔH_{EX}^{sol} (eqn. 67) has a value of only 3 meV (the ion pair with μ of 67 D would have $\Delta H_{EX}^{sol} \approx 4$ eV). For a molecule like PAQ, with the components separated by ca. 14 Å, the interaction is very small as shown by the values of H_{rp}. As the interaction varies from 0 to 0.25 eV, the value of ΔH_{EX}° varies from $-\Delta H_{EX}^{sol}$ to $-\Delta H_{EX}^{sol}$ - 0.14 eV.

Using Kapinus' [44] relation between the enthalpy ΔH and entropy ΔS of formation in the reaction between an excited donor-acceptor molecule and its exciplex,

$$\Delta H = \Delta H_0 + \beta_K \Delta S \qquad 96$$

where ΔH_0 = -17.7 kJ mol^{-1} (-0.183 eV) and β_K = 244 K, the entropy corresponding to -0.03 eV is 0.74 meV K^{-1} (71 J mol^{-1} K^{-1}). The free energy of reaction forming the exciplex, -0.22 eV, is then almost entirely due to entropy. It should be noted that a larger value of the triplet exciplex dipole moment would yield a larger exciplex enthalpy of reaction and a correspondingly smaller entropy.

Table 4.2. Binding energy of the ^{3}PAQ exciplex

solvent	$\Delta E°$ [a]	U_{stab} [b]	E_{EX} [c]	$-\Delta H°_{EX}$ [d]
		/ eV		
BzCN	1.45	0.37	1.40	0.003
MeCl	1.40	0.32	1.40	0.003
MeCN	1.41	0.33	1.40	0.003

a Redox potential $\Delta E° = E°_{P/P^-} - E°_{Q/Q^-}$[5]. Error = ± 0.040 V.[5]

b Exciplex stabilization energy from eqn. 65, using β = 0 eV, μ = 2D, and ρ = 7.5 Å.

c Exciplex enthalpy of formation from eqn. 64.

d Exciplex enthalpy of formation from the triplet state using eqn. 1.37. Error = ± 0.04 eV.

It may be useful to compare these values with those of the exciplex to ion pair transition state shown in Table 4.3, where the approximation of eqn. 39 is assumed. The activation entropy $\Delta S^{\ddagger}$ is calculated by equating the formulas for the rate constant from activated complex theory

$$k = \frac{k_B T}{h} \exp\left(-\frac{\Delta H^{\ddagger} - T\Delta S^{\ddagger}}{k_B T}\right) \qquad 99$$

and from an Arrhenius analysis

$$k = A\exp\left(-\frac{\Delta H^{\ddagger} + k_B T}{k_B T}\right) \qquad 100$$

so that

$$\Delta S^{\ddagger} = k_B\left[\ln\left(\frac{Ah}{k_B T}\right) - 1\right] \qquad 101$$

and $\Delta G^{\ddagger} = \Delta H^{\ddagger} - T\Delta S^{\ddagger}$. It can be seen that in benzonitrile and in methylene chloride, $\Delta H^{\ddagger} < \Delta H_{EX}^{\circ}$ implying that the exciplex is much more stabilized by the solvent than supposed above. This agrees with the negative values of $\Delta S^{\ddagger}$ which imply the exciplex to be in a more ordered state than ^{3}PAQ, possibly due to ordering of solvent molecules about an exciplex with significant degree of charge transfer character.

Applying the activated complex theory to the condition $k_{-EX} >> k_{IP}$ requires that $\Delta S_{-EX}^{\ddagger} - \Delta S_{IP}^{\ddagger} > 0$ or $\Delta H_{-EX}^{\ddagger} - \Delta H_{IP}^{\ddagger} < 0$. As seen in Fig. 1.4, a negative

Table 4.3. Activation parameters[a]

solvent	E_a / eV	$\Delta H^{\ddagger}$ / eV	$\Delta S^{\ddagger}$ / meV K^{-1}	$\Delta G^{\ddagger}$ / eV
BzCN	-0.095	-0.120	-1.98	0.47
MeCl,inc	-0.142	-0.167	-2.05	0.44
" ,dec	-0.140	-0.165	-2.05	0.44
MeCN,inc	0.074	0.048	-1.57	0.51
" ,dec	0.063	0.037	-1.62	0.52

a All parameters are for the reaction $^3P^*AQ \rightleftharpoons {}^3(P^{\bullet+}AQ^{\bullet-})^{\ddagger}$

b Activation enthalpy, defined by eqn. 62

c Activation entropy, defined by eqn. 101.

d Activation Gibbs energy from $\Delta G^{\ddagger} = \Delta H^{\ddagger} - T\Delta S^{\ddagger}$.

activation energy is inconsistent with the latter condition. Since the measured change in entropy from ^{3}PAQ to the transition state between the exciplex and the ion pair $\Delta S^{\ddagger} = \Delta S_{EX}^{\circ} + \Delta S_{IP}^{\ddagger}$ is a large negative value, then the first condition is realized if the transition state between the triplet porphyrin and the triplet exciplex has an entropy near that of the locally excited porphyrin. Thus, it is possible that there is a fast equilibrium between the ^{3}PAQ and the exciplex before the step for electron transfer to the ion pair.

A similar system,[98] involving bimolecular quenching of triplet TPP by benzoquinone, gave rate constants about four orders of magnitude lower than the rate constant for the quenching of fluorescence; this result could not be explained using Marcus theory. This is similar to the decrease in quenching rate constants seen in this study compared to quenching of fluorescence in the same molecule.[5] Preliminary experiments by Schmidt[4] in a variety of solvents also confirmed the slowness of quenching of triplets in freebase porphyrins.

CHAPTER 5

CONCLUSIONS

In a porphyrin-quinone molecule, covalently linked by an amide bridge, the triplet state of the porphyrin was quenched by the presence of the quinone relative to the corresponding states with a hydroquinone component. Due to the energy levels of the two constituents, it is presumed that the quenching is due to electron transfer from the porphyrin to the quinone. There seems to be a triplet exciplex between the triplet porphyrin and the triplet radical-ion pair state. A fast equilibrium between the triplet porphyrin and the exciplex is then established before electron transfer to the ion pair state occurs as the rate-limiting step. Subsequently, the electron may return to form the ground state porphyrin. The existence of such an exciplex is indicated, but by no means conclusively, by the observation of negative or small positive activation energies for the quenching of $^3P^*AQ$.

Thus, it cannot be determined if Marcus electron transfer theory applies to each elementary step, since the Gibbs energy of the postulated exciplex intermediate and the reorganization energies between this and the adjacent states are not known. If such an exciplex does not exist then the relation between the quenching rates and the available free energy in a variety of solvents shows that Marcus electron transfer theory does not describe the system studied, in contrast to its experimental confirmation in the case of singlet states in the same molecule.

Given that neither the radical-ion-pair nor the exciplex were observed as intermediate products, it is not possible to conclusively identify the pathway of deexcitation of the porphyrin triplet state.

The results determined here have limited application to the study of photosynthesis as most plants, algae, and bacteria usually have carotenoids to quench the (bacterio)chlorophyll triplet state and the complete absence of oxygen is not their normal physiological environment. These results may have more application in the design of solar cells, especially in a solid device where it may be possible to keep oxygen at low levels.

APPENDIX A

COMPUTER PROGRAMS

GAUSS[85] (Aptech Systems, Inc., Maple Valley, WA) is a matrix-oriented language for programming mathematical problems. In version 2.0 for an IBM AT compatible computer, every variable is considered to be a 2-dimensional dynamically allocated floating point matrix unless otherwise specified and every operation can operate directly on these matrices (subsequent versions have been developed solely for the 386 and higher computers; these allow up to 16 dimensions). This allows programming to be done without the necessity of many explicit loops (they are still available if needed). Also many high-level mathematical and statistical manipulations are provided as intrinsic or extrinsic functions or procedures. The language was created primarily for statistical use and has no direct ability to access external data acquisition devices, although it supplies hooks to other major languages through which the user could add a third-party device driver.

APPENDIX A.1. CAT8WCBK

```
/*        This program, CAT8WCBK, was written by David Fraser,
 to convert a light on/off pair of 8k WAVEFORM-CATALYST 3.0
files to averaged absorbance data and store it
as an integer GAUSS dataset.

Ask which file list is to be converted.            lines   27 -  39
Initialize, start loop, clear variables            lines   41 -  60
Get desired 8k data file created by WAVEFORM-CAT   lines   62 -  74

Convert the parameters                             lines   76 - 116
Check proper data and convert data                 lines  118 - 171
Strip beginning and end points                     lines  173 - 192

Find transient start channel                       lines  194 - 260
Average data into 20 channels per block            lines  246 - 254
Calculate absorbance                               lines  262 - 269
Store the parameters and data
as a two-byte integers in a GAUSS data file        lines  271 - 280
Loop return to get next file or end.               lines  282 - 294
*/

#lineson;

catpath = "C:\\CAT\\DATA\\";        @ where W-CAT stores data    @
gcat = "C:\\gauss\\cat\\";          @ where GAUSS stores the data@

newstart:
?; ?; "Running CAT8WCFI"; ?;
"Enter set of files as year month date  (yymmdd)  eg   91se20 ";;
filedate = cons; ?; ?;
"Enter number of first transient file as dd  eg    01 ";;
fileno = con(1,1); ?;
"Enter number of last transient file as dd   eg    23 ";;
filelast = con(1,1); ?;

if fileno > filelast;
    "First file > last file.    Try again.";
    goto newstart;
endif;

yymm = strsect(filedate,1,4);
gcatyymm = gcat $+ yymm $+ "\\";
block = 20;
format /rdn 3,0;
do while fileno <= filelast;
    k=1;
start:
    clear ampl, ans, bits_val, blk_chnl, byte_val, cdata, ch, cs1;
    clear cs1, cs2, datatype, ds, expper, f1, f2, filename;
```

```
50      clear filespec, idata, msg, nr, numblks, numrecs, numvals;
51      clear params, period, ptr, ptrstart, pxstart, skipbyt;
52      clear strtchnl, trigtime, v, vals_blk, vals_rec, voffset;
53      clear x, y, yfile, yname, z, zy;
54
55      if k == 1;
56          filename = filedate $+ ftocv(fileno,2,0);
57          outname = filename;
58      elseif k == 2;
59          filename = filedate $+ ftocv(fileno+1,2,0);
60      endif;
61
62      filespec = catpath $+ filename;
63      ds = getf(filespec,1);
64      ?; "loading and converting " filespec
65                                  "       Takes about 20 seconds.";
66      @   See WAVEFORM-CATALYST user's manual  pp A1-A3, A6-A7    @
67      v = strsect(ds,1,1);
68      if v $/= "K"; "Invalid file   try again";  goto start; endif;
69      cs1 = vals(strsect(ds,2,1));
70      cs2 = vals(strsect(ds,37,1));
71      if cs1 /= 34 and cs2 /=34;
72          "Lost the record delimiter at 2 and 37 = " cs1 cs2;
73          goto start;
74      endif;
75
76      ch = vals(strsect(ds,3,cs1));       @ header @
77      vals_blk = ch[1,1]  + ch[2,1]*256;
78      bits_val = ch[3,1]  + ch[4,1]*256;
79                          @ bits/value may be from 8 to 32, eg 12 @
80      period   = ch[5,1]  + ch[6,1]*256  + ch[7,1]*65536
81                                         + ch[8,1]*16777216;
82      /* units of 0.1 ns:   80 0C 00 00  ==  3200 * 0.1 ns = 320 ns
83                            40 06 00 00  ==  1600 * 0.1 ns = 160 ns
84                            20 03 00 00  ==   800 * 0.1 ns =  80 ns
85                            90 01 00 00  ==   400 * 0.1 ns =  40 ns
86                            C8 00 00 00  ==   200 * 0.1 ns =  20 ns
87                            64 00 00 00  ==   100 * 0.1 ns =  10 ns
88                            32 00 00 00  ==    50 * 0.1 ns =   5 ns
89      */
90      voffset  = ch[9,1]  + ch[10,1]*256;  @ corresponds to 0.0 V @
91      trigtime = ch[11,1] + ch[12,1]*256 + ch[13,1]*65536
92                                         + ch[14,1]*16777216;
93      /*    point when stop trigger received:
94                                    on a 1/8 * 32k memory boundary */
95      ampl     = ch[15,1] + ch[16,1]*256 + ch[17,1]*65536
96                          + ch[18,1]*16777216;     @ units of uV @
97      skipbyt  = ch[19,1] + ch[20,1]*256;
98          /*  actual data starts after missing this number of bytes
99                                   plus the first 16 data points   */
100     numblks  = ch[21,1] + ch[22,1]*256;
```

```
101       datatype = ch[23,1] + ch[24,1]*256;
102       if datatype /= 0;
103           "Not single channel data";
104           goto start;
105       endif;
106       blk_chnl = ch[25,1] + ch[26,1]*256;
107       strtchnl = ch[27,1] + ch[28,1]*256;
108       expper   = ch[29,1] + ch[30,1]*256;
109       msg = strsect(ds,39,128) $+ strsect(ds,169,32);
110
111       byte_val = int((bits_val+7)/8);
112       vals_rec = 128/byte_val;
113       numvals  = numblks*vals_blk;
114       numrecs  = numvals/vals_rec;
115       period   = period/1e+4;      * set default units of us *
116       periodb  = period*block;
117
118       /*
119         Waveform-Catalyst delimits the last record of each
120         8 kB data block by the same delimiter as the last record
121         at the end of all the data (128 = 80h).                    */
122       if numblks == 2;
123           test80a = 203 + 130*63;
124           test80b = test80a + 129;
125           if     vals(strsect(ds,test80a,1)) /= 128
126               OR vals(strsect(ds,test80b,1)) /= 128;
127               "error in " filespec " coding:  end of intermediate";
128               "8k data block not delimited by value 128 ( = 80h )";
129               stop;
130           endif;
131           chrs81 = chrs(81);
132           ds = strchnge(ds,chrs81,test80a);
133           ds = strchnge(ds,chrs81,test80b);
134       endif;
135
136       /*   Waveform Catalyst delimits each 128 byte physical record
137         by the value 129 = 81h.                                    */
138       nr = 1;
139       if byte_val == 1;
140           do while nr <= numrecs;
141               ptrstart = vals(strsect(ds,203+(nr-1)*130,1));
142               if ptrstart == 128 XOR nr == numrecs;
143                   "error:  end /= calculated end";
144                   stop;
145                   goto start;
146               endif;
147               cdata = vals(strsect(ds,204+(nr-1)*130,128));
148               if nr /= 1;      y = y ¦ cdata;
149               else;       y = cdata[skipbyt+16+1:128,1];
150               endif;
151               nr = nr + 1;
```

```
152         endo;
153     elseif byte_val == 2;
154         do while nr <= numrecs;
155             ptrstart = vals(strsect(ds,203+(nr-1)*130,1));
156             if ptrstart == 128 XOR nr == numrecs;
157                 "error: end /= calculated end";
158                 stop;
159                 goto start;
160             endif;
161             cdata = vals(strsect(ds,204+(nr-1)*130,128));
162             cdata = reshape(cdata,64,2);
163             idata = zeros(64,1);
164             idata[.,1] = cdata[.,1] + cdata[.,2]*256;
165             if nr /= 1;       y = y | idata;
166             else;         y = idata[(skipbyt/2)+16+1:64,1];
167             endif;
168             nr = nr + 1;
169         endo;
170     else; "number of bytes per value /= 1 nor 2";     goto start;
171     endif;
172
173     numvals = numvals - skipbyt/byte_val - 32;
174         /*  1 "value" = 1 channel.  The first 16 plus skipbyt
175             values have already been removed from the data by the
176             assignment to y when nr == 1.  The above statement
177             deletes these first 16, plus the last 16, plus
178             skipbyt values from the number of values in the data
179             file.  The following statement removes the last 16
180             values from the data                                  */
181     y = y[1:numvals,1];   @ y now contains the useful bit data  @
182
183         /*  skipbyt = 0, 1, 2, or 3.  Therefore numvals has a
184             minimum value of        8192 - 32 - 3 = 8157
185                             or      4096 - 32 - 3 = 4061
186             Therefore to make calculations easy, I will make the
187             pretransient be the first 2000 data points and the
188             posttransient the 2000 or 6000 data points after
189             (but including) the transient as determined in the
190             following, for a total of 4000 or 8000 data points.*/
191
192     y = (y-voffset)*ampl/1000;              @    convert to mV    @
193
194     if k == 1;                  @    transient signal   @
195         numvals  = int(numvals/4000)*4000;  @   4000  or  8000  @
196         p1or5999 = numvals - 2001;          @   1999  or  5999  @
197         numbloks = numvals/block;           @ total # of blocks @
198
199         zeropos = -9999;  @ zeropos will denote transient start @
200         startest = 2010;
201         endtest  = 2090;        @  zero is near position 2049   @
202         pretron = y[1:2000];
```

```
203         avprtron = meanc(pretron);
204         sdpretrn = stdc(pretron);
205         clear pretron;
206           /*  First point before and including transient max or
207               laser pulse min that grows to more than
208               0.7 * height (max/min - avprtron)
209               is declared to be zero time.  0.7 is arbitrary.  */
210         mintrans = minc(y[startest:endtest]);
211         maxtrans = maxc(y[startest:endtest]);
212         height = avprtron - mintrans;
213         if height >= 6*sdpretrn;     @ test for of laser pulse  @
214             "laser pulse determines start time";  ?;
215             height07 = height * 0.7;
216             testpos =  startest;
217             do while testpos <  endtest;
218                 testht = avprtron - y[testpos];
219                 if testht >= height07;
220                     goto breakk1; @ laser pulse = zero position @
221                 endif;
222                 testpos = testpos + 1;
223             endo;
224         else;                    @   laser pulse does not appear @
225             height = maxtrans - avprtron;
226             if height >= 6*sdpretrn;      @ test for transient  @
227                 "transient maximum determines start time"; ?;
228                 height07 = height * 0.7;
229                 testpos = startest;
230                 do while testpos < endtest;
231                     testht = y[testpos] - avprtron;
232                     if testht >= height07;
233                         goto breakk1; @start of transient = zero@
234                     endif;
235                     testpos = testpos + 1;
236                 endo;
237             endif;
238         endif;
239         if zeropos == -9999;
240             testpos = 2044 - 16;
241             "Could not find start of transient - set to 2028"; ?;
242             "\g\g";
243         endif;
244       breakk1:
245         zeropos = testpos;
246         y = y[zeropos-2000:zeropos+p1or5999];    @ 4000 or 8000 @
247         y = reshape(y,numbloks,block);      @  divide by block  @
248         lighton = meanc(y');       @ average of light on blocks @
249         clear y;
250       else;                       @ k = 2: light off signal       @
251         y = y[zeropos-2000:zeropos+p1or5999];    @ 4000 or 8000 @
252         y = reshape(y,numbloks,block);      @  divide by block  @
253         lightof = meanc(y');      @ average of light off blocks @
```

```
254         clear y;
255       endif;
256
257       k = k+1;
258       if k <=2;
259           goto start;
260       endif;
261
262       numprblk = 2000/block;     @  number of pretransient blocks  @
263       endprblk = numprblk - 3;   @  do not include near transient  @
264       Io = lightof[1:endprblk] - lighton[1:endprblk];
265       avIo = meanc(Io);
266       y = log(avIo/(lightof - lighton));
267       y = avprtron ¦ sdpretrn ¦ avIo ¦ period ¦ block
268                                              ¦ numbloks ¦ zeropos ¦ y;
269       clear Io,lightof,lighton,avprtron,sdpretrn;
270
271       yfile = gcatyymm $+ outname;
272       create f2 = ^yfile with y,1,4;
273                          @  4-byte single-precision GAUSS data file @
274       if f2 == -1;
275           ?; "can't create output file in \gauss\cat";
276           f2 = close(f2);
277           goto start;
278       endif;
279       zy = writer(f2,y);           @ store all data from \cat\data @
280       f2 = close(f2);                      @ close file @
281
282   endofile:    fileno = fileno + 2;  ?; ?;
283   endo;
284
285   "End of program"; ?;
286   ans = "N";
287   "Get another set of data?     Y/N     (Default = N) ";;
288   ans = cons; ?;
289   if ans $== "y" or ans $== "Y";
290       goto newstart;
291   endif;
292   ?; ?;
293
294   end;
295
```

APPENDIX A.2 CATGRDBK

```
/*      CATGRDBK   program written by David Fraser
        to read absorbance data from CAT8WCBK created datasets,
        make initial guesses for 4 fits, calls (5)=marqcalc(6),
        saves coeffts and calls PRCANAL4 to print them.
        To graph results run CAPBKYRS

Initialize program                                    lines   21 -  41
Ask which file list is to be analyzed                         43 -  65
Set up files for storing coefficients                         67 -  90
Start loop; get file created by CAT8WCBK                      92 - 119
Find range of first contiguous nonzero transient             121 - 138
Initialize fitting loop                                      140 - 155
Single exponential fit                                       157 - 200
Double exponential fit                                       202 - 307
Second order fit                                             309 - 329
First and second order fit                                   331 - 344
End fitting and file loops                                   346 - 356
Print results and ask if more data                           357 - 365
*/

#lineson;

external matrix f0;        @   f0 used by gradients in marqcalc @
external matrix numbloks;
external matrix savefit,sigmay;
external string filename;
external proc marqcalc,f1exp,f2exp,f2ord.f12ord,sgn;
external proc indexcat;
external proc linearft;
external proc prcanal4;

declare matrix f0 != 0;
declare matrix x != 0;
declare matrix y != 0;
declare matrix sigmay != 1;
declare matrix savefit != 1;  @ tells other procs coeffts saved @
declare matrix numbloks != 400;
declare string filename != "";

gcat = "c:\\gauss\\cat\\";          @ path where data is stored @
prfitdir = "C:\\GAUSS\\CAT\\FIT\\"; @ path to save fit coeffts  @

newstart:
?; ?; "Running CATGRDBK"; ?;
"Enter set of files as year month date  (yymmdd)  eg   92ap20 ";;
filedate = cons; ?; ?;
"Enter number of first transient file as dd  eg    01 ";;
fileno = con(1,1); ?;
"Enter number of last transient file as dd   eg    23 ";;
```

```
filelast = con(1,1); ?;

if fileno > filelast;
    "First file > last file.    Try again.";
    goto newstart;
endif;

"Do you want a printout of the parameters?  Y/N (Default = Y) ";;
printans = cons; ?; ?;
if printans $/= "N" AND printans $/= "n";
    printans = "Y";
endif;

closeall f1,fsg,fdb,fsc,ffs;
yymm = strsect(filedate,1,4);
gcatyymm = gcat $+ yymm $+ "\\";

prdate = prfitdir $+ filedate;
single = prdate $+ "sg";
double = prdate $+ "db";
second = prdate $+ "sc";
firsec = prdate $+ "fs";
open fsg = ^single;
if fsg == -1;           @    file not found  == does not exist? @
    fsg = close(fsg);
    let sgnames = filenam   b i ssr a1 sa1 k1 sk1  Von sVon avIo;
    let dbnames = filenam s b i ssr a1 sa1 k1 sk1 a2 sa2 k2 sk2;
    let scnames = filenam   b i ssr a0 sa0 k2 sk2;
    let fsnames = filenam   b i ssr a0 sa0 k1 sk1 k2 sk2 a0k2
                                                          sa0k2;
    create fsg = ^single with ^sgnames,0,8;
    create fdb = ^double with ^dbnames,0,8;
    create fsc = ^second with ^scnames,0,8;
    create ffs = ^firsec with ^fsnames,0,8;
else;
    fsg = close(fsg);
    open fsg = ^single FOR APPEND;
    open fdb = ^double FOR APPEND;
    open fsc = ^second FOR APPEND;
    open ffs = ^firsec FOR APPEND;
endif;

do while fileno <= filelast;
    clear tx,x,yabs,y,yfit;

    filename = filedate $+ ftocv(fileno,2,0);
    yfile = gcatyymm $+ filename;
    open f2 = ^yfile;
    rowsf2 = rowsf(f2);
    y = readr(f2,rowsf2);
    f2 = close(f2);
```

```
101       Von      = y[1];
102       sVon     = y[2];
103       avIo     = y[3];
104       period   = y[4];
105       block    = y[5];
106       numbloks = y[6];
107       zeropos  = y[7];
108       yabs     = y[8:rowsf2];
109       npretrbk = 2000/block;  @ the number of pretransient blocks @
110       npostrbk = numbloks - npretrbk; @ # of posttransient blocks @
111       endprebk = npretrbk - 3; @ avoid neighbourhood of transient @
112       firstrbk = npretrbk + 2; @ skip first block of transient pts@
113       firstr_1 = firstrbk - 1;
114       periodb = period*block;
115       tx1 = (-2000 + block/2)*period;
116       tx = seqa(tx1,periodb,numbloks);  @ x sequence to above yabs@
117       y = yabs[firstrbk:numbloks];
118       sigmay = stdc(yabs[1:endprebk]);
119
120       firstzer = npostrbk; @ one more than number of pts now in y @
121       zerolowr = zeros(2,1);
122       zerolowr = -10 ¦ 0;
123       firstzer = indexcat(abs(y),zerolowr);
124       if scalerr(firstzer) == 13;
125           firstzer = npostrbk;
126       else;
127           firstzer = firstzer[1];
128       endif;
129
130       x = tx[firstrbk:numbloks];
131
132       clear fastx,fasty;
133       fastnum = firstzer - 1;
134       f14num = int(fastnum/4);
135       f34num = fastnum - f14num;
136       fastx = x[1:firstzer-1];
137       fasty = y[1:firstzer-1];
138
139       gradtype = 2;
140       bfixed = 0;
141       fittype = 1;
142       do while fittype <= 4;
143           filename; ?;
144           schemenr =  0;
145           breakfit = 0;
146           numiter = 0;
147           ssr = 0;
148
149       /*    For the initial estimates of parameters, make them all
150             greater than zero, even if only by a tiny amount.
151             All rate constants are in units of us-1 for better
```

```
152             scaling in Marqcalc (see discussion of scaling and
153             condition number).
154             Convert to s-1 before saving coefficients.          */
155
156           if fittype == 1;        @  A = b[1]*exp(-b[2]*t) @
157               let binit[2];
158               signabs = sgn(fasty[1]); @ to take note of bleaching@
159               lnfasty = ln(abs(fasty));
160               weight = fasty/sigmay;
161               { binit,sigb,bomb } = linearft(fastx,lnfasty,weight);
162                 ?;  "return single exp: binit,bomb = " binit' bomb;
163               if binit[2] >= 0; @ possibly due to too small signal@
164                   breakfit = 6;
165                   coeffts = zeros(1,4);
166                   params = filename~breakfit~numiter~ssr~coeffts
167                                                       ~Von~sVon~avIo;
168                   z = writer(fsg,params);
169                   coeffts = zeros(1,8);
170                   params = filename~schemenr~breakfit~numiter~ssr
171                                                            ~coeffts;
172                   z = writer(fdb,params);
173                   coeffts = zeros(1,4);
174                   params = filename~breakfit~numiter~ssr~coeffts;
175                   z = writer(fsc,params);
176                   coeffts = zeros(1,8);
177                   params = filename~breakfit~numiter~ssr~coeffts;
178                   z = writer(ffs,params);
179                   goto endofFit;
180               endif;
181               if bomb;
182                   binit[2] =
183                     ln(fasty[1]/fasty[fastnum])/(fastnum*periodb);
184                   binit[1] = fasty[1]*exp(binit[2]*fastx[1]);
185               else;
186                   binit[1] = signabs*exp(binit[1]);
187                   binit[2] = -binit[2];
188               endif;
189
190               let bname[2] = "A1"   "K1";
191               { numiter,breakfit,b1,stderr,ssr }
192             = marqcalc(fittype,gradtype,&fiexp,binit,bfixed,bname);
193               bsave = b1[1] ¦ b1[2]*1e6;      @  save rate as s-1 @
194               stderr = stderr[1] ¦ stderr[2]*1e6;
195               coeffts = vec((bsave~stderr)')';
196                           @ creates row of alternating b & stderr @
197               params = filename~breakfit~numiter~ssr~coeffts~Von
198                                                       ~sVon~avIo;
199               z = writer(fsg,params);
200
201           elseif fittype == 2;
202               /*  Cannot have either binit[1 3] = 0, because this
```

```
203                 will cause singular matrix m due to entire column
204                 of gradient = 0.  See anlytgrd in ratefns.g    */
205             ssrtest = 1e6*ones(4,1);
206             bf2 = ones(4,1);
207             ni2 = ones(4,1);
208             b2 = ones(4,4);
209             stderr2 = ones(4,4);
210             let bname[4] = "A1"   "K1"    "A2"    "K2";
211             let binit[4];
212             fast34x  = fastx[f34num:fastnum];
213             fast34y  = fasty[f34num:fastnum];
214             weight34 = fast34y/sigmay;
215             lnfas34y = ln(abs(fast34y));
216             { binit[3:4],sigb,bomb }
217                             = linearft(fast34x,lnfas34y,weight34);
218             if bomb or binit[3] > 0 or binit[4] > 0;
219                 ssrtest[1] = 1000;
220                 goto tailbomb;
221             else;
222                 binit[3] = signabs*exp(binit[3]);
223                 binit[4] = -binit[4];
224             endif;
225             if fasty[1] >= binit[3]*exp(-binit[4]*fastx[1]);
226                 fast14x = fastx[1:f14num];
227                 fast14y = fasty[1:f14num];
228                 fast14y =fast14y-binit[3]*exp(-binit[4]*fast14x);
229                 f14zer = indexcat(fast14y,zerolowr);
230                 if scalerr(f14zer) == 13;
231                     f14zer = f14num + 1;
232                 else;
233                     f14zer = f14zer[1];
234                     if f14zer > 3;
235                         fast14x = fast14x[1:f14zer-1];
236                         fast14y = fast14y[1:f14zer-1];
237                     else;
238                         ssrtest[1] = 2000;
239                         goto tailbomb;
240                     endif;
241                 endif;
242                 weight14 = fast14y/sigmay;
243                 lnfas14y = ln(abs(fast14y));
244                 { binit[1:2],sigb,bomb }
245                             = linearft(fast14x,lnfas14y,weight14);
246                 if bomb or binit[1] > 0 or binit[2] > 0;
247                     ssrtest[1] = 3000;
248                     goto tailbomb;
249                 else;
250                     binit[1] = signabs*exp(binit[1]);
251                     binit[2] = -binit[2];
252                 endif;
253                 i2 = 1;
```

```
254                 { ni2[i2],bf2[i2],b2[.,i2],stderr2[.,i2],
255                                                   ssrtest[i2] } =
256                 marqcalc(fittype,gradtype,&f2exp,
257                                                 binit,bfixed,bname);
258             endif;
259         tailbomb:
260             binit[1] = b1[1];
261             binit[2] = b1[2];
262             binit[3] = b1[1]/10;
263             binit[4] = b1[2]/10;
264             i2 = 2;
265             { ni2[i2],bf2[i2],b2[.,i2],stderr2[.,i2],ssrtest[i2]}
266           = marqcalc(fittype,gradtype,&f2exp,binit,bfixed,bname);
267             binit[1] = b1[1];
268             binit[2] = b1[2];
269             binit[3] = b1[1]/10;
270             binit[4] = b1[2]*10;
271             i2 = 3;
272             { ni2[i2],bf2[i2],b2[.,i2],stderr2[.,i2],ssrtest[i2]}
273           = marqcalc(fittype,gradtype,&f2exp,binit,bfixed,bname);
274             binit[1] = b1[1]/2;
275             binit[2] = b1[2]/2;
276             binit[3] = b1[1]/3;
277             binit[4] = b1[2]*3;
278             i2 = 4;
279             { ni2[i2],bf2[i2],b2[.,i2],stderr2[.,i2],ssrtest[i2]}
280           = marqcalc(fittype,gradtype,&f2exp,binit,bfixed,bname);
281             schemenr = minindc(ssrtest);       @  scheme number @
282             numiter = ni2[schemenr];
283             breakfit = bf2[schemenr];
284             b2 = b2[.,schemenr];
285             stderr = stderr2[.,schemenr];
286             ssr = ssrtest[schemenr];
287             if b2[4] > b2[2];  @ put faster rate constant first @
288                 bfast = b2[4];
289                 b2[4] = b2[2];
290                 b2[2] = bfast;
291                 afast = b2[3];
292                 b2[3] = b2[1];
293                 b2[1] = afast;
294                 errbfast  = stderr[4];
295                 stderr[4] = stderr[2];
296                 stderr[2] = errbfast;
297                 errafast  = stderr[3];
298                 stderr[3] = stderr[1];
299                 stderr[1] = errafast;
300             endif;
301             bsave = b2[1] | b2[2]*1e6 | b2[3] | b2[4]*1e6;
302             stderr = stderr[1] | stderr[2]*1e6
303                                       | stderr[3] | stderr[4]*1e6;
304             coeffts = vec((bsave~stderr)')';
```

```
305             params=filename~schemenr~breakfit~numiter~ssr~coeffts;
306              z = writer(fdb,params);
307
308           elseif fittype == 3;
309              let binit[2];
310              invfasty = 1/fasty;
311              weight = fasty.*fasty/sigmay;
312              { binit,sigb,bomb }=linearft(fastx,invfasty,weight);
313              if bomb;
314                 binit[1] = fasty[1];
315                 binit[2] = (1/fasty[fastnum] - 1/fasty[1])
316                                                 /(fastnum*periodb);
317              else;
318                 binit[1] = 1/binit[1];
319              endif;
320
321              let bname[2] = "A0" "K2/\127\238";
322              { numiter,breakfit,b3,stderr,ssr }
323         = marqcalc(fittype,gradtype,&f2ord,binit,bfixed,bname);
324              bsave = b3[1] ¦ b3[2]*1e6;
325              stderr = stderr[1] ¦ stderr[2]*1e6;
326              coeffts = vec((bsave~stderr)')';
327              params = filename~breakfit~numiter~ssr~coeffts;
328              z = writer(fsc,params);
329
330           elseif fittype == 4;
331              let bname[3] = "A0" "K1" "K2/\127\238";
332              let binit[3];
333              binit[1] = b1[1];
334              binit[2] = b1[2];
335              binit[3] = 0;
336              { numiter,breakfit,b4,stderr,ssr }
337         = marqcalc(fittype,gradtype,&f12ord,binit,bfixed,bname);
338              bsave = b4[1] ¦ b4[2]*1e6 ¦ b4[3]*1e6 ¦ b4[4]*1e6;
339              stderr = stderr[1] ¦ stderr[2]*1e6
340                                 ¦ stderr[3]*1e6 ¦ stderr[4]*1e6;
341              coeffts = vec((bsave~stderr)')';
342              params = filename~breakfit~numiter~ssr~coeffts;
343              z = writer(ffs,params);
344           endif;
345           fittype = fittype + 1;
346        endo;   @   endo fittype   @
347     endoffit:
348        clear lnfasty,fast34x,fast34y,fast14x,fast14y,f14zer;
349        clear weight,weight34,weight14,lnfas34y,lnfas14y,invfasty;
350        clear binit,bname,stderr,stderr2;
351
352     endofile:   fileno = fileno + 2;
353     endo;
354
355     closeall fsg,fdb,fsc,ffs;
```

```
356   if printans $== "Y";  call prcanal4(filedate,0);  endif;
357
358   ?; "End of program"; ?;
359   "Get another set of data?     Y/N     (Default = N) ";;
360   ans = cons; ?; ?;
361   if ans $== "y" or ans $== "Y";
362       goto newstart;
363   endif;
364   ?; ?;
365
366   clear fastx,fasty,tx,x,yabs,y;
367   end;
```

APPENDIX A.3 MARQCALC

```
/*    MARQCALC.ARC

Purpose:
Nonlinear least squares fit using a Marquardt algorithm
adapted from Bevington, P.R., Data Reduction and Error Analysis
for the Physical Sciences, McGraw-Hill, New York, 1969, p237.
and NONLIN.PRG (GAUSS 1.49b documentation manual pp489-494).
Uses analytical calculation of gradient as default.

Format:
{ iter,breakfit,b,stderr,ssr } =
            marqcalc(fittype,gradtype,&fnfit,binit,bfixed,bname);

Inputs:
fittype -   scalar.  Code for the type of fit.
            1 = single exponential
            2 = double exponential
            3 = second order
            4 = first and second
            5 = coupled first and second order d.e.'s

gradtype -  Scalar.  Code for type of gradient calculation.
            0 = numerical gradient
            1 = other combination of analytical and numerical
            2 = analytical gradient (default)

&fnfit --   Function (or procedure) you want to be fitted,
            must already be defined as a function
            or procedure in the current subdirectory
            or in the file \GAUSS\SRC\RATEFNS.ARC

binit  --   k x 1 matrix.   The initial guesses of the k
            fitting coefficients.

bfixed --   Column vector.  Parameters and fixed coefficients.

bname  --   k x 1 matrix.   The names of the variables
            for printing the results.

Outputs:
iter  ----  scalar.  The number of gradient calculations
            required before the system converged.

breakfit -  scalar.  A description of the best fit results.
                0 : ok
                1 : converging too slowly (>10 grad calcns)
                2 : may be trapped in a local minima (>10 invs)
              3,4 : gradient moment matrix singular
                5 : next matrix iteration yields invalid params
```

```
b ------   k x 1 matrix.   The best fit coefficients.
           For fittype 4, also the product a0k2 is returned.

stderr -   k x 1 matrix.   The standard error in the
           coefficients.  For fittype 4, the standard error of
           the product a0k2 is also returned.

ssr -----  scalar.   Sum of the Squared Residuals.
               (unweighted chi-squared)

Globals:
x ------   n x 1 matrix.   The independent variable data.
y ------   n x 1 matrix.   The dependent variable data.
           ie. In the main program x,y form the n data pairs.

filename -  string.   The name of datafile being fit..

savefit -   scalar.   0 if not in set of files; then ok to print
               fitting results.    1 if in such a set; then the
               results are being saved to a dataset before
               being printed in a different format.

sigmay --   scalar.   The standard deviation of the noise level.

f0 ------   n x 1 matrix.   The calculated yfit for use in
               the analytical gradient calculation.

Remarks:
EXTERNAL proc marqcalc;
          should be be put at the top of the calling program

This program does not use weighted fitting, assuming all
weights are equal (= sigmay).  This is included at the end
to calculate the reduced chi-square.
*/

#lineson;

proc (5) = marqcalc(fittype,gradtype,&fi,binit,bfixed,bname);

    external proc anlytgrd,marqtest;
    external string filename;
    external matrix f0,x,y,savefit,sigmay;

    local fi:proc;

    local ans,b,breakfit,bsave,db,dbsave,e,fixed,i,inverts;
    local invertsv,iter,k,lambda,lambda1,n,tol,t0,t1;
    local g,gu,m,m0,minv,ssr,ssr1,u,relcovar;
    local df,momtsave,pvt,sa0k2,sigsq,stderr,t,vc_ml,weight;
    local dh,e,v1;
```

```
101       clear b,breakfit,e,iter,k,n,t0,t1;
102       clear df,momtsave,pvt,sigsq,t,vc_m1;
103
104       fixed = 1;       @   dummy variable in this procedure    @
105       lambda1 = 0;
106       ans = "N";
107       k = rows(binit);
108       n = rows(x);
109       weight = 1/(sigmay*sigmay);
110       df = n - k;
111       dh = 1e-6;
112
113       stderr = ones(k,1);
114       if k == 1;
115           lambda = .005;
116       elseif k == 2;      @ see D.V.O'Connor and  D. Phillips,      @
117           lambda = .01;   @ Time-correlated Single Photon Counting,@
118       elseif k == 3;      @ Academic Press, London, 1984, p175.     @
119           lambda = .02;
120       else;         /*  if k == 4;  */
121           lambda = .05;
122       endif;
123       b = binit;
124       bsave = binit;
125       tol = abs(binit)/1e4;
126       db = binit/100;
127       dbsave = db;
128       u = y - fi(b,bfixed);
129       ssr = u'u;          @  initial ssr   @
130       ?;
131       format /rd 8,0;
132       filename;
133       format /ren 13,4;
134       "b(initial) = " b';
135       format /rd 8,3;
136       "reduced chisqr(initial) = " ssr*weight/df; ?;
137
138
139       t0 = hsec;
140       do until abs(db) < tol;
141           clear inverts,invertsv;
142           gosub gradcalc;
143   invert: inverts = inverts+1;
144           m = diagrv(m0,diag(m0)*(1+lambda));
145           if iter == 0 and inverts == 1;   momtsave = m0;  endif;
146           trap 1;
147           minv = inv(m);
148           trap 0;
149           if scalerr(minv);
150               lambda = lambda*10;
151               inverts = inverts - 1;
```

```
152             if lambda > 1e6;
153                 breakfit = 4; @singular matrix; lambda too large@
154                 goto jumpend;
155             endif;
156             goto invert;        @ try again with larger lambda  @
157         endif;
158         db = minv*gu;
159         b = b + db;
160         if marqtest(fittype,b);
161             breakfit = 5;                 @ invalid parameters  @
162             goto jumpend;
163         endif;
164
165 b_ok:   u = y - fi(b,bfixed);
166         ssr = u'u;
167         if ssr1 <= ssr;
168             if abs(db) < tol;
169                 ssr = ssr1;
170                 breakfit = 2;   @   local minima?   @
171                 goto jumpend;
172             else;
173                 if lambda > 1e6;
174                     breakfit = 2;   @   local minima?   @
175                     goto jumpend;
176                 endif;
177                 lambda = lambda*10;
178                 goto invert;  @  try again with larger lambda   @
179             endif;
180         endif;
181
182     endinv:  iter = iter+1;
183         bsave = b;
184         dbsave = db;
185         momtsave = m0;
186         invertsv = inverts;
187         format /rd 2,0;
188         "iteration # " iter;;
189         "    # inverts = " inverts;;
190         format /re 6,0;
191         "    lambda = " lambda;
192         lambda = lambda/10.;
193         format /ren 13,4;
194         "b  = " b';
195         "db = " db';
196         format /rd 8,3;
197         "reduced chisqr =  " ssr*weight/df; ?;
198         if iter > 20;
199             breakfit = 1;   @   system converging too slowly    @
200             goto jumpend;
201         endif;
202         tol = abs(b)/1e4;
```

```
203       endo;   @   abs(db) < tol   @
204       lambda1 = 1;
205       goto gradcalc;
206
207   jumpend:
208       format /rd 2,0;
209       "jumpend:    breakfit = " breakfit;
210       inverts = inverts - 1;
211       if inverts == 0;
212           inverts = invertsv;
213       else;
214           iter = iter + 1;
215       endif;
216       b = bsave;
217       ssr = ssr1;
218       m0 = momtsave;
219       db = dbsave;
220
221   normend:
222       sigsq = ssr/df;
223       trap 1;
224       minv = inv(m0);  @ with lambda = 0  for errors in coeffts   @
225       trap 0;
226       if scalerr(minv);
227           breakfit = 3;
228           if m0 == momtsave;  goto results;  endif;
229           goto jumpend;   @   singular matrix m without lambda!   @
230       endif;
231       vc_m1 = sigsq*minv;    @ estimates variance of coefficients @
232       stderr = sqrt(diag(vc_m1));  @ if y weights are all equal   @
233       if breakfit > 0;
234           relcovar = ones(k,k);
235       else;
236           relcovar = vc_m1./(b*b');    @   relative covariance    @
237       endif;
238       if fittype == 4;
239           b = b ¦ b[1]*b[3];
240           sa0k2 = sqrt(relcovar[1,1] + relcovar[3,3]
241                                      + 2*relcovar[1,3])*b[4];
242           stderr = stderr ¦ sa0k2;
243           bname = bname ¦ "K2A0";
244       endif;
245   /*  t = b./stderr;  @ null t-statistic  ie  t = (b - 0)./stderr @
246       pvt = 2*cdftc(abs(t),df);          */
247
248   results:
249       if ans $== "N";
250           t1 = hsec;
251       endif;
252       ?; "\g";
253       format /rd 8,0;
```

```
254       filename;
255       i = 1;
256       do until i>k;
257           format /ld 6,6;  print $bname[i];;
258           if strindx(bname[i]."A",1);
259               print "       =   ";;
260           else;
261               print " (s-1) =   ";;
262           endif;
263           format /ro 12,4; b[i]  "  +/-  ";;
264           format /ro 10,3;    stderr[i];
265       i = i+1;
266       endo;
267
268       format /rd 8,3;
269       "reduced chisqr = " sigsq*weight;
270       format /rd 3,3;
271       " time = " (t1-t0)/100. " s ";;
272       "  #iter = " iter;;
273       "  #inv = " inverts;
274       if inverts > 1;
275           "   fit will not get better.";
276       endif;
277       ?;
278       if breakfit /= 0;
279           if breakfit == 1;
280   "The fit is converging too slowly;  breakfit = " breakfit;
281           if breakfit == 2;
282   "This matrix iteration may be trapped (local minima in ssr?)";
283           elseif breakfit == 3 or breakfit == 4;
284   "The matrix becomes singular;  breakfit = " breakfit;
285           elseif breakfit == 5;
286   "The next matrix iteration produces invalid parameters:";
287           endif;
288       endif;      @   breakfit /= 0   @
289
290       if not savefit;
291           "relative covariance matrix: error\253[i,j]/(b[i]*b[j])";
292           format /ro 12,4;
293           relcovar; ?; ?;
294       endif;
295
296       retp(iter,breakfit,b,stderr,sigsq*weight);
297
298
299   gradcalc:
300       clear g,m,m0,minv,u,gu,ssr,ssr1;
301       g = zeros(n,k);
302
303       if gradtype == 0;
304           g = gradp2(&fi,b,bfixed);       @   numerical gradient  @
```

```
305                 /*  elseif gradtype == 1;
306                         g = othrgrad(fittype,b,bfixed);          */
307         else;  * default *
308             f0 = fi(b,bfixed);  *   required in procedure anlytgrd  *
309             g = anlytgrd(fittype,b,bfixed);
310         endif;
311         m0 = moment(g,0);
312         u = y - f0;
313         gu = g'u;
314         ssr1 = u'u;
315         if lambda1;     ssr = ssr1;     goto normend;       endif;
316         return;
317
318     endp;
```

APPENDIX A.4 LINEARFT

```
1   /*    Procedure LINEARFT performs a linear least squares analysis
2         on Y-weighted data.                    */
3
4   proc (3) = linearft(x,y,weight);
5
6   #lineson;
7       local xweight,yweight,wsumsig2,wsumx,wsumx2,wsumy,wsumy2;
8       local deltax,deltay,r,b,sigb,wsumxy;
9
10      let b[2] = 0 0;
11      let sigb[2] = 1 1;
12
13      if rows(weight) == 1 and cols(weight) == 1;
14          weight = weight*ones(rows(y),1);
15      endif;
16      xweight  = x .* weight;
17      yweight  = y .* weight;
18      wsumsig2 =   weight' *   weight;
19      wsumx    =   weight' *  xweight;
20      wsumx2   =  xweight' *  xweight;
21      wsumy    =   weight' *  yweight;
22      wsumy2   =  yweight' *  yweight;
23      wsumxy   =  xweight' *  yweight;
24
25      deltax = wsumsig2*wsumx2 - wsumx*wsumx;
26      if abs(deltax) < 1e-15;
27          retp(b,sigb,1);
28      else;
29          deltay = wsumsig2*wsumy2 - wsumy*wsumy;
30          b[1] = (wsumx2*wsumy - wsumx*wsumxy)/deltax;
31          b[2] = (wsumsig2*wsumxy - wsumx*wsumy)/deltax;
32          sigb[1] = wsumx2/deltax;
33          sigb[2] = wsumsig2/deltax;
34          if abs(deltay) > 1e-15;
35              r = b[2]*sqrt(deltax)/sqrt(deltay);
36          endif;
37          retp(b,sigb,0);
38      endif;
39
40  endp;
```

APPENDIX A.5 RATEFNS.ARC

```
1   /*  RATEFNS.ARC - Library of functions and analytical gradients
2   **                to which data is fit.  Also procedure MARQTEST
3   **                to check whether MARQCALC has produced
4                     invalid parameters                              */
5
6   #LINESON;
7
8   proc fexpxb(x,b2);
9
10  /*  for an expoenetial decay,
11                    fexp assumes the rate constant, b2, is positive
12      Note here: the x is passed by argument, it is not external */
13
14      local ftot,last,n,period,safe,xsafe;
15      n=rows(x);
16      period = x[2] - x[1];
17
18  /*  Need to know how far to go in x without causing an underflow.
19              4e-300 = exp(-b2 * (last * period) )     */
20
21      last = int(ln(4e-300)/(-b2*period));
22
23      if last GE n;
24          retp(exp(-b2*x));
25      else;
26          ftot = zeros(n,1);
27          xsafe = x[1:last];
28          ftot[1:last] = exp(-b2*xsafe);
29          retp(ftot);
30      endif;
31  endp;
32
33
34  proc fexp(b2);
35
36      external matrix x;
37
38      local ftot,last,n,period,safe,xsafe;
39
40      n=rows(x);
41      period = x[2] - x[1];
42
43      last = int(ln(4e-300)/(-b2*period));
44
45      if last GE n;
46          retp(exp(-b2*x));
47      elseif last == 0;
48          retp(zeros(n,1));
49      else;
```

```
50          ftot = zeros(n,1);
51          xsafe = x[1:last];
52          ftot[1:last] = exp(-b2*xsafe);
53          retp(ftot);
54      endif;
55  endp;
56
57
58  proc f1exp(b,bfixed);
59
60      external proc fexp;
61
62      retp(b[1]*fexp(b[2]));
63
64  endp;
65
66
67  proc f1_5exp(b,bfixed);
68
69      external proc fexp;
70
71      retp(b[1]*fexp(b[2]) +  b[3]*fexp(bfixed));
72
73  endp;
74
75
76  proc f2exp(b,bfixed);
77
78      external proc fexp;
79
80      retp(b[1]*fexp(b[2]) +  b[3]*fexp(b[4]));
81
82  endp;
83
84
85  proc f2ord(b,bfixed);
86
87      external matrix x;
88
89      local A0,K2;
90
91      A0 = b[1];
92      K2 = b[2];
93
94      retp(1/(1/A0 + K2*x));
95
96  endp;
97
98
99
100
```

```
101   proc f12ord(b,bfixed);
102
103       external proc fexp;
104       external matrix x;
105
106       local A0,K1,K2;
107       local ftot,last,n,period,safe,xsafe;
108       n=rows(x);
109       period = x[2] - x[1];
110
111       A0 = b[1];
112       K1 = b[2];
113       K2 = b[3];
114
115       if K1 < 0;
116           retp(1/((1/A0 + K2/K1)*exp(K1*x) - K2/K1));
117       endif;
118
119   /*      Need to know if exp(K1 * (last# * period)) will overflow
120           i.e. if 1/[exp(k1*(last#*period))] will underflow
121           4e300 = exp(K1*last*period)                                  */
122
123       last = int(ln(4e300)/(K1*period));
124       if last GE n;
125           retp(1/((1/A0 + K2/K1)*exp(K1*x) - K2/K1));
126       elseif last == 0;
127           retp(zeros(n,1));
128       else;
129           ftot = zeros(n,1);
130           xsafe = x[1:last];
131           ftot[1:last] = 1/((1/A0 + K2/K1)*exp(K1*xsafe) - K2/K1);
132           retp(ftot);
133       endif;
134   endp;
135
136
137   proc fe12ord(b,bfixed);
138
139       external proc fexp,f12ord;
140
141       retp(b[1]*fexp(b[2]) +  f12ord(b[3:5],bfixed));
142
143   endp;
144
145
146
147
148
149
150
151
```

```
/*  proc anlytgrd(i,b,bfixed)
**
**  purpose:    Calculates analytical gradients.
**
**  inputs: i       scalar.  Chooses function to take gradient of.
**                       i = 1   f1exp
**                       i = 2   f2exp
**                       i = 3   f2ord
**                       i = 4   f12ord
**
**          b       k x 1 vector.  The adjustable coefficients
**
**          bfixed fixed coefficients.
**
**  output  g   n x k matrix.  The gradient of fn i wrt the b[k]
**
**  remark      gradtype = 2 (or /= 0,1) chooses anlytgrd
*/

proc anlytgrd(i,b,bfixed);

    local g,a0,k,k1,k2,n,k1x,expk1x,f02,f5,f52;

    external matrix x,f0;
    external proc fexp,f12ord;

    k = rows(b);
    n = rows(x);
    g = zeros(n,k);
    if i == 1;          @       i = fittype     @
        g[.,1] = f0/b[1];
        g[.,2] = -x.*f0;
    elseif i == 2;
        g[.,1] = fexp(b[2]);
        g[.,2] = -b[1]*x.*g[.,1];
        if k == 4;
            g[.,3] = fexp(b[4]);
            g[.,4] = -b[3]*x.*g[.,3];
        elseif k == 3;
            g[.,3] = fexp(bfixed);
        endif;
    elseif i == 3;
        f02 = f0.*f0;
        g[.,1] = f02/(b[1]*b[1]);
        g[.,2] = -f02.*x;
    elseif i == 4;
        a0 = b[1];
        k1 = b[2];
        k2 = b[3];
        k1x = k1*x;
        expk1x = exp(k1x);
```

```
203             f02 = f0.*f0;
204             g[.,1] = f02.*expk1x/(a0*a0);
205             g[.,2] = -f02.*(x.*expk1x/a0
206                                 + ((k1x-1).*expk1x+1)*k2/(k1*k1));
207             g[.,3] = -f02.*(expk1x - 1)/k1;
208         elseif i == 5;
209             g[.,1] = fexp(b[2]);
210             g[.,2] = -b[1]*x.*g[.,1];
211             a0 = b[3];
212             k1 = b[4];
213             k2 = b[5];
214             k1x = k1*x;
215             expk1x = exp(k1x);
216             f5 = f12ord(b[3:5],bfixed);
217             f52 = f5.*f5;
218             g[.,1] = f52.*expk1x/(a0*a0);
219             g[.,2] = -f52.*(x.*expk1x/a0
220                                 + ((k1x-1).*expk1x+1)*k2/(k1*k1));
221             g[.,3] = -f52.*(expk1x - 1)/k1;
222         endif;
223
224         retp(g);
225
226     endp;
227
228
229     proc marqtest(fittype,b);
230
231             if fittype == 1;
232                 if b[2] <= 0;
233                     retp(1);
234                 endif;
235             elseif fittype == 2;
236                 if b[2] <= 0 or b[4] <= 0 or sgn(b[1]) /= sgn(b[3]);
237                     retp(1);
238                 endif;
239             elseif fittype == 3;
240                 if sgn(b[1]) /= sgn(b[2]);
241                     retp(1);
242                 endif;
243             elseif fittype == 4;
244                 if sgn(b[1]) /= sgn(b[3]);
245                     retp(1);
246                 endif;
247             endif;
248
249         retp(0);
250
251     endp;
```

APPENDIX A.6 PRCANAL4

```
1   /*
2   **      Procedure PRCANAL4 written by David Fraser,
3   **              PRint Catalyst data ANALyzed by 4 fittypes
4   **      to produce output of the results of the 4 fits
5   **      (single exponential, double exponential, second order,
6   **      first+second order)
7   **      to the analytical solutions to triplet kinetic data.
8   */
9
10  proc (0) = prcanal4(mondate,fit);
11
12  #lineson;
13
14  local single,double,second,firsec;
15  local sgmask,dbmask,scmask,fsmask,sgfmt,dbfmt,scfmt,fsfmt;
16  local headsame,headsg,headsg1,headsg2,headdb,headsc,headfs1;
17  local headfs2,headfs,units_1,units_2,r,z,fsg,fdb,fsc,ffs;
18
19  mondate = "\\GAUSS\\CAT\\FIT\\" $+ mondate;
20
21  single = mondate $+ "sg";
22  double = mondate $+ "db";
23  second = mondate $+ "sc";
24  firsec = mondate $+ "fs";
25
26                                          @ 0 = string, 1 = number  @
27  let sgmask[1,11] = 0    1 1  1   1 1   1 1   1 1 1;
28  let dbmask[1,13] = 0  1 1 1  1   1 1   1 1   1 1   1 1;
29  let scmask[1,8]  = 0    1 1  1   1 1   1 1;
30  let fsmask[1,12] = 0    1 1  1   1 1   1 1   1 1   1 1;
31  let sgfmt[11,3] = "-s  "      8 8            @   signal name @
32                    "lf "       4 0            @   breakfit    @
33                    "lf  "      2 0            @   #iterations @
34                    "lf  "      7 3            @   ssr         @
35                    "lf \241"  10 5            @   a1 +/-      @
36                    "lf  "      8 5            @   stderr a1   @
37                    "lE \241"  13 3            @   k1 +/-      @
38                    "lE  ¦ "    9 1            @   stderr k1   @
39                    "lf \241"   8 2            @   Von +/-     @
40                    "lf  "      7 2            @   sVon        @
41                    "lf"        9 2;           @   Io          @
42  let dbfmt[13,3] = "-s  "      8 8
43                    "lf  "      1 0            @   scheme      @
44                    "lf "       1 0            @   breakfit    @
45                    "lf  "      2 0            @   #iterations @
46                    "lf  "      7 3            @   ssr         @
47                    "lf \241"  10 5
48                    "lf  "      8 5
49                    "lE \241"  13 3
```

```
                    "1E  "      9 1
                    "1f \241" 10 5            @   a2          @
                    "1f  "      8 5           @   stderr a2   @
                    "1E \241" 13 3            @   k2          @
                    "1E"        9 1;          @   stderr k2   @
let scfmt[8,3] =    "-s  "      8 8
                    "1f "       4 0           @   breakfit    @
                    "1f  "      2 0           @   #iterations @
                    "1f  "      7 3           @   ssr         @
                    "1f \241" 10 5            @   a0          @
                    "1f  "      8 5           @   stderr a0   @
                    "1E \241" 13 3            @   k2          @
                    "1E"        9 1;          @   stderr k2   @
let fsfmt[12,3] =   "-s  "      8 8
                    "1f "       4 0           @   breakfit    @
                    "1f  "      2 0           @   #iterations @
                    "1f  "      7 3           @   ssr         @
                    "1f \241" 10 5            @   a0          @
                    "1f  "      8 5           @   stderr a0   @
                    "1E \241" 13 3            @   k1          @
                    "1E  "      9 1           @   stderr k1   @
                    "1E \241" 13 3            @   k2          @
                    "1E  "      9 1           @   stderr k2   @
                    "1E \241" 13 3            @   a0k2        @
                    "1E"        9 1;          @   stderr a0k2 @
headsame = "Signal    s  b  i     X\eS1v\253\eT       ";
headsg1 =
      "   a1   \241   \235a1          k1     \241    \235k1    ";
headsg2 = "  ¦     Von  \241   \235Von       Io";
headdb  =
     "       a2   \241   \235a2          k2     \241    \235k2";
headsc  ="   a0   \241   \235a0          K2     \241    \235K2";
headfs1 ="   a0   \241   \235a0          K1     \241    \235K1";
headfs2 = "          K2     \241    \235K2          "\
                                      "a0K2    \241   \235a0K2";
headsg = headsame $+ headsg1;
headsg2 = headsg $+ headsg2;
headdb = headsg $+ headdb;
headsc = headsame $+ headsc;
headfs = headsame $+ headfs1 $+ headfs2;

units_1  =  "s" $+ "\eS0" $+ "-1" $+ "\eT";
units_2  =  "mV";

output file = lpt1 on;
outwidth 140;
lpwidth 140;
lprint "\015";   /*  sets printer spacing to condensed mode
                     i.e.   to 17.1 cpi = 136.8 c per line  */
```

```
101   if fit == 0 or fit == 1;
102       lprint headsg2;
103       lprint (chrs(ones(63,1)*32) $+ units_1
104            $+ chrs(ones(22,1)*32) $+ units_2
105            $+ chrs(ones(13,1)*32) $+ units_2);
106       open fsg = ^single;
107       r = rowsf(fsg);
108       z = printfm(readr(fsg,r),sgmask,sgfmt);
109       fsg = close(fsg); ?; ?;
110   endif;
111
112   if fit == 0 or fit == 2;
113       lprint headdb;
114       lprint (chrs(ones(63,1)*32) $+ units_1
115            $+ chrs(ones(45,1)*32) $+ units_1);
116       open fdb = ^double;
117       r = rowsf(fdb);
118       z = printfm(readr(fdb,r),dbmask,dbfmt);
119       fdb = close(fdb); ?; ?;
120   endif;
121
122   if fit == 0 or fit == 3;
123       lprint headsc;
124       lprint (chrs(ones(63,1)*32) $+ units_1);
125       open fsc = ^second;
126       r = rowsf(fsc);
127       z = printfm(readr(fsc,r),scmask,scfmt);
128       fsc = close(fsc); ?; ?;
129   endif;
130
131   if fit == 0 or fit == 4;
132       lprint headfs;
133       lprint (chrs(ones(63,1)*32) $+ units_1
134            $+ chrs(ones(23,1)*32) $+ units_1
135            $+ chrs(ones(23,1)*32) $+ units_1);
136      open ffs = ^firsec;
137       r = rowsf(ffs);
138       z = printfm(readr(ffs,r),fsmask,fsfmt);
139       ffs = close(ffs);
140   endif;
141
142   lprint "\r\l";
143
144   outwidth 80;
145   lpwidth 80;
146   lprint "\018";      /*  turns condensed mode off  */
147   output off;
148
149   endp;
```

REFERENCES

1. Schmidt, J.A.; Siemiarczuk, A.; Weedon, A.C.; Bolton, J.R. *J. Am. Chem. Soc.* **1985**, *107*, 6112-6114.
2. Schmidt, J.A. *Ph.D. Thesis: Intramolecular Photochemical Electron Transfer in Porphyrin-Quinone Molecules*; University of Western Ontario: London, Ontario, 1986.
3. Connolly, J.S.; Bolton, J.R. In *Photoinduced Electron Transfer. Part D. Photoinduced Electron Transfer Reactions: Inorganic Substrates and Applications*; Fox, M.A.; Chanon, M., Eds.; Elsevier: Amsterdam, 1988; pp 303-393.
4. Schmidt, J.A.; McIntosh, A.R.; Weedon, A.C.; Bolton, J.R.; Connolly, J.S.; Hurley, J.K.; Wasielewski, M.R. *J. Am. Chem. Soc.* **1988**, *110*, 1733-1740.
5. Schmidt, J.A.; Liu, J.-Y.; Bolton, J.R.; Archer, M.D.; Gadzekpo, V.P.Y. *J. C. S. Faraday I* **1989**, *85*, 1027-1041.
6. Liu, J.-Y.; Bolton, J.R. *J. Phys. Chem.* **1992**, *96*, 1718-1725.
7. Wayne, R.P. *Photochemistry*; American Elsevier: New York, 1970.
8. Bolton, J.R.; Archer, M.D. In *Electron Transfer in Inorganic, Organic, and Biological Systems, Advances in Chemistry Series 228*; Bolton, J.R.; Mataga, N.; McLendon, G.L., Eds.; American Chemical Society: Washington, 1991; pp 7-23.
9. Siebrand, W., Williams, D.F. *J. Chem. Phys.* **1968**, *49*, 1860-1871.

10. Michl, J.; Bonačić-Koutecký, V. *Electronic Aspects of Organic Photochemistry*; Wiley Interscience: New York, 1990.

11. McManis, G.E.; Golovin, M.N.; Weaver, M.J. *J. Phys. Chem.* **1986**, *90*, 6563-6570.

12. Kosower, E.M. *J. Am. Chem. Soc.* **1985**, *107*, 1114-1118.

13. Gilbert, A.; Baggott, J.E. *Essentials of Molecular Photochemistry*; Blackwell Scientific: Oxford, 1991.

14. Gouterman, M.; Khalil, G.-E. *J. Mol. Spectrosc.* **1974**, *53*, 88-100.

15. McGlynn, S.P.; Azumi, T.; Kinoshita, M. *Molecular Spectroscopy of the Triplet State*; Prentice-Hall: Englewood Cliffs, NJ, 1969.

16. Levine, I.N. *Quantum Chemistry*; 3rd ed.; Allyn and Bacon: Newton, MA, 1983.

17. Calvert, J.G.; Pitts, J.N.Jr. *Photochemistry*; John Wiley & Sons: New York, 1966.

18. McGlynn, S.P.; Smith, F.J.; Cilento, G. *Photochem. Photobiol.* **1964**, *3*, 269-294.

19. Gouterman, M. In *The Porphyrins, v.III*; Dolphin, D., Ed.; Academic Press: New York, 1978; pp 1-165.

20. Whitten, D.G. *Rev. Chem. Intermed.* **1978**, *2*, 107-138.

21. Weiss, C. In *The Porphyrins, vol III*; Dolphin, D., Ed.; Academic Press: New York, 1978; pp 211-223.

22. Dilung, I.I.; Kapinus, E.I. *Russ. Chem. Rev.* **1978**, *47*, 43-53; tr. from *Uspekhi Khimii* **1978**, *47*, 83-100.

23. Adar, F. In *The Porphyrins, v.III*; Dolphin, D., Ed.; Academic Press: New York, 1978; pp 167-209.

24. Pekkarinen, L.; Linschitz, H. *J. Am. Chem. Soc.* **1960**, *82*, 2407-2416.

25. Yasuike, M.; Shima, M.; Koseki, K.; Yamaoka, T.; Sakuragi, M.; Ichimura, K. *J. Photochem. Photobiol. A* **1992**, *64*, 115-122.

26. Carnieri, N.; Harriman, A. *Inor. Chim. Acta* **1982**, *62*, 103-107.

27. Gasyna, Z.; Browett, W.R.; Stillman, M.J. *Inorg. Chem.* **1985**, *24*, 2440-2447.

28. Newton, M.D.; Sutin, N. *Ann. Rev. Phys. Chem.* **1984**, *35*, 437-480.

29. Marcus, R.A.; Sutin, N. *Biochim. Biophys. Acta* **1985**, *811*, 265-322.

30. Archer, M.D.; Gadzekpo, V.P.Y.; Bolton, J.R.; Schmidt, J.A.; Weedon, A.C. *J. C. S. Faraday II* **1986**, *82*, 2305-2312.

31. Parker, C.A. *Photoluminescence of Solutions*; Elsevier: Amsterdam, 1968.

32. Cannon, R.D. *Electron Transfer Reactions*; Butterworths: London, 1980.

33. Marcus, R.A. *J. Chem. Phys.* **1965**, *43*, 679-701.

34. Newton, T.W. *J. Chem. Educ.* **1968**, *45*, 571-575.

35. Wasielewski, M.R.; Niemczyk, M.P.; Svec, W.A.; Pewitt, E.B. *J. Am. Chem. Soc.* **1985**, *107*, 1080-1082.

36. Bixon, M.; Jortner, J. *Faraday Discussions of the Chemical Society* **1982**, *74*, 17-29.

37. Jortner, J. *J. Chem. Phys.* **1976**, *64*, 4860-4867.

38. Miller, J.R.; Beitz, J.V.; Huddleston, R.K. *J. Am. Chem. Soc.* **1984**, *106*, 5057-5068.

39. The accepted definition of an exciplex is "an electronically excited atomic or molecular complex of definite stoichiometry, which is dissociated in its electronic ground state."[40] This has been slightly extended by Birks[41] to "...dissociative (i.e. would dissociate in the absence of external restraints) in its electronic ground state." However, Weller[42] incudes such ground state complexes (also termed electron donor acceptor complexes or EDA complexes) as a legitimate type of exciplex.

40. Lim, E.C. (Ed.) *Molecular Luminescence*; W.A. Benjamin: New York, 1969, p 907.

41. Birks, J.B. In *The Exciplex*; Gordon, M.; Ware, W.R., Eds.; Academic Press. N.Y., 1975; pp 39-73.

42. Weller, A. *The Exciplex*; Gordon, M.; Ware, W.R., Eds.; Academic Press: N.Y., 1975; pp 23-38.

43. Mataga, N.; Ottolenghi, M. In *Molecular Association, vol 2*; Foster, R., Ed.; Academic Press: London, 1979; pp 1-78.

44. Kapinus, E.I.; Dilung, I.I. *Russ. Chem. Rev.* **1988**, *57*, 620-633; tr. from *Uspekhi Khimii* **1988**, *57*, 1087-1109.

45. Harrima. *A J. C. S. Faraday I* **1980**, *76*, 1978-1985.

46. Wilford, J.H.; Archer, M.D.; Bolton, J.R.; Ho, T.-F.; Schmidt, J.A.; Weedon, A.C. *J. Phys. Chem.* **1985**, *89*, 5395-5398.

47. Trommsdorff, H.P. *J. Chem. Phys.* **1972**, *56*, 5358-5372.

48. Itoh, T. *Spectrochimica Acta* **1984**, *40A*, 387-389.

49. Becker, R.S. *Theory and Interpretation of Fluorescence and Phosphorescence*; Wiley Interscience: New York, 1969.

50. Flaig, W., Salfeld, J.-C., Baume, M. *Anal. Chem.* **1958**, *618*, 117-129.

51. Braude, E.A. *J. Chem. Soc.* **1945**, 490-497.

52 Wasielewski, M.R.; Neis, J.R.; Bowman, M.K. *Faraday Discussions of the Chemical Society* **1984**, *78*, 279-288.

53. Ware, W.R. In *Time-Resolved Fluorescence Spectroscopy in Biochemistry and Biology*; Cundall, R.B.; Dale, R.E., Eds.; Plenum Press: New York, 1983; pp 341-362.

54. Baggott, J.E. *Photoinduced Electron Transfer. Part B. Experimental Techniques and Medium Effects*; Fox, M.A.; Chanon, M., Eds.; Elsevier: Amsterdam, 1988; pp 385-419.

55. Gorman, A.A.; Gould, I.R.; Hamblett, I. *J. Am Chem. Soc.* **1982**, *104*, 7098-7194.

56. Weller, A. *Z. Phys. Chem. Neue Folge* **1982**, *133*, 93-98.

57. Williams, W.P. In *Primary Processes of Photosynthesis*; Barber, J. Ed.; Elsevier: Amsterdam, 1977; pp 99-147.

58. Deisenhofer, J.; Michel, H. *EMBO J.* **1989**, *8*, 2149-2170.

59. Chang, C. -H.; Tiede, D.; Tang, J.; Smith, U.; Norris, J.; Schiffer, M. *FEBS Lett.* **1986**, *205*, 82-86.

60. Huber, R. *Angew. Chem. Int. Ed. Engl.* **1989**, *28*, 848-869.

61. Koyama, Y. *J. Photochem. Photobiol. B: Biol.* **1991**, *9*, 265-280.

62. Truscott, T.G. *J. Photochem. Photobiol. B: Biol.* **1990**, *6*, 359-371.

63. Cogdell, R.J.; Frank, H.A. *Biochim. Biophys. Acta* **1987**, *895*, 63-79.

64. Rehm, D.; Weller, A. *Israel J. Chem.* **1970**, *8*, 259-271.

65. Miller, J.R.; Calcaterra, L.T.; Closs, G.L. *J. Am. Chem. Soc.* **1984**, *106*, 3047-3049.

66. Wasielewski, M.R.; Johnson, D.G.; Svec, W.A. In *Supramolecular Photochemistry*; Balzani, V., Ed.; D. Reidel: Dordrecht, 1987; pp 255-266.

67. Irvine, M.P.; Harrison, R.J.; Beddard, G.S.; Leighton, P.; Sanders, J.K.M. *Chem. Phys.* **1986**, *104*, 315-324.

68. Gould, I.R.; Ege, D.; Moser, J.E.; Farid, S. *J. Am. Chem. Soc.* **1990**, *112*, 4290-4301.

69. Levin, P.P.; Plushnikov, P.F.; Kuzmin, V.A. *Chem. Phys.* **1989**, *137*, 331-344.

70. Vogelmann, E.; Rauscher, W.; Kramer, H.E.A. *Photochem. Photobiol.* **1979**, *29*, 771-776.

71. Verhoeven, J.W. *Pure & Appl. Chem.* **1990**, *62*, 1585-1596.

72. Kavarnos, G.J. In *Topics in Current Chemistry, v.156*; Mattay, J., Ed.; Springer-Verlag: Berlin, 1990; pp 21-58.

73. Perrin, D.D.; Armarego, W.L.F.; Perrin, D.R. *Purification of Laboratory Chemicals*; 2nd ed.; Pergammon Press: Oxford, 1980.

74. Duhaime, R.M.; Lombardo, D.A.; Skinner, I.A.; Weedon, A.C. *J. Org. Chem.* **1985**, *50*, 873-879.

75. Grimmett, M.R. *Advances in Heterocyclic Chemistry, vol. 12*; Katritzky, A.R.; Boulton, A.J., Eds.; Academic Press: New York, 1970; pp 103-183.

76. Windholz, M., ed. *Merck Index*; 9th ed.; Merck & Co.: Rahway, NJ, 1976; compound 4807.

77. Hampel, B. *DMS UV Atlas of Organic Compounds*; Butterworths: London, 1980; spectrum G1/7.

78. Liu, J.-Y. private communication.

79. Kong, J.L.Y.; Loach, P.A. *J. Heterocyclic Chem.* **1980**, *17*, 737-743.

80. Ho, T.-F.; McIntosh, A.R.; Weedon, A.C. *Can. J. Chem.* **1984**, *62*, 967-974.

81. Liu, J.-Y. *Ph.D. Thesis: Solvent Dependence of Photoinduced Intramolecular Electron Transfer*; University of Western Ontario: London, Ontario, 1991.

82. Sassoon, R.E.; Rabani, J. *J. Phys. Chem.* **1980**, *84*, 1319-1325.

83. Linschitz, H.; Sarkanen, K. *J. Am. Chem. Soc.* **1958**, *80*, 4826-4832.

84. Boag, J.W. *Trans. Faraday Soc.* **1968**, *64*, 677-685.

85. *GAUSS 2.0*; Aptech Systems, Inc.: Maple Valley, WA., 1988.

86. Bevington, P.R. *Data Reduction and Error Analysis for the Physical Sciences*; McGraw Hill: New York, 1969.

87. Gorman, D.S.; Connolly, J.S. *Int. J. Chem. Kinetics* **1973**, *5*, 977-989.

88. Linschitz, H.; Steel, C.; Bell, J.A. *J. Phys. Chem.* **1962**, *66*, 2574-2576.

89. Press, W.H.; Flannery, B.P.; Teukolsky, S.A.; Vetterling, W.T. *Numerical Recipes: The Art of Scientific Computing (FORTRAN version)*; Cambridge University Press: Cambridge, 1989.

90. *HP 8450 UV/VIS Spectrophotometer Operators Manual*; Hewlett Packard: Palo Alto, CA, 1981.

91. Schmidt, J. A., unpublished work.

92. Carmichael, I.; Hug, G.L. *J. Phys. Chem. Ref. Data* **1986**, *15*, 1-250.

93. Moore, T.A.; Benin, D.; Tom, R. *J. Am. Chem. Soc.* **1982**, *104*, 7356-7357.

94. Connolly, J.S.; Gorman, D.S.; Seely, G.R. *Ann. N.Y. Acad. Sci.* **1973**, *206*, 649-669.

95 Seely, G.R.; Jensen, R.G. *Spectrochimica Acta* **1965**, *21*, 1835-1845.

96. *Landolt-Bornstein*, 6 Auf., II Band, 8 Teil; Springer-Verlag: Berlin, 1959; pp 5-587, 5-623, 5-655.

97. *Landolt-Bornstein*, 6 Auf., II Band, 6 Teil; Springer-Verlag: Berlin, 1959; pp 673, 685, 686.

98. Connolly, J.S.; Hurley, J.K.; Bell, W.L. In *Supramolecular Photochemistry*; Balzani, V., Ed.; D. Reidel: Dordrecht, 1987; pp 299-318.